Abstract

Due to the effects of climate change and the potential shortage of resources like water and fertilizer, the use of novel techniques in agriculture has become a major priority on the global scene. The focus of this research is the application of proximal sensing methods for precision soil and crop management and sustainable use of water and nitrogen. The research has been focused on sweet maize (*Zea mays* var. saccharata L.) crop. The main objectives of the thesis were to i) describe the spatial variability of the experimental site; ii) analyse the sensitivity of spectral information to explain the physiological and yield response of sweet maize under various nitrogen and water management; iii) evaluate the relationship between bio-physiological crop parameters and hyperspectral vegetation indices (VIs); iv) identify suitable red-green-blue (RGB) indices for estimating crop properties.

The experimental trial on sweet maize was conducted at the Mediterranean Agronomic Institute of Valenzano, Bari (Southern Italy), in the growing seasons 2020 and 2021. Sweet maize was grown and tested under three irrigation regimes (full irrigation, deficit irrigation, and rainfed) and two nitrogen levels (300 and 50 kg ha^{-1}).

As the first step of the experimental set-up, an electromagnetic induction sensor (EMI) was used to measure apparent electrical conductivity, in order to characterize the soil spatial variability and define the experimental layout. Our results highlighted the great potential of using proximal geophysical sensors to better guide experimental agronomic trials.

Thereafter, during the growing seasons ground-based, aerial-based and bio-physiological measurements were acquired. Hyperspectral reflectance and canopy temperature were measured using proximal sensors. Concerning bio-physiological measurements leaf gas exchanges, relative water content, leaf chlorophyll concentration, leaf area index, dry-above-ground biomass and yield were measured. In addition, RGB images were captured by an RGB camera installed on the drone.

The data of hyperspectral reflectance were used to evaluate the crop physiological parameters of sweet maize. Principal component analysis (PCA) was applied to determine which wavelengths were most important to describe sweet maize performance. Correlation analysis and multiple linear regression, with a stepwise algorithm, were used to select the best-performing vegetation indices (VIs) for monitoring the yield and physiological response of sweet maize grown under different water and nitrogen availability. The multivariate regression results showed that red-edge group indices, such as CARI (Chlorophyll Absorption Reflectance Index), DD (Double Difference Index), REIP (Red- Edge Inflection Point), and $Cl_{red\text{-}edge}$ (Chlorophyll Red-Edge) were good predictors of yield and physiological parameters, confirming the crucial role of the red-edge spectral region that also emerged

through PCA. DD, REIP, and $Cl_{red-edge}$ VIs were able to discriminate water stress at the mid-season stage, as well as to separate water and N stress levels.

Moreover, we evaluated the sensitivity of hyperspectral indices to different water and nitrogen treatments. The DATT index, based on near-infrared and red-edge wavelengths, performed better than other indices in explaining the variation in chlorophyll content, whereas the double difference index (DD) showed the greatest correlation with the leaf gas exchange. The modified normalized difference vegetation index (NNDVI) and the ratio of water band index to normalized difference vegetation index (WBI/NDVI) showed the highest capacity to distinguish the interaction of irrigation x nitrogen, and the best discriminating capability of these indices was observed under a low nitrogen level. Moreover, red-edge-based indices had higher sensitivity to nitrogen levels compared to the structural and water band indices. This study highlighted that it is crucial to choose proper narrow-band vegetation indices to monitor the plant's eco-physiological response to water and nitrogen stresses.

To overcome some environmental limitations in crop production, remote sensing measures may be utilized to quickly evaluate crop performance and to cost-effectively monitor a large number of plots. Hence, we examined how well a set of RGB indices and hyperspectral vegetation indices were able to describe the crop growth. The greatest ability was found for the Green-Area index (GA) predicting Leaf Area Index (LAI) in 2020 (R^2=0.61) and Leaf Chlorophyll Concentration (CC) in 2021 (R^2=0.49). Moreover, the capacity of predicting gas-exchange parameters by red-edge region was demonstrated. Several red-edge indices, including $Cl_{red-edge}$, NDRE, MTCI, DD, and REIP, were shown to be the best predictors of the bio-physiological parameters. The usefulness of RGB-derived indices, which are less expensive and less time-consuming compared to hyperspectral indices, has been assessed in this study.

Sintesi

A causa degli effetti del cambiamento climatico e della potenziale carenza di risorse come acqua e fertilizzanti, l'uso di nuove tecniche in agricoltura è diventata una delle principali priorità sulla scena globale. L'obiettivo di questo progetto di ricerca è l'applicazione di metodi di rilevamento prossimale per la gestione sostenibile del suolo, delle colture e delle risorse (acqua e azoto). Lo studio è stato effettuato su una coltura di mais dolce (*Zea mays* var. saccharata L.). Gli obiettivi principali del progetto sono stati: i) descrivere la variabilità spaziale del suolo del sito sperimentale; ii) analizzare la sensibilità delle informazioni spettrali per spiegare la risposta fisiologica e produttiva del mais dolce in diverse modalità di gestione dell'azoto e dell'acqua; iii) valutare il legame tra parametri colturali bio-fisiologici e indici vegetazionali iperspettrale (VIs); iv) determinare gli indici rosso-verde-blu (RGB) adatti per la stima delle proprietà delle colture.

La prova sperimentale sul mais dolce è stata condotta presso i campi sperimentali dell'Istituto Agronomico Mediterraneo di Valenzano, Bari (Italia), negli anni 2020 e 2021. Il mais dolce è stato coltivato e testato in tre regimi irrigui (irrigazione ottimale, irrigazione in deficit e in assenza di irrigazione) e due livelli di azoto (300 e 50 kg ha^{-1}).

Una fase preliminare della sperimentazione ha previsto l'impiego di un sensore ad induzione elettromagnetica (EMI) per misurare la conduttività elettrica apparente del suolo e definire il disegno sperimentale. I nostri risultati hanno evidenziato il grande potenziale dell'utilizzo di sensori geofisici prossimali anche al fine di impostare le prove agronomiche sperimentali.

Successivamente, sono state effettuate misurazioni a terra, aeree e biofisiologiche. Le misure di riflettanza iperspettrale e di temperatura della canopy sono state effettuate attraverso sensori prossimali. Per quanto riguarda le misurazioni biofisiologiche, sono stati rilevati i seguenti parametri: gli scambi gassosi a livello fogliare, il contenuto idrico relativo nelle foglie, il contenuto di clorofilla fogliare, l'indice di area fogliare, la biomassa della coltura e la produzione. Inoltre, le immagini RGB sono state catturate da una telecamera RGB installata sul drone.

I dati della riflettanza iperspettrale sono stati utilizzati per valutare i parametri fisiologici della coltura. L'analisi delle componenti principali (PCA) è stata applicata per identificare quali lunghezze d'onda sono risultate essere più efficaci nel descrivere la risposta della coltura. L'analisi di correlazione e la regressione lineare multipla, con un algoritmo stepwise, sono state utilizzate per selezionare gli indici di vegetazione (VIs) che sono risultati essere i più efficienti per monitorare la risposta produttiva e quella fisiologica del mais dolce coltivato in diverse disponibilità di acqua e azoto. I risultati della regressione multivariata hanno mostrato che gli indici vegetazionali che considerano la regione del red-edge, come gli indici CARI (Chlorophyll Absorption Reflectance Index), DD (Double Difference Index), REIP (Red- Edge Inflection Point) e $Cl_{red\text{-}edge}$ (Chlorophyll Red-Edge) sono stati buoni

predittori della produzione e dei parametri fisiologici, a conferma del ruolo cruciale di questa regione spettrale così come anche emerso attraverso la PCA. I VIs DD, REIP e $Cl_{red\text{-}edge}$ sono stati in grado di discriminare le condizioni di stress in condizioni di stress idrico e nutrizionale.

I risultati hanno anche mostrato come l'indice DATT, basato sulle lunghezze d'onda del vicino infrarosso e del red-edge, si sia comportato meglio di altri indici nello spiegare la variazione del contenuto di clorofilla, mentre l'indice DD abbia mostrato la maggiore correlazione con gli scambi gassosi. L'indice di vegetazione NNDVI e il rapporto WBI/NDVI hanno mostrato la più alta capacità di distinguere l'interazione di irrigazione x azoto, mentre la migliore capacità discriminante di questi indici è stata osservata in condizioni di azoto limitato. Gli indici basati sul red-edge hanno mostrato una maggiore sensibilità ai livelli di azoto rispetto agli indici strutturali e di "water band". Questo studio ha evidenziato l'importanza nella scelta di adeguati indici di vegetazione "narrow band" per monitorare la risposta eco-fisiologica della pianta agli stress idrici e nutrizionali.

Inoltre, lo studio ha evidenziato la possibilità di utilizzare misure da remoto per valutare rapidamente le prestazioni delle colture ampliando le superfici di monitoraggio, pur riducendo i costi. Pertanto, sono state confrontate le potenzialità di indici RGB e indici di vegetazione iperspettrali. L'indice GA ha mostrato la migliore capacità predittiva nei riguardi dell'indice di area fogliare (LAI) nel 2020 (R^2= 0,61) e della concentrazione di clorofilla fogliare (CC) nel 2021 (R^2= 0,49). Inoltre, è stata la regione "red-edge" ha evidenziato ancora una volta la migliore capacità predittiva per i parametri di scambi gassosi. Risultati simili sono stati riscontrati anche per gli indici $Cl_{red\text{-}edge}$, NDRE, MTCI, DD e REIP. La ricerca ha dunque dimostrato l'utilità degli indici RGB che, pur essendo meno costosi e richiedendo meno tempo rispetto agli indici iperspettrali, hanno dimostrato essere ugualmente efficienti.

Author's address Milica Colovic
Department of Soil and Food Science
University of Bari Aldo Moro
Piazza Umberto I, 1, 70121 Bari (BA)
milica.colovic@uniba.it/m.colovic94@gmail.com

Supervisor Prof. Dr. Anna-Maria Stellaci
Department of Soil and Food Science
University of Bari Aldo Moro

Tutors Dr. Rossella Albrizio
National Research Council of Italy, Institute for Agricultural and Forestry Systems in the Mediterranean (CNR-ISAFOM)

Dr. Nicola Lamaddalena
Sustainable Water and Land Management in Agriculture program, department of Land and Water Resources Management, Mediterranean Agronomic Institute of Bari, Italy

This dissertation is dedicated to all my beloved people who believed in me and supported me on this interesting journey.

Acknowledgements

I am deeply thankful for the many mentors, collaborators, friends, and family who have supported and inspired my work over the past three years.

First and foremost, thank you to my supervisor Prof.Dr. Anna-Maria Stellacci and my Tutor Dr. Rossella Albrizio for their enormous investment of time and energy in my growth as a researcher. They provided invaluable guidance and support while always giving me the space to explore my interests freely. Their dedication will help me as a model throughout my career.

Many thanks to my Tutors Dr. Nicola Lamaddalena. His diverse and creative insights and advices have greatly improved this work. I appreciate his generosity and many efforts to support my professional development.

I am especially grateful to PhD program course coordinator Prof. Fabio Minervini for his invaluable support, time, and energy he has given to the program during these three years. I would also like to thank the many other mentors and teachers at the University of Bari and CIHEAM Bari who have guided and inspired my path. Special thanks to my dear professor Mladen Todorovic, who always had brilliant ideas and useful critiques of this research work.

Many thanks to Dr. Kang Yu for his kindness and hospitality during my internship at the Technical University of Munich (Germany), Department of Precision Agriculture. His help has been crucial and he has always found time for my doubts and questions.

I am heartily thankful to Carlo Ranieri, Mimmo Tribuzio, Vito Raspatelli, Giovanna Dragonetti and Marco Nicastro for their support and help during the field trials and lab work.

I would like to give special thanks to my lovely parents Milenko and Novka for their unconditional love, understanding and support. I will forever be indebted to my sisters Bojana and Jelena who have stood by my side through the successes, failures, and adventures of my life. Special thanks to my special love – my nephew Tadija – who brought new energy and happiness to my life. Finally, I owe my deepest gratitude to Majmi Aymen Sawassi for his love, encouragement, advices and sharing unforgettable moments.

List of Figures

List of Tables

Table of contents

Chapter 1

Introduction

"Advances in medicine and agriculture have saved vastly more lives than have been lost in all the wars in history." -
Carl Sagan

1.1. Motivation and background

A rise in human population, a shift in lifestyle, and growth in industrial and agricultural output have all contributed to a greater water demand. Due to an increase in the frequency of droughts, urbanization, and population expansion in cities, the demand for water resources has increased and will keep increasing in the upcoming years. Deforestation, higher fertilizer and pesticide usage, all have a significant negative impact on water supplies. Since the Mediterranean area has been designated as one of the most sensitive places to the effects of climate change in the world, the actual pattern of climate change and land use clearly predicted an increase in water demand and a shortage of water and agricultural land in that region (Pascual *et al.*, 2017).
According to Pereira *et al.* (2009), the sector with the largest water use is agriculture and a lack of water is the most significant abiotic stressor for agricultural production, frequently reducing plant growth, yield, and quality (Gerhards *et al.*, 2016). Additionally, in arid and semi-arid countries where in-season rainfall is insufficient to cover crop water requirements, irrigation is a crucial component of agricultural input. Knowing the appropriate amount of water to apply, as well as the duration and frequency of irrigation, can help to reduce crop yield loss due to water stress, maximize yield response to other management practices, and optimize yield per unit of water applied (i.e. irrigation efficiency), which can then help to maximize the farmer's profit (Khanal *et al*., 2017). Within the Mediterranean area, there are significant disparities in freshwater supplies and irrigation methods, especially between the northern and southern portions of the Mediterranean Basin. Irrigation is the greatest water user, accounting for 69% of all water consumption overall (Malek and Verburg, 2017). In order to deal with this complicated scenario, the Mediterranean area needs precise and real-time monitoring techniques. To pursue such a goal, remote and proximal sensing can be used.
For farmers dealing with water constraints, developing sustainable irrigation techniques is a leading issue (Bell *et al.*, 2018). However, agriculture is a complex system and many factors may affect

production. For example, in order to maximize output, nitrogen (N) is essential for achieving this aim (Spiertz, 2009). Moreover, N has a crucial role in the photosynthetic processes and the production and duration of leaves; these aspects are directly associated with increased yield (Leghari *et al.*, 2016). Hence, nitrogen, as well as other fertilizers, needs to be applied at the level required for optimal crop growth based on crop requirements and agro-climatic considerations ensuring protection of the environment and human health (Gruhn *et al.*, 2000). One of the main challenges in agriculture is to understand how different levels of irrigation and fertilizers have significant effects on crop production, growth and water productivity (Javed *et al.*, 2022).

Due to fundamental tenet of increasing yields by applying the proper quantity of input at the proper location and time, at the same time reducing production costs and agricultural practices negative effects on the environment, precision agriculture is also gaining popularity today. Many farm managers strive to use new technology for decision-making in order to achieve this aim, including when and where to water, fertilize, grow crops, apply herbicides, etc. Data collection/analysis, information management, computer processing, field positioning, yield monitoring, remote sensing, and sensor design are all part of precision agriculture.

Several non-destructive remote sensing techniques may be used to offer valuable performance on canopy coverage, plant growth, development, and the detection of numerous environmental challenges that restrict plant productivity. From the ground, air, and space-based platforms, detailed geographical and temporal information on plants reactions to environment is delivered (Pinter *et al*., 2003).

1.2. Research questions

This thesis addresses four main questions build upon previous studies with the goal of answering additional questions and developing new methods to analyze data obtained by crop canopy sensors. This has led us to the four overarching research questions addressed in this dissertation:

1. To characterize soil spatial variability of the experimental site;
2. To study the sensitivity of spectral information, in order to describe the physiological and yield response of sweet maize under different water and nitrogen management;
3. To investigate the relationship between hyperspectral vegetation indices (VIs) and both biometric and physiological crop parameters, during the growing season;
4. To assess the suitability of red-green-blue (RGB) indices to estimate crop parameters.

This dissertation addresses these objectives through different methodologies for analysing crop spectral information, bio-physiological parameters, as well as RGB images. Question 1 focuses on using a proximal geophysical sensor for soil variability characterization. The obtained information, together with data from soil analysis, helped to define the experimental design and to improve data analysis. The physiological and yield response of sweet maize under various water and nitrogen management is described in response to question 2; in this approach the sensitivity of spectral information was investigated. To this aim, the factors extracted through Principal Component Analysis (PCA) and selected VIs were analysed using correlation analysis and multiple linear regression (MLR) with a stepwise algorithm. Thereafter, their performance was evaluated and discussed. In Question 3 the overall objective was to assess the performance of various narrow-band vegetation indices and sensitivity to different irrigation and nitrogen levels and their interaction, while the specific objective was to find the best correlation in determining which vegetation index is the most efficient predictor of crop eco-physiological parameters. Finally, in question 4 the performance of different RGB indices was assessed, as well as their interactions with bio-physiological parameters. The responses of those research questions facilitated understanding of the behaviour of different VIs, their performance under different growth conditions, as well as the potential of proximal and low-cost aerial RGB images to detect and monitor crop stress.

The remainder of this dissertation is organized as follows. Chapter 2 covers the theoretical and conceptual framework used in this dissertation and connects the dots between all the upcoming chapters.

Chapter 3 includes four sub-chapters, where the first one introduces the use and the results of EMI proximal sensor for soil characterization. The second sub-chapter applies PCA and MLR for sensitivity analysis of the spectral information. Thereafter, the performance of narrow-band VIs and their ability to differentiate between irrigation and nitrogen treatment is described in sub-chapter three. The fourth sub-chapter explained the trend of RGB VIs, as well as their correlation with bio-physiological parameters. Finally, Chapter 4 concludes with methodological contributions of the dissertation, and a discussion of insights across the applications, limitations, and potential for future development of the planning framework.

The sub-chapters 2, 3 and 4 are presented as stand-alone papers. This technique enables chapters to be read and used independently without having to go through the entire dissertation.

1.3. References

Pascual, D., Pla, E., Fons, J., and Abdul-Malak, D. (2017). Climate change impacts on water availability and human security in the intercontinental biosphere reserve of the Mediterranean (Morocco-Spain). In *Environmental Change and Human Security in Africa and the Middle East* (pp. 75-93). Springer, Cham.

Pereira L. S., Cordery I. and Iacovides I. (2009). *Coping with water scarcity: Addressing the challenges*. Springer Science & Business Media.

Gerhards M., Rock G., Schlerf M. and Udelhoven T. (2016). Water stress detection in potato plants using leaf temperature, emissivity, and reflectance. *International journal of applied Earth observation and geoinformation*, *53*, 27-39.

Khanal S., Fulton J. and Shearer S. (2017). An overview of current and potential applications of thermal remote sensing in precision agriculture. *Computers and Electronics in Agriculture*, *139*, 22-32.

Malek Ž. and Verburg P. H. (2018). Adaptation of land management in the Mediterranean under scenarios of irrigation water use and availability. *Mitigation and adaptation strategies for global change*, *23*(6), 821-837.

Bell J. M., Schwartz R., McInnes K. J., Howell T. and Morgan C. L. (2018). Deficit irrigation effects on yield and yield components of grain sorghum. *Agricultural water management*, *203*, 289-296.

Spiertz J. H. J. (2009). Nitrogen, sustainable agriculture and food security: a review. *Sustainable agriculture*, 635-651.

Leghari A. H., Laghari G. M., Ansari M. A., Mirjat M. A., Laghari U. A., Leghari S. J. and Abbasi Z. A. (2016). Effect of NPK and boron on growth and yield of wheat variety TJ-83 at Tandojam soil. *Advances in Environmental Biology*, *10*(10), 209-216.

Gruhn P., Goletti F. and Yudelman M. (2000).*Integrated nutrient management, soil fertility, and sustainable agriculture: current issues and future challenges*. Intl Food Policy Res Inst.

Javed T., Indu I., Singhal R. K., Shabbir R., Shah A. N., Kumar P. and Siuta D. (2022). Recent advances in agronomic and physio-molecular approaches for improving nitrogen use efficiency in crop plants. *Frontiers in Plant Science*, *13*.

Pinter Jr P. J., Hatfield J. L., Schepers J. S., Barnes E. M., Moran M. S., Daughtry C. S. and Upchurch D. R. (2003). Remote sensing for crop management. *Photogrammetric Engineering & Remote Sensing*, *69*(6), 647-664.

Chapter 2

Theoretical and Conceptual Framework

The previous chapter provided a general introduction concerning the necessity of agricultural modernization and use of novel, more precise technologies for maximizing yield, optimizing inputs and decreasing the negative impact on the environment. Here, we present the theoretical and conceptual framework of the entire dissertation by addressing the what, why, and how questions in the above literature. In order to address such questions, it is important to 1) investigate the use of remote and proximal sensing techniques to monitor soil and crop behaviour; 2) comprehend the types of remote and proximal sensing techniques and their role in precision agriculture; 3) understand the crop spectral response and behaviour of vegetation indices under different growth conditions. In this study, all the above-listed points have been developed by focusing on the sweet maize (*Zea mays* L., var. Saccharata) crop, as it is one of the most important staple foods in the world that can be grown in a variety of environments.

2.1. Use of remote and proximal sensing to monitor soil and sweet maize crop behavior

Maize crop has a duplex attitude: a source of energy for animal diets as well as an alternative crop for the generation of biogas. Due to its high degree of adaptation to environmental factors and ease of planting, maize is grown in 170 different nations (Klein and Luna, 2022). Even though maize is a very adaptable crop, environmental factors have a significant impact on the production of maize grains as well as their qualitative characteristics (Finke *et al.*, 1999). Water stress (drought) is one of the main abiotic stressors associated with climate change, and negatively affects the production and quality of many field crops (Alqudah *et al.*, 2011; Lu *et al.*, 2012). When non-limited water was accessible during the flowering and grain-filling periods, both maize grain production and protein content increased (Butts-Wilmsmeyer *et al.*, 2019). In comparison to no-stress circumstances, severe water stress enhanced the protein content in maize while decreasing the grain yield and starch (Da Ge *et al.*, 2010).

Moreover, it was proved that an optimal supply of N fertilizer boosts crop yield and overall biomass production; however, at lower N fertilizer supplies, plants accumulate less dry matter in their reproductive organs, which lowers grain output (Monneveux *et al.*, 2005). Thus, in order to guarantee enough grain crop production throughout the world and take into account global food security, water

and N supply is a key necessity (Thompson *et al.*, 2015; Correndo *et al*., 2021). Corn is extensively cultivated in the Northern part of Italy and has about one million hectares and a mean grain yield of approximately 9.4 t ha^{-1}, while in Central and Southern Italy, characterized by a Mediterranean climate, cultivation accounts for 130,000 ha and due to the water-limited conditions, the average grain yield is about 7.4 t ha^{-1} (ISTAT sources, 2006).

Since this study on sweet maize was carried out in Southern Italy, which is one of the most water-scarce regions in the world, irrigation management should be applied as a powerful strategy for increasing crop production and coping with the challenging climatic conditions (Piscitelli et al., 2021). Furthermore, the application of both remote and proximal sensing can provide valuable information for maize crop management, particularly concerning the detection of water stress, N deficiency and diseases. Many previous studies confirmed the great potential of these techniques used in precision agriculture to fulfil the main aim, which is maximizing yields by giving the right amount of input at the right place and at the right time and, at the same time, reducing production costs and environmental impacts of agricultural practices (Pinter, 2003). For example, Gabriel *et al.* (2017) tested the suitability of proximal and airborne sensing for the assessment of maize N nutritional status and reported that higher accuracy was obtained with indices combining chlorophyll estimation with canopy structure. Hedley *et al.* (2010) applied proximal sensing methods for mapping soil water status in an irrigated maize field. Numerous recent research focused on using spectral reflectance answers to evaluate the water stress level of maize (Alvino *et al*., 2020; Kim, 2021; Martens et al., 2021; Ndlovu *et al.,* 2021; Spisic *et al.,* 2022). Moreover, remote sensing techniques were successfully used, in maize crop, also in precision nitrogen management (Paiao *et al.,* 2020; Kizilgeci *et al.,* 2021; Wen *et al.,* 2021), detecting different types of diseases in maize crop (Meng *et al.*, 2020; Furuya *et al.,* 2021) and light use efficiency (Gitelson *et al.,* 2018; Liu *et al*., 2020).

2.2. Remote sensing in precision agriculture (PA)

The fourth revolution in agriculture is currently underway, largely thanks to developments in information and communication technologies (Delgado *et al.*, 2019). Application and use of water, fertilizer, pesticides, seeds, fuel, labour, etc. are a few examples of how PA involves a management strategy that uses a variety of advanced information, communication, and data analysis techniques in the decision-making process. This helps to increase crop production while minimizing water and nutrient losses as well as adverse environmental effects. Data collection, analysis, and management are all part of precision agriculture, along with global positioning systems (GPS), geographic

information systems (GIS), Internet of things (IoT), Big Data analysis, artificial intelligence (AI), field location, yield monitoring, and sensor design (Mulla, 2013). Remote sensing and proximal sensing, which are used to track and map agricultural lands throughout the world in a variety of conditions, are among the most effective tools for precision agriculture.

For the sustainable management of natural resources at the local, regional, and national levels, researchers long time ago recognized the necessity to map soil and land use (Metternicht, 2018). The term "remote sensing" was first used in 1958.

Remote and proximal sensing may be categorized according to (i) sensor platform and (ii) sensor type (Lechner *et al.,* 2020). There are several platforms available for collecting remotely sensed data, including satellite, aerial (planes, unmanned aerial vehicles, etc.), and ground-based (handheld radiometers) (Vélez-Nicolás *et al.,* 2021). They might be gathered by a variety of tools, such as sensors, digital cameras.

The technology of remote sensing has advanced significantly as a result of the deployment of satellites. Sentinel 2, for instance, with a temporal resolution of 5–12 days, spatial resolution of 10–60 meters, and 12 spectral bands encompassing the visible, near-infrared, and short-wave infrared spectrum, can greatly support management in agriculture, especially over the large areas (Zhang *et al.*, 2017; Segarra *et al.,* 2020). On the other hand, unmanned aerial vehicles (UAVs) have experienced a significant increase in use over the past ten years because of their flexibility and cost-effectiveness for getting the high-resolution (cm-scale) photographs required for PA applications (Norasma *et al.*, 2019). However, cloud cover frequently restricts the availability of remote sensing photographs from satellite and aerial platforms, whereas ground-based remote and proximal sensing is much less impacted by this restriction (Mulla, 2013). Ground-based platforms that are most often used in precision agriculture can be categorized into three groups: (i) hand-held, (ii) freestanding in the field, and (iii) installed on tractors or other farm equipment. Since ground-based platforms are situated much closer to the target surface (a land surface or plant) than aerial or satellite-based ones, they are also known as proximal remote sensing systems (Ferguson and Rundquist, 2018). The attached sensors vary based on their spatial, spectral, radiometric, and temporal resolution (Sishodia *et al.,* 2020).

2.3. Spectral reflectance and vegetation indices

By definition, remote sensing refers to theory technology that allows the identification, measurement and analysis of objects of interest without physical contact (Campbell and Wynne, 2011). Remote

sensing measures the amount of energy that is emitted from any surface. Electromagnetic waves are considered to be the transmitters of detection information.

For each wavelength in the visible (400-750 nm), near-infrared (750-1200 nm), and shortwave infrared (1200-2400 nm) spectral regions, the ratio of the intensity of reflected light to the intensity of the irradiated light is used to characterize the object spectral signature (Li et al., 2014). The percentage of irradiated light that is reflected by vegetation is known as reflectance. The crop spectral reflectance is affected by the properties of pigments, leaf physiological structure, and leaf water content (Reddy *et al.*, 2001). In the visible range, the canopy has low reflectivity because of the significant absorption by photoactive pigments (chlorophylls, anthocyanins, and carotenoids). When compared to the blue, yellow, and red-light bands, which are absorbed by photoactive pigments, the green light band (550 nm), which is reflected rather efficiently, gives the leaves their green color.

In healthy environment, the canopy displays a high reflectivity in the near-infrared wavebands (760-900 nm) as a result of repeated scattering at the air-cell interfaces in the interior leaf tissue (Yang *et al.*, 2007). On the contrary, plants responses to stress alter how incident visible and NIR light is absorbed and reflected (Karteer and Knapp, 2001). The sharp rise in reflectance between the red and NIR regions is identified as the red-edge position (Tarpley et al., 2000). Moreover, healthy leaves show poor reflectance in a wide range of shortwave infrared wavelengths due to absorption by water, proteins, and other carbon components. Likewise, plants emit radiation in thermal infrared band (≈10 μm) according to their temperature. The fluctuation in spectral reflectance provides highly reliable information of crop status.

Numerous vegetation indices (VIs) have been developed using different bands of the spectrum. These indices provide important information about plant structure and growth conditions. In most cases, the index is a sum, difference, ratio, or other linear combination of reflectance or radiance from two or more wavelength intervals (Wiegand *et al.,* 1991). The broadband wavelength-based VIs are largely used in many studies. They were reported as indices suitable to detect nutrient deficiencies, as they are strongly correlated to Leaf Area Index (LAI) modifications and senescence (Broge and Leblanc, 2001). Another group of vegetation indices is narrow-band VIs, the combination of narrow (<10 nm) bands. In particular, those based on red-edge position are strongly related to leaf chlorophyll content changes (Raper and Varco, 2015). A third group is given by the water band indices, that use the reflectance based on NIR region at 950± 20 nm and provide valuable information about leaf and canopy water content (Sims and Gamon, 2003).

In the following chapters, it will be given more information about previously described and grouped VIs, as well as their relationships with other important bio-physiological parameters.

2.4. References

Klein H. S. and Luna F. V. (2022). The Impact of the Rise of Modern Maize Production in Brazil and Argentina. Historia agraria: Revista de agricultura e historia rural, (86), 273-310.

Finke C., Möller K., Schlink S., Gerowitt B. and Isselstein J. (1999). The environmental impact of maize cultivation in the European Union: Practical options for the improvement of the environmental impact: case study Germany. Forschungs-und Studienzentrum Landwirtschaft und Umwelt in Zusammenarbeit mit der Abteilung Futterbau und Grünlandwirtschaft des Institutes für Pflanzenbau und Pflanzenzüchtung, Georg-August Universität Göttingen.

Alqudah A. M., Samarah N. H. and Mullen R. E. (2011). Drought stress effect on crop pollination, seed set, yield and quality. In Alternative farming systems, biotechnology, drought stress and ecological fertilisation (pp. 193-213). Springer, Dordrecht.

Lu Y., Xu J., Yuan Z., Hao Z., Xie C., Li X. and Xu Y. (2012). Comparative LD mapping using single SNPs and haplotypes identifies QTL for plant height and biomass as secondary traits of drought tolerance in maize. Molecular Breeding, 30(1), 407-418.

Butts-Wilmsmeyer C. J., Seebauer J. R., Singleton L. and Below F. E. (2019). Weather during key growth stages explains grain quality and yield of maize. Agronomy, 9(1), 16.

Da Ge T., Sui F. G., Nie S. A., Sun N. B., Xiao H. A. and Tong C. L. (2010). Differential responses of yield and selected nutritional compositions to drought stress in summer maize grains. Journal of plant nutrition, 33(12), 1811-1818.

Monneveux P, Zaidi PH, Sanchez C (2005) Population density and low nitrogen affects yield-associated traits in tropical maize. Crop Sci 45:535–545

Thompson L. J., Ferguson R. B., Kitchen N., Frazen D. W., Mamo M., Yang H. and Schepers J. S. (2015). Model and sensor-based recommendation approaches for in-season nitrogen management in corn. Agronomy JouCorrendo, A. A., Rotundo, J. L., Tremblay, N., Archontoulis, S., Coulter, J. A., Ruiz-Diaz, D., ... & Ciampitti, I. A. (2021). Assessing the uncertainty of maize yield without nitrogen fertilization. Field Crops Research, 260, 107985.rnal, 107(6), 2020-2030.

Piscitelli L., Colovic M., Aly A., Hamze M., Todorovic M., Cantore V. and Albrizio R. (2021). Adaptive Agricultural Strategies for Facing Water Deficit in Sweet Maize Production: A Case Study of a Semi-Arid Mediterranean Region. Water, 13(22), 3285.

Pinter Jr P. J., Hatfield J. L., Schepers J. S., Barnes E. M., Moran M. S., Daughtry C. S. and Upchurch D. R. (2003). Remote sensing for crop management. Photogrammetric Engineering & Remote Sensing, 69(6), 647-664.

Gabriel J. L., Zarco-Tejada P. J., López-Herrera P. J., Pérez-Martín E., Alonso-Ayuso M. and Quemada M. (2017). Airborne and ground level sensors for monitoring nitrogen status in a maize crop. Biosystems Engineering, 160, 124-133.

Hedley C. B., Yule I. J., Tuohy M. P. and Kusumo B. H. (2010). Proximal sensing methods for mapping soil water status in an irrigated maize field. In Proximal Soil Sensing (pp. 375-385). Springer, Dordrecht.

Alvino F. C., Aleman C. C., Filgueiras R., Althoff D. and da Cunha F. F. (2020). Vegetation indices for irrigated corn monitoring. Engenharia Agrícola, 40, 322-333.

Ndlovu H. S., Odindi J., Sibanda M., Mutanga O., Clulow A., Chimonyo V. G. and Mabhaudhi T. (2021). A comparative estimation of maize leaf water content using machine learning techniques and unmanned aerial vehicle (UAV)-based proximal and remotely sensed data. Remote Sensing, 13(20), 4091.

Spišić J., Šimić D., Balen J., Jambrović A. and Galić V. (2022). Machine Learning in the Analysis of Multispectral Reads in Maize Canopies Responding to Increased Temperatures and Water Deficit. Remote Sensing, 14(11), 2596.

Wen P., Shi Z., Li A., Ning F., Zhang Y., Wang R. and Li J. (2021). Estimation of the vertically integrated leaf nitrogen content in maize using canopy hyperspectral red edge parameters. Precision Agriculture, 22(3), 984-1005.

Paiao G. D., Fernández F. G., Spackman J. A., Kaiser D. E. and Weisberg S. (2020). Ground-based optical canopy sensing technologies for corn–nitrogen management in the Upper Midwest. Agronomy Journal, 112(4), 2998-3011.

Kizilgeci F., Yildirim M., Islam M. S., Ratnasekera D., Iqbal M. A. and Sabagh A. E. (2021). Normalized difference vegetation index and chlorophyll content for precision nitrogen management in durum wheat cultivars under semi-arid conditions. Sustainability, 13(7), 3725.

Meng R., Lv Z., Yan J., Chen G., Zhao F., Zeng L. and Xu B. (2020). Development of spectral disease indices for southern corn rust detection and severity classification. Remote Sensing, 12(19), 3233.

Furuya D. E. G., Ma L., Pinheiro M. M. F., Gomes F. D. G., Gonçalvez W. N., Junior J. M. and de Castro Jorge L. A. (2021). Prediction of insect-herbivory-damage and insect-type attack in maize plants using hyperspectral data. International Journal of Applied Earth Observation and Geoinformation, 105, 102608.

Gitelson A. A., Arkebauer T. J. and Suyker A. E. (2018). Convergence of daily light use efficiency in irrigated and rainfed C3 and C4 crops. Remote sensing of environment, 217, 30-37.

Liu G., Yang Y., Liu W., Guo X., Xie R., Ming B. and Li S. (2022). Optimized canopy structure improves maize grain yield and resource use efficiency. Food and Energy Security, e375.

Kim H. (2021). Quantifying plant physiological responses to drought and high-temperature stress in the Midwest US: Through scaling from proximal hyperspectral sensing to satellite monitoring (Doctoral dissertation, University of Illinois at Urbana-Champaign).

Delgado JA, Short NM Jr, Roberts DP, Vandenberg B (2019) Big data analysis for sustainable agriculture on a geospatial cloud framework. Front Sustain Food Syst 3:54.

Mulla D. J. (2013). Twenty five years of remote sensing in precision agriculture: Key advances and remaining knowledge gaps. Biosystems engineering, 114(4), 358-371.

Metternicht G. (2018). Land use and spatial planning: Enabling sustainable management of land resources. Springer.

Lechner A. M., Foody, G. M., & Boyd, D. S. (2020). Applications in remote sensing to forest ecology and management. One Earth, 2(5), 405-412.

Vélez-Nicolás M., García-López, S., Barbero, L., Ruiz-Ortiz, V., & Sánchez-Bellón, Á. (2021). Applications of unmanned aerial systems (UASs) in hydrology: A review. Remote Sensing, 13(7), 1359.

Zhang T., Su J., Liu C., Chen, W. H., Liu, H., & Liu, G. (2017, September). Band selection in Sentinel-2 satellite for agriculture applications. In 2017 23rd international conference on automation and computing (ICAC) (pp. 1-6). IEEE.

Segarra J., Buchaillot M. L., Araus J. L. and Kefauver S. C. (2020). Remote sensing for precision agriculture: Sentinel-2 improved features and applications. Agronomy, 10(5), 641.

Norasma C. Y. N., Fadzilah M. A., Roslin N. A., Zanariah Z. W. N., Tarmidi Z. and Candra F. S. (2019, April). Unmanned aerial vehicle applications in agriculture. In IOP Conference Series: Materials Science and Engineering (Vol. 506, No. 1, p. 012063). IOP Publishing.

Ferguson R. and Rundquist D. (2018). Remote sensing for site-specific crop management. Precision agriculture basics, 103-117.

Sishodia R. P., Ray R. L. and Singh S. K. (2020). Applications of remote sensing in precision agriculture: A review. Remote Sensing, 12(19), 3136.

Campbell J. B. and Wynne R. H. (2011). Introduction to remote sensing. Guilford Press.

Li M., Zang S., Zhang B., Li S. and Wu C. (2014). A review of remote sensing image classification techniques: The role of spatio-contextual information. European Journal of Remote Sensing, 47(1), 389-411.

Reddy G. S., Rao C. N., Venkataratnam L. and Rao P. K. (2001). Influence of plant pigments on spectral reflectance of maize, groundnut and soybean grown in semi-arid environments. International Journal of Remote Sensing, 22(17), 3373-3380.

Yang C., Everitt J. H. and Bradford J. M. (2007). Airborne hyperspectral imagery and linear spectral unmixing for mapping variation in crop yield. Precision Agriculture, 8(6), 279-296.

Carter G. A. and Knapp A. K. (2001). Leaf optical properties in higher plants: linking spectral characteristics to stress and chlorophyll concentration. American journal of botany, 88(4), 677-684.

Tarpley L., Reddy K. R. and Sassenrath-Cole G. F. (2000). Reflectance indices with precision and accuracy in predicting cotton leaf nitrogen concentration. Crop science, 40(6), 1814-1819.

Wiegand C. L., Richardson A. J., Escobar D. E. and Gerbermann A. H. (1991). Vegetation indices in crop assessments. Remote sensing of Environment, 35(2-3), 105-119.

Broge N. H. and Leblanc E. (2001). Comparing prediction power and stability of broadband and hyperspectral vegetation indices for estimation of green leaf area index and canopy chlorophyll density. Remote sensing of environment, 76(2), 156-172.

Raper T. B. and Varco J. J. (2015). Canopy-scale wavelength and vegetative index sensitivities to cotton growth parameters and nitrogen status. Precision Agriculture, 16(1), 62-76.

Sims D. A. and Gamon J. A. (2003). Estimation of vegetation water content and photosynthetic tissue area from spectral reflectance: a comparison of indices based on liquid water and chlorophyll absorption features. Remote sensing of environment, 84(4), 526-537.

Chapter 3

Results and Discussions

3.1. Characterization of soil spatial variability in the experimental site by using proximal EMI sensor

3.1.1. Introduction

Proximal, as well as other remote sensing techniques, offers an advanced array of methods for obtaining soil property information and determining soil variability for precision agriculture (Saifuzzaman et al., 2019). Lukas et al. (2011) reported that remote sensing may identify any changes in soil variability that affects crop growth. Numerous types of research have shown a high potential of remote sensing for monitoring spatial soil variability, with high resolution and performance (Thompson et al., 2004; Adamchuk et al., 2011; Mulder et al., 2011, 2013). Likewise, many on-the-go soil-sensing instruments (Adamchuk et al., 2004) offer a great chance of studying spatial variability of measured parameters (e.g. electrical resistivity/conductivity, optical reflectance, mechanical resistance, etc.) allowing to identify homogeneous within-field areas. Among many proximal sensors for soil properties monitoring, electromagnetic induction (EMI) sensors are used for measuring apparent electrical conductivity (ECa) (De Benedetto et al., 2013). In-situ measurement of electrical conductivity has caused considerable interest as a potential technique in many soil applications; in particular, it has received substantial attention from precision agriculture (Corwin and Lesch, 2005). The ability to use on-the-go EMI sensors and map soil ECa at high resolution can support site-specific management (Hossain, 2008).

3.1.2. Materials and methods

3.1.2.1. Electromagnetic induction (EMI) measurements

Electromagnetic induction (EMI) sensors are used to measure apparent electrical conductivity (ECa) in agricultural soils. For the purpose of this study, CMD Mini-Explorer (GF instruments), which measures ECa in mS m^{-1}, has been used (Fig.1 left). The CMD Mini-Explorer probe is 1.275m long, 0.05m in diameter and weighs 1.8 kg.

The Mini-Explorer is a low-frequency EM sensor and operates at 30 kHz; it has three receivers (Rx) coils (spaced 0.32 m, 0.71 m and 1.18 m from the transmitter (Tx) coil) and two coil arrangements; a

horizontal coplanar (HCP) configuration (in the vertical dipole orientation or the 'full depth' range) and, when the instrument is rotated through 90°, a vertical coplanar (VCP) configuration (in the horizontal coil dipole orientation or the 'half depth' range) (Bonsall et al., 2013).

Specifically, the manufacturer indicates that the instrument has an effective depth range of 0.25 m, 0.5m and 0.9m for VCP in the horizontal coil dipole orientation (half depth range); this is extended to 0.5 m, 1.0m and 1.8m by rotating the orientation of the Tx/Rx coils by 90° to use HCP in the vertical coil dipole orientation (full depth range).

As the CMD Mini-Explorer must be used in either the full depth (HCP, vertical dipole orientation) or the half depth (VCP, horizontal dipole orientation) mode, two surveys 'sweeps' are required over a given area if depth data from both dipole orientations are desired. The probe is used in conjunction with a control unit, which is usually connected via Bluetooth (which operates in the GHz band and does not impact the 30 kHz operating frequency of the EM sensor). The Bluetooth connection allows for either a pedestrian hand-held survey or a GPS-enabled sledge/cart-mounted survey if required. The instrument can be set up efficiently within 3 minutes. Internal temperature compensation automatically provides absolute calibration of apparent conductivity data prior to each line or profile of data collected, which limits drift across the dataset. The sensor can be held comfortably in one hand at the optimum probe height of approximately 0.05m above the ground in order to ensure maximum depth of penetration. The probe height can be adjusted using a telescopic handle when encountering sites of variable terrain or vegetation cover (Bonsall et al., 2013).

3.1.2.2. Soil morphology

Brief morphological analysis (identification of genetic horizons) of soil cores has been performed by the use of augers (20 cm core length). Soil samples were collected for each 20 cm soil depth interval (0-20; 20-40; 40-60; 60-80 cm), (Fig. 1-right).

Figure 1. Apparent electrical conductivity (ECa) measurements using CMD Mini Explorer (left) and soil sampling (right)

3.1.3. Results and discussion

3.1.3.1. Electrical conductivity

In order to characterize the soil spatial variability of the experimental site, a geophysical survey was carried out using an electromagnetic induction (EMI) sensor (CMD Mini-Explorer) on 23rd January 2020.

EMI data were collected both at full depth (vertical coil dipole orientation by using horizontal coplanar configuration, HCP) and at half depth (horizontal coil dipole orientation by using vertical coplanar configuration, VCP) mode. After data pre-treatment and processing, maps of apparent electrical conductivity (ECa, mS m^{-1}) for different soil layers were produced using the Surfer software. In particular, measurements taken in the vertical coil dipole orientation provided a survey of ECa at depths of 50, 100 and 180 cm, whereas measurements taken in the horizontal coil dipole orientation provided a survey of ECa at 25, 50 and 90 cm.

In Figure 2 and Figure 3, the ECa maps obtained by measurements taken in vertical and horizontal coil dipole orientation, respectively, are reported. From a visual inspection of the maps, a greater heterogeneity was observed in the upper soil layers (25 cm and 50 cm); in addition, the right side and the southern corner of the experimental field showed on average higher values of apparent electrical conductivity.

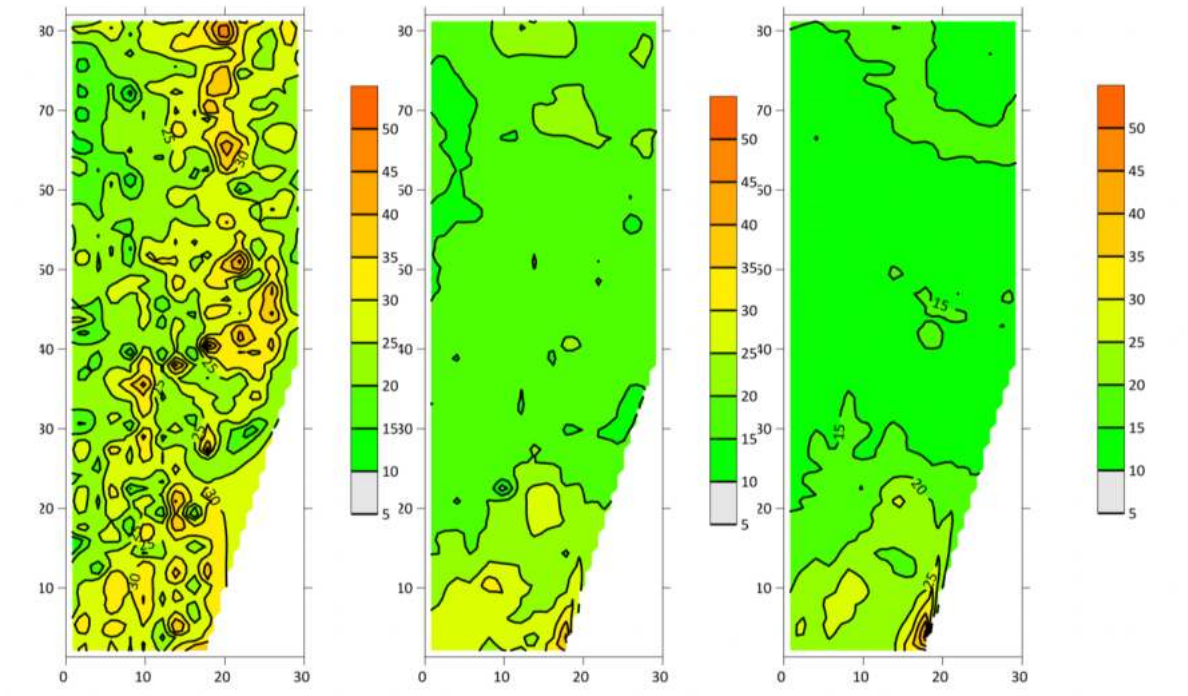

Figure 2. ECa maps obtained by measurements taken in vertical coil dipole orientation showing depths of 50, 100 and 180 cm. In the legend, ECa values (mS m^{-1}) are reported.

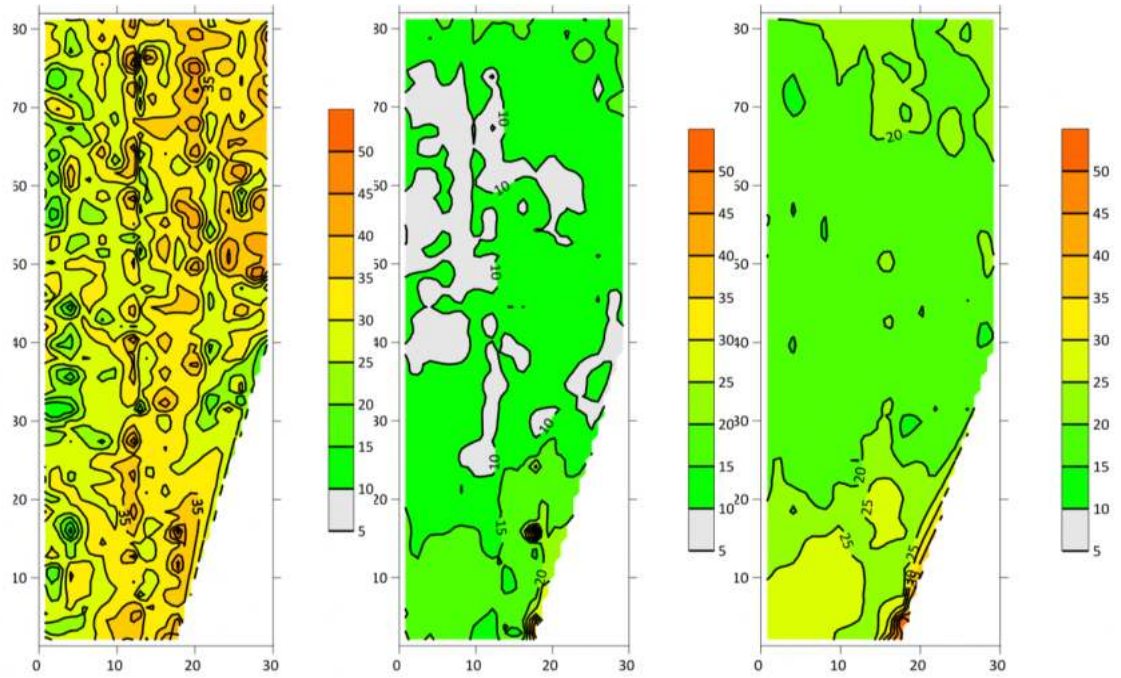

Figure 3. ECa maps obtained by measurements taken in horizontal coil dipole orientation showing depths of 25, 50 and 90 cm. In the legend, ECa values (mS m^{-1}) are reported.

Differences in apparent electrical conductivity can be related to variations in chemical and physical soil properties, such as soil water content, texture, salinity, and porosity. Therefore, in order to understand the causes of the observed variability, two soil transects were identified in the experimental site and nine soil cores were collected at distances of 6 m, as shown in Figure 4. The spatial variation from lower (green in the figure) towards higher apparent electrical conductivity corresponds to (i) the occurrence of Bt soil horizons (thus clay illuviated horizons) (ii) redder subsoil and (iii) an increase (although not always consistent) of soil depth. Consequently, on some soil core samplings, ECe, pH, texture and calcareous content was determined in the lab.

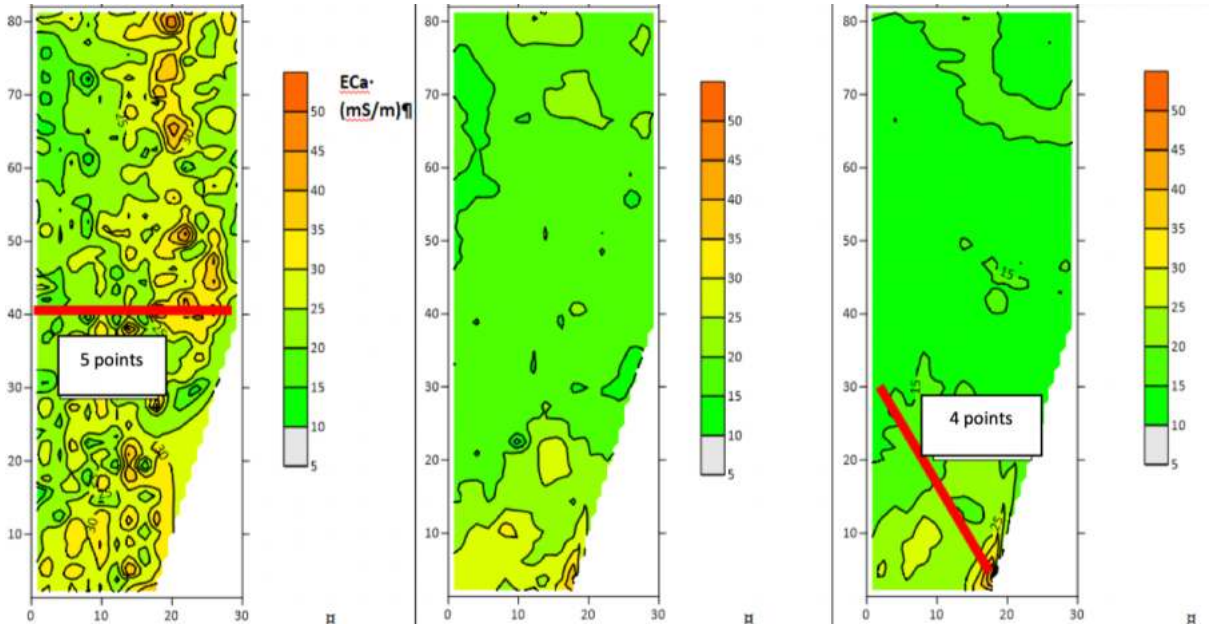

Figure 4. Soil sampling scheme with location of soil transects and number of sampling points.

3.1.3.2. Soil characterization to define the experimental design

The analysis of the soil samples, collected along the areas showing the maximum variation of the electromagnetic induction, indicated that all soils showed a texture varying from silty-clayey loam to silty (USDA), a sub-alkaline pH with moderate (5%) to high (10%) contents of calcium carbonate. Moreover, the areas having low electromagnetic induction values (ECa<20 mS m^{-1}) had shallow soils (50-60 cm) while those areas having higher electromagnetic induction values (e.g. ECa> 35 mS m^{-1}\) had deeper soils (up to 70-80 cm). Most interestingly these deeper soils showed the presence of an argillic horizon (Bt), that is a subsoil horizon characterized by clayey illuviation.

These results, therefore, confirm an interesting correlation between electromagnetic induction values and soil morphology, with deeper and more fertile soils in areas with higher electromagnetic induction values. These results also highlight the great potential of using proximal geophysical sensors to better guide experimental agronomic trials.

Then, further data analysis was performed to define the experimental design. To this aim, the information deriving from proximal electromagnetic induction sensor data, and from plant growth and yield recorded in previous years in the experimental site, were considered. The objective of this analysis was to identify within-field homogeneous portions in order to allocate the blocks of the experimental design. The EMI data collected at full depth, with vertical coil dipole orientation, which provided a survey of apparent electrical conductivity (ECa) at depths of 50 cm, 100 cm and 180 cm, were used in this analysis.

Data analysis was carried out according to the following procedure. Each dataset was firstly rasterized and then all three rasters were stacked into a single raster. Before applying the clustering procedure on the merged raster, the silhouette method was used with the aim of estimating the best-suited number of clusters. In fact, the (spatial) clustering procedure is intrinsically unable to estimate the right number of clusters underlying the spatial dataset; on the contrary, after the user provided a number of clusters, the cluster analysis segments the overall area into the best-suited sub-areas according to the number assessed by the silhouette method (Rousseeuw, 1987).

The clustering method applied was the multivariate k-means (MacQueen, 1967). K-means clustering is a method of vector quantization that aims to partition n observations into k clusters in which each observation belongs to the cluster with the nearest mean (cluster centers or cluster centroid). K-means clustering minimizes within-cluster variances (squared Euclidean distances) and maximizes variances between clusters. All the computations were carried out within the R environment (RStudio Team, 2020; R Core Team, 2013) including the graphic representation section.

Results of cluster analysis are reported in Figure 5 and in Table 1, where the mean values of ECa (mS m^{-1}) for the three clusters per each soil depth considered are reported.

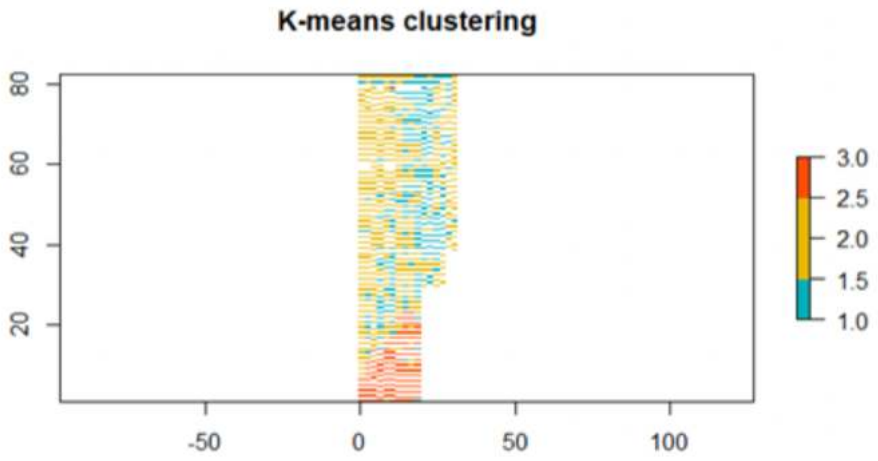

Figure 5. Maps of the three clusters identified in the experimental site using proximal EMI sensor data.

Table 1. Mean values of ECa (mS m^{-1}) for the three clusters per each soil depth considered

Cluster	X50cm	X100cm	X180cm
1	31.38983	18.59021	14.43719
2	20.92742	16.95180	13.63745
3	29.36374	26.23983	23.98930

By a visual inspection of the map, the distribution of the three clusters seemed to resemble the main sources of variability observed for ECa in the shallower soil layer, which was characterized by the

greatest heterogeneity, with the right side and the southern corner of the experimental field showing on average the highest values.

The main distinguishing behaviour was represented by the cluster "3" in the southern corner which showed the highest ECa values in all the three soil layers (Table 1); the other two clusters tended to show instead a greater overlapping.

For this reason, and considering also the increasing trend of productivity moving from the northern to the southern portion of the field recorded in the previous years on the experimental field, the experimental area was divided into three transversal blocks (Fig.6). Afterwards, within the blocks, the treatments were allocated according to a hierarchical split-plot experimental design with water regime as the main plot factor and N as the sub plot factor (Fig.6).

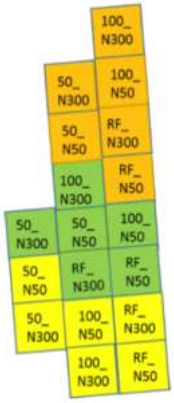

Figure 6. Layout of the experimental design.

3.1.4. Conclusion

Electromagnetic induction (EMI) was used to measure apparent electrical conductivity, as it is one of the most efficient and non-invasive proximal sensors for soil characteristics monitoring. The obtained spatial variation from lower to higher apparent electrical conductivity may correspond to the occurrence of clay illuviated horizons, redder subsoil and/or an increase of soil depth. However, in order to understand the causes of the observed variability, the soil samples in certain soil transects is necessary. Our results highlighted the great potential of using proximal geophysical sensors to better guide experimental agronomic trials since an interesting correlation between electromagnetic induction values and soil morphology was found. Nevertheless, in order to define the experimental site, a part of the information deriving from proximal electromagnetic induction sensor data, plant growth and yield recorded in previous years in the experimental site, must be considered.

3.1.5. References

Saifuzzaman M., Adamchuk V., Buelvas R., Biswas A., Prasher S., Rabe N. and Ji W. (2019). Clustering Tools for Integration of Satellite Remote Sensing Imagery and Proximal Soil Sensing Data. Remote Sensing, 11(9), 1036.

Lukas V., Neudert L. and Křen J. (2011). Mapování variability půdy a porostů v precizním zemědělství. Brno: Mendelova univerzita v Brně.

Thompson A. N., Shaw J. N., Mask P. L., Touchton J. T. and Rickman D. (2004). Soil sampling techniques for Alabama, USA grain fields. Precision Agriculture, 5(4), 345-358.

Adamchuk V. I., Rossel R. A. V., Marx D. B. and Samal A. K. (2011). Using targeted sampling to process multivariate soil sensing data. Geoderma, 163(1-2), 63-73.

Mulder V. L., de Bruin S. and Schaepman M. E. (2013). Representing major soil variability at regional scale by constrained Latin Hypercube Sampling of remote sensing data. International Journal of Applied Earth Observation and Geoinformation, 21, 301-310.

Mulder V. L., De Bruin S., Schaepman M. E. and Mayr, T. R. (2011). The use of remote sensing in soil and terrain mapping—A review. Geoderma, 162(1-2), 1-19.

Adamchuk V. I., Hummel J. W., Morgan M. T. and Upadhyaya S. K. (2004). On-the-go soil sensors for precision agriculture. Computers and electronics in agriculture, 44(1), 71-91.

De Benedetto D., Castrignano A., Diacono M., Rinaldi M., Ruggieri S. And Tamborrino R. (2013). Field partition by proximal and remote sensing data fusion. Biosystems engineering, 114(4), 372-383.

Corwin D. L. and Lesch S. M. (2005). Characterizing soil spatial variability with apparent soil electrical conductivity: I. Survey protocols. Computers and electronics.

Hossain B., Frazier P. and Lamb D. (2008). EM38 for measuring and mapping soil moisture in a cracking clay soil.

Bonsall J., Fry R., Gaffney C., Armit I., Beck A. and Gaffney V. (2013). Assessment of the CMD Mini-Explorer, a new low-frequency multi-coil electromagnetic device, for archaeological investigations. Archaeologica Prospection, 20(3), 219-231.

Rousseuw P. and Vanzomeren B. (1987). Identification of multivariate outliers and leverage points by means of robust covariance matrices.

MacQueen J. (1967). Some methods for classification and analysis of multivariate observations. In Proceedings of the fifth Berkeley symposium on mathematical statistics and probability (Vol. 1, No. 14, pp. 281-297).

3.2. Selection of Hyperspectral Vegetation Indices for Monitoring Yield and Physiological Response in Sweet Maize under Different Water and Nitrogen Availability

This chapter has been adapted from a previously published paper:
Sellami, M. H., Albrizio, R., Čolović, M., Hamze, M., Cantore, V., Todorovic, M., Piscitelli, L & Stellacci, A. M. (2022). Selection of Hyperspectral Vegetation Indices for Monitoring Yield and Physiological Response in Sweet Maize under Different Water and Nitrogen Availability. Agronomy, 12(2), 489.

Abstract:
This study used hyperspectral reflectance data to evaluate the crop physiological parameters of sweet maize. Principal component analysis (PCA) was applied to identify the wavelengths that primarily contributed to each selected PC. Correlation analysis and multiple linear regression, with a stepwise algorithm, were used to select the best-performing vegetation indices (VIs) for monitoring the yield and physiological response of sweet maize grown under different water and nitrogen availability. The spectral reflectance measurements of crops were taken during the mid-season stage, for two consecutive growing seasons. The multivariate regression results showed that red-edge group indices, such as CARI (Chlorophyll Absorption Reflectance Index), DD (Double Difference Index), REIP (Red-Edge Inflection Point), and Clred-edge (Chlorophyll Red-Edge) indices were good predictors of yield and physiological parameters, confirming the crucial role of the red-edge spectral region that also emerged through PCA. Moreover, DD, REIP, and Clred-edge VIs were able to discriminate transient temporary stress at the mid-season stage, as well as to separate water and N stress levels. Therefore, hyperspectral reflectance VIs can provide valid information to growers, helping them identify and discriminate between different stress conditions.

Keywords: hyperspectral proximal sensing; principal component analysis (PCA); multiple linear regression (MLR); variable selection; water and nitrogen deficiency

3.2.1. Introduction

Water and nitrogen (N) represent two major limiting factors for maize production (Li *et al.*, 2020). Water stress acts directly on growth and development, photosynthesis, dry mass production; in addition, yield (Zhang and Zhou, 2019) might be severely diminished, especially if water deficiency is prolonged (Shin *et al.,* 2015). Nitrogen is considered the most crucial nutrient for proper growth

and development, as it is the principal regulator of many physiological and biochemical processes, and is strongly linked to chlorophyll content (Maheswari *et al.*, 2009; Massignam *et al.*, 2009; Leghari *et al.*, 2016;) and quantity of yield (Li *et al.*, 2020). Matching N supply to water availability, both spatially and temporally, is essential to accomplish optimal crop response, offering opportunities for precision agriculture (Tilling *et al*., 2007). In recent years, proximal and remote sensing methods have been widely used as effective tools for precision agriculture, as they allow rapid, non-destructive monitoring of growth, along with both water and nutrient stress (Pinter *et al.*, 2003). These methods can be efficiently utilized to measure vegetation's spectral reflectance, which is related to biophysical and biochemical components (such as chlorophyll, nitrogen content, dry mass production, and water status) (Solari *et al*., 2008; Taghvaeian *et al.,* 2012; Genc *et al.,* 2013; Walsh *et al.,* 2013; DeJonge *et al.*, 2016).

There are numerous biophysical, physiological, and biochemical crop parameters that can be monitored using spectral reflectance data generated by remote/proximal sensing techniques. Timely observation of plant biophysical properties and eco-physiological status, such as leaf area, chlorophyll, and nitrogen contents, have become critical to diagnose plant responses to environmental stress (Zhao *et al.*, 2013; Din *et al.,* 2017).

All environmental stresses, such as water deficit, salinity, and nutrient deficiency, evoke a similar plant response, as they tend to decrease leaf area, and numerous stresses cause stomatal closure. As a result, diagnosing or monitoring the impact of a specific stress based on a single observed response is frequently challenging (Jones and Vaughan, 2010).

The use of spectral signatures can reveal not only the pigment composition of the leaves, but also the leaf area, and even the canopy's water content. In this case, stress responses can be detected and quantified using any or all of these spectral signature properties. However, many of the proposed spectral indices are rather limited in their applicability, because they were developed using empirical regression techniques for one specific experiment and cannot be easily extrapolated to other situations (Jones and Vaughan, 2010). Hence, any spectral index should be thoroughly validated for the specific site conditions (Jones and Vaughan, 2010).

Crops under optimal growing conditions have a very high reflectance in the near-infrared region (NIR, 760–900 nm), high in the green (520–600 nm), and low in blue (450–520 nm) and red (630–690 nm) spectra (Jain *et al.,* 2007), where they absorb almost all of the incident light. Under stress conditions, plants change their absorption of incident light in the visible and NIR ranges (Carter and Knapp, 2001; Mahajan *et al.,* 2014). Therefore, the variation of reflectance in the green and far-red (690–720 nm) spectra provides a particularly standard pigment-related response and provides reliable indications of stress conditions (Carter *et al.,* 2002).

Field spectroradiometers can generate a continuous spectrum for any object (Li et al., 2020) because of their ability to collect spectral signatures in narrow (<10 nm) and contiguous wavelengths in the visible and near-infrared region; thus, they represent effective tools to estimate crop status (Feng *et al.*, 2015), as well as morpho-physiological (Gomez-Casero *et al.*, 2010) and biochemical plant traits at different phenological stages (Stellacci *et al*., 2016).

However, weak spectral information, caused by crop structure characteristics and soil background conditions (Mahajan *et al.*, 2014), as well as information redundancy due to the high degree of correlation of hundreds of neighbouring wavebands (Ye *et al*., 2008), poses a challenge in terms of data analysis and interpretation (Kale *et al*., 2017). For this reason, data pre-processing and analysis are essential to extract crucial information from raw spectral data and estimate crop status efficiently. The main approaches used to analyze hyperspectral data of vegetation are focused on the computation of vegetation indices (VIs), and on exploring the whole reflectance spectrum through multivariate statistical analysis methods. The analysis of the whole spectrum is usually aimed at identifying the narrow bands (optimal bands) able to capture most of the information on crops properties (Thenkabail *et al.,* 2004; Jain *et al.*, 2007; Stellacci *et al.*, 2016). However, it can also be focused on extracting derived variables or factors capable of summarizing spectral information and predicting crop behavior. Principal component analysis (PCA) is the most-applied method among multivariate approaches. PCA is an unsupervised dimensionality-reduction method that is often used to reduce the dimensionality of the multivariate data set, while holding most of the variation within the data (Choi *et al.,* 2004; Kale *et al*., 2017). Several studies on the investigation of hyperspectral plant response showed the effectiveness of PCA in coping with multicollinearity problems occurring along many wavelengths (Kale *et al.*, 2017), and selecting important wavelengths crucial for discriminating the effects of N availability (Jain *et al*., 2007; Stellacci *et al.,* 2012; Stellacci *et al.,* 2016), water regimes (Ray *et al.*, 2010), and plant diseases (Krezhova *et al.,* 2017).

Computation of VIs is among the most studied and widespread methods for crop status estimation from spectral reflectance data (Morcillo-Pallares *et al.,* 2019). The most traditional VIs are those using broadband wavelengths. Among them, the most used are the Normalized Difference Vegetation Index (NDVI, Charlson and Ripley, 1997), which is strictly associated with variation of both leaf area index (LAI) and fractional vegetation cover, and all its alternatives, including the Soil Adjusted Vegetation Index (SAVI, Huete, 1988), the Optimized Soil Adjusted Vegetation Index (OSAVI, Rondeaux *et al*., 1996), and the Enhanced Vegetation Index (EVI, Huete *et al.*, 2002). The last ones (SAVI, OSAVI and EVI) have been used to overcome the main constraints given by the disturbance of soil or background reflectance. The Green Normalized Difference Vegetation Index (GNDVI,

Gitelson and Merzlyak, 1998) is related to the fraction of active photosynthetic radiation intercepted by crops (Cristiano *et al.*, 2010).

All these indices have an intrinsic aggregated nature; this results in an evident loss of spectral information, which is available when analysing narrow spectral bands (Hansen and Schjoerring, 2003).

When moving from broadband toward hyperspectral sensors, more indices can be calculated; in the last four decades, many VIs, acquired by both ground and remote sensing, have been published (Glenn *et al*., 2008). Recently, Morcillo-Pallarés et al. classified VIs on the basis of their sensitivity towards (i) LAI, (ii) leaf chlorophyll content, and (iii) leaf water content. The broadband VIs belong mainly to the first group, strongly correlated to LAI modifications and senescence. In the second category are VIs such as the Transformed Chlorophyll Absorption in Reflectance Index (TCARI, (Haboudane, 2004), the Cl_{green} and $Cl_{red\text{-}edge}$ chlorophyll indices (Gitelson *et al*., 2003; Gitelson *et al*., 2006), chlorophyll red-edge (Wu *et al.*, 2008), the double difference index (DD), and the double-peak index (DPI, (Main *et al*., 2011). The red-edge position has been found to have an excellent correlation to chlorophyll content, and it is obtained by the point of maximum slope between the red chlorophyll absorption region and the region of high NIR reflectance (Horler *et al*., 1983). The shape and position of the red edge are affected by chlorophyll content modifications, which are always strictly linked to change in leaves structure, and thus strongly influenced by variation in the water and nitrogen status of vegetation (Main *et al*., 2011). In the third group are VIs classified as water indices, such as the Water Band Index (WBI) and the Normalized Water Index (Prasad *et al*., 2007). These indices use the reflectance-based NIR region at 950± 20 nm, where there is a water absorption band and a reference wavelength reflectance at 900 nm. The ratio of these reflectance values can offer a powerful opportunity to assess the water status of vegetation (Peñuelas *et al*., 1997)

Many VIs are designed for a diverse array of applications and research purposes, and often the similarity of acquired information requires the use of rigorous approaches to select the most informative and sensitive indicators for assessing plant status and the onset of stress conditions. Correlation analysis and multiple linear regression (MLR), through a stepwise algorithm, are commonly employed for this purpose.

MLR is a statistical technique that uses several explanatory variables to predict the outcome of a response variable. The goal of MLR is to model the linear relationship between the spectral reflectance bands and crop characteristics (Hayes, 2021). MLR can be used not only to establish relationships between spectral VIs and investigated crop characteristics, but also to select the most informative variables for the estimation of crop properties (Stellacci *et al*., 2016). Previously published studies have reported MLR as a widely used method for rapidly estimating crop leaf N

concentration (Huang *et al*., 2004; Wang *et al*., 2010) and grain yield (Kefauver *et al.,* 2017; Romero *et al.,* 2017;). In detail, Gracia-Romero *et al*. (2017) used correlation analysis and MLR with a forward stepwise method to compare the capability of ground-based and aerially assessed VIs in predicting grain yield and leaf phosphorous content in maize. Kefauver *et al*. (2017) applied a stepwise selection algorithm to compare the capacity of the field and UAV-based RGB and multispectral indices to differentiate the nitrogen-related performance in barley.

In this study, the sensitivity of spectral information, derived by both analysis of the whole spectrum and the computation of VIs, was investigated to describe the physiological and yield response of sweet maize under different water and nitrogen management. To this aim, the factors extracted through PCA and selected VIs were analysed using correlation analysis and MLR with a stepwise algorithm. In the following sections, their performance is assessed and discussed.

3.2.2. Materials and Methods

3.2.2.1. Study Area

Two-year research was conducted at the experimental field of the Mediterranean Agronomic Institute of Bari (IAMB) in Valenzano (41 ◦ 03 ′ N, 16 ◦ 53 ′ E, 77 m above sea level). The experimental site is characterized by typical Mediterranean climate conditions, with mild winters and hot, dry summers. The average annual precipitation is about 550 mm (30 years average), distributed mostly during autumn and winter. The average monthly air temperature ranges from 8◦ C in January to 24◦C in July and August. The soil of the study area is silty-clay-loam. Meteorological data were obtained from the weather station next to the experimental field.

Sweet maize (*Zea mays* var. saccharata L., hybrid Centurion F1) was cultivated in the 2019 and 2020 growing seasons in rows 0.5 m apart, with a distance between plants in the row of 0.2 m and a plant density of 10 plants per square meter.

The crop was grown under three water regimes (WR) in combination with two N levels. Water regimes were: (i) full irrigation (I_{100}), (ii) deficit irrigation (I_{50}), and (iii) rainfed treatment (I_0). Deficit irrigation was obtained by applying 50% of the irrigation requirements, while rainfed treatment was watered only once, immediately after sowing. N levels were: (i) 50 kg ha^{-1} (low level - LN) and (ii) 300 kg ha^{-1} (high level-HN).

Treatments were arranged in a split-plot experimental design, with three replicates, with water regime as a main-plot factor and N as a sub-plot, sized 10 × 10 m.

Irrigation was performed by surface drip method, using a drip line for each row and drippers (2.2 L h^{-1}) spaced 0.20 m apart. Crop water balance and irrigation scheduling were managed using an Excel-

based model (Todorovic, 2006) that estimates day-by-day crop evapotranspiration and irrigation water requirements through the standard procedure proposed by the FAO 56 document. As reported by Piscitelli *et al.* (2021), 8 and 12 irrigations were applied in the first and second year, respectively, with the corresponding seasonal irrigation amounts equal to 281 and 291 mm in I 100 treatments. Half of these amounts were applied in I50 treatments.

In both years and before sowing, fertilizers were applied to the total cropping surface as follows: N, 50 kg ha −1 as urea (46% of N); phosphorus (P_2O_5), 100 kg ha −1 as pyrophosphate (20% P_2O_5); and potassium (K_2O), 200 kg ha^{-1} as potassium sulfate (51% K_2O). At a sixth-leaf stage, N 250 kg ha^{-1}, as urea, was supplied to the HN treatment.

3.2.2.2. Measurements

Leaf gas exchanges, leaf chlorophyll content, and vegetation reflectance measurements were taken at about one-week intervals, 5 times in 2019 (from the end of June to the end of July) and 4 times in 2020 (from mid-July to mid-August), all of them within the mid-season stage. All measurements were acquired on clear sunny days around 11:00–13:00 h (solar time).

3.2.2.2.1. Leaf Gas Exchange

Net photosynthetic CO_2 assimilation rate (A, μ mol m^{-2} s^{-1}), stomatal conductance (gs, mol m^{-2} s^{-1}), and leaf transpiration (Tr, mmol m^{-2} s^{-1}) were measured using a portable open-system gas-exchange analyser (Li-6400XT (Li-Cor Biosciences, Lincoln, NE, USA)) provided by an external bottled CO_2 source supplying 400 μ mol^{-1} CO_2 concentration inside the leaf chamber. The instrument software calculated the various gas-exchange parameters on the basis of the von Caemmerer and Farquhar model. Intrinsic water use efficiency (WUEi, μ mol^{-1}) was calculated as the ratio of net photosynthetic rate to stomatal conductance. Measurements were taken on intact, healthy, green, and well-exposed leaves, over a clipped leaf surface of 6.0 cm^2. Each measurement was replicated three times per plot.

3.2.2.2.2. Leaf Chlorophyll Content

The Chlorophyll Content Index (CCI) of leaves was indirectly measured by means of an optical meter (SPAD-502, Konica Minolta, Osaka, Japan) on 25 replicates per plot.

3.2.2.2.3. Plant Reflectance

Plant reflectance was measured by using a high spectral resolution ASD FieldSpec Hand-Held 2 Spectro-radiometer (Analytical Spectral Devices, Inc., Boulder, CO, USA). This instrument measures reflectance with a wavelength range of 325–1075 nm, an accuracy of ±1 nm, and a resolution of <3

nm at 700 nm. The field of view (FOV) of the bare fiber-optic probe was 25°. The spectrum of a white ($BaSO_4$) reference panel with known reflectance properties was acquired to derive the reflectance of the target.

Measurements were acquired on three plants for each plot. The vegetation spectrum was measured from a distance of 10 cm above the crop, with a spot size of approximately 14 cm^2. Gradually, as maize grew and expanded, the distance from the vegetation increased to 60 cm. Thereafter, data were processed by means of View Spec software.

The reflectance data were restricted to the 395–1004 nm interval, which was considered noise-free. Then, statistical analyses were performed. The reflectance measurements were averaged over 10 nm to reduce collinearity and overfitting (Min and Lee, 2005). In this way, 61 derived reflectance variables were obtained; the name of the variables indicated the central wavelength. The spectral indices used in this study were computed from narrow bands reflectance measurements and are reported in Table 2.

Table 2. Indices are derived from the hyperspectral visible and near-infrared wavelengths.

Acronym	Indices	Equation	Reference
	Broadband Greenness for Structure		
NDVI	Normalized Difference Vegetation Index	(R860 − R650) / (R860 + R650)	Rouse *et al.,*1974
mNDVI	Modified Normalized Difference Vegetation Index	(R775 – R670) / (R775 + R670)	Jurgens,1997
RDVI	Renormalized Difference Vegetation Index	(R800 − R670) / ((R800 + R670)$^{0.5}$)	Roujean and Breon (1995)
SAVI	Soil Adjusted Vegetation Index	(R860 – R650) / (R860 + R650 + L) * (1 + L)	Huete (1988)
		Low vegetation, L = 1, intermediate, 0.5, and high 0.25	
GNDVI	Green Normalized Difference Vegetation Index	(R860 − R550) / (R860 + R550)	Gitelson and Merzlyak (1998)
EVI	Enhanced Vegetation Index	2.5*(R860 – R650) / (R860 + (6*R650) − (7.5*R470) + 1)	Huete et al. (2002)
OSAVI	Optimized Soil Adjusted Vegetation Index	(R860 – R650) / (R860 + R650 + 0.16)	Rondeaux *et al.* (1996)
	Narrowband Greenness for Chlorophyll, Carotenoids, and light use efficiency		
CARI	Chlorophyll Absorption Reflectance Index	[(R700 – R670) – 0.2 × (R700 – R550)]	Kim (1994)
MCARI	Modified Chlorophyll Absorption Reflectance Index	[(R700 – R670) – 0.2 × (R700 – R550)] × (R700/R670)	Daughtry *et al.*(2000)
TCARI	Transformed Chlorophyll Absorption in Reflectance Index	3 × [(R700- R670) – 0.2 × (R700 – R550) × (R700/R670)]	Haboudane *et al.* (2002)
TCARI/OSAVI	Integrated TCARI and OSAVI		Haboudane *et al.* (2002)
Cl_{green}	Chlorophyll Indices	(R730/R530) – 1	Gitelson *et al.* (2003)
$Cl_{red\text{-}edge}$		(R850/R730) - 1	Gitelson *et al.* (2006)
$CI_{rededge710}$	Chlorophyll Red-Edge	(R750/R710) - 1	Wu *et al.,* 2008
DD	Double Difference Index	(R749-R720)- (R701-R672)	Main *et al.,* 2011

DPI	Double Peak Index	$R688+R710/(R697)^2$	Main *et al.,* 2011
PSRI	Plant Senescence Reflectance Index	(R680-R500)/R750	Merzlyak *et al.* (1999)
PRI	Photochemical Reflectance Index	(R531 – R570) / (R531 + R570)	Gamon *et al.* (1992)
SIPI	Structure Insensitive Pigment Index	(R800-R445) / (R800-R680)	Penuelas *et al.*(1995)
REIP	Red-Edge Inflection Point	700+40*[(((R670+R780)/2)-R700) / (R740-R700)]	Vogelmann *et al.,* 1993
NDRE	Normalized Difference Red-Edge	(R790-R720) / (R790+R720)	Barnes *et al.* (2000)
RVSI	Red-Edge Vegetation Stress Index	(R714 + R752)/2 – R733	Merton and Huntington (1999)
Canopy Water Content			
WBI	Water Band Index	R970/R900	Wang *et al.*, 2007
NWI1	Normalized Water Index	(R970 − R900)/(R970 + R900)	Babar *et al.* (2006)
NWI2		(R970 − R850)/(R970 + R850)	
WBI:NDVI		WBI/NDVI	Peñuelas *et al.* (1997)

R represents the reflectance value at specified wavelengths in nm.

3.2.2.2.4. Fresh Grain Yield

Harvesting was completed on 9 August and on 3 September in the first and in the second years, respectively, when grain reached about 30% in dry matter, by sampling 2 m^2 in the middle of each plot. The total weight of the ears was determined after the removal of the bracts. Fresh grain yield is reported in the text as GY.

3.2.2.2.5. Agronomic Water Productivity

Agronomic Water Productivity (WP) was calculated as the ratio of fresh grain yield to the total amount of water supplied (irrigation and rainfall) and expressed as kg m^{-3}.

3.2.2.2.6. Plant Nitrogen Uptake

At maturity, 10 plants per plot were harvested and the fresh weight was measured for the determination of total biomass. The dry plant was ground, and aliquots were weighted in tubes for digestion prior to total N determination through the Kjeldahl method. Plant nitrogen uptake (NUptake) was calculated as the product of N percentage by dry weight.

3.2.2.3. Statistical Analysis

Dependent variables—fresh grain yield (GY), agronomic water productivity (WP), and nitrogen uptake (NUptake)—were preliminarily evaluated for normal distribution and homogeneity of

variance according to the Kolmogorov–Smirnov test and Bartlett's test, respectively. Since the normality assumption was violated, factorial nonparametric analysis of variance for mixed designs was used by applying the Aligned Rank Transform analysis. Analysis of variance from the 3 × 2 factorial experiments in a split-plot design was then conducted, and the significance of differences was tested using Fisher's Least Significant Difference (LSD) at a 5% probability level. This analysis was carried out using the software packages agricolae (De Mendiburu, 2009) and ARTool (Wobbrock et al., 2022) in R studio software (R Core Team). This package is available via the Comprehensive R Archive Network (CRAN, https://cran.r-project.org (accessed on 12 April 2020)).

A multivariate analysis approach was applied to select the optimal spectral bands using XLSTAT 2020 (Addinsoft, New York, NY, USA, (Addinsoft, 2021). Principal component analysis (PCA) was performed on 61 derived variables from the mid-season stage of each growing season. PCA was carried out on the correlation matrix of 61 variables to obtain a few new components, explaining most of the variation of the initial spectral data. PCA outputs included treatment component scores and variable loadings for each selected component.

The Principal Components (PCs) with eigenvalues greater than one, and cumulatively explaining more than 90% of the total variance, were selected for the ordination analysis (Dunteman, 1989); variable loadings were examined to identify the wavelengths that most contributed to each selected component (Matus et al., 1999). Within each extracted component, the five bands with the highest loadings (in absolute value) were selected (Jain *et al,* 2007).

The Pearson correlation was used to determine the relationship between GY, WP, NUptake, physiological parameters (A, gs, Tr, WUEi, and LCC), vegetation indices, and the components extracted using PCA. This analysis was carried out using the software package Corrplot (Friendly, 2002) in R studio software.

The multiple linear regression using the stepwise technique was applied to explain GY, WP, NUptake, and physiological variables variation from VIs across different water supplies and nitrogen treatment on both growing seasons, satisfying the criteria of probability-of F-to-enter ≤ 0.05 and probability-to-remove ≥ 0.05. The overall model's performance was evaluated by its coefficient of determination (R^2), a measure of the proportion of variance in variables estimated that can be predicted by the explanatory variables (VIs). This analysis was carried out using a regression analysis procedure of SAS software (University Edition, SAS Institute, Inc., Cary, NC, USA).

3.2.3. Results

3.2.3.1. Agronomic Water Productivity, Nitrogen Uptake and Yield Response

Table 3 reports the results of the analysis of variance for fresh grain yield (GY), agronomic water productivity (WP), and plant nitrogen uptake (NUptake) for two consecutive growing seasons. The rainfed treatment did not reach the reproductive stage because of strong and prolonged drought. The GY of both growing seasons varied significantly in relation to the amount of available water. In 2020, GY increased as a consequence of N fertilization, but in 2019 this increment only showed a trend towards significance ($p = 0.08$). In both seasons, GY was almost the same in the full irrigation treatment, with the production of about 15 t ha^{-1}. GY was 72.2% and 44.9% less in the I_{50} treatment for the 2019 and 2020 growing seasons, respectively, compared to the full irrigation treatment. In both years, the interaction between water regime and nitrogen level was not significant for GY.

WP was strongly affected by the N level in both growing seasons. By increasing the water supply from I_{50} to I_{100}, WP increased more than double in 2019 and no significant change was observed in 2020. Under a high amount of N, as an average of I_{50} and I_{100} treatments, WP was 28 and 32.5% higher than under a low amount of N, for the 2019 and 2020 growing seasons, respectively.

N uptake was significantly and positively affected by the increase in water and N supply and considerably higher in 2019 than in 2020. A significant interaction was also observed between WR and N levels in both growing seasons.

Table 3. Effects of irrigation regime and nitrogen levels on fresh grain yield (GY), agronomic water productivity (WP) and nitrogen uptake (NUptake) of sweet maize plants grown in 2019 and 2020.

Treatment		GY (t ha^{-1})		WP (kg m^{-3})		NUptake (kg ha^{-1})	
		2019	2020	2019	2020	2019	2020
Water Regime (WR)	**Nitrogen(N)**						
I_0	Low	-	-	-	-	62.81 ± 4.04 d	39.57 ± 2.81 d
	High	-	-	-	-	69.38 ± 8.86 d	52.67 ± 6.4 cd
Average		**-**	**-**	**-**	**-**	***66.09 ± 7.14 b***	***46.12 ± 8.43 b***
I_{50}	Low	2.66 ± 0.95	7.56 ± 0.51	1.03 ± 0.37 c	3.74 ± 0.25	155.38 ± 26.81 c	94.49 ± 15.38 bc
	High	6.20 ± 0.09	9.74 ± 1.64	2.39 ± 0.03 b	4.82 ± 0.81	215.18 ± 16.29 b	195.9 ± 14.23 a
Average		***4.43 ± 2.03 b***	***8.65 ± 1.61 b***	***1.71 ± 0.78 b***	***4.28 ± 0.80***	***185.28 ± 38.29 a***	***145.2 ± 57.1 a***
I_{100}	Low	15.88 ± 0.28	13.33 ± 2.08	3.97 ± 0.07 a	3.84 ± 0.60	159.8 ± 27.76 c	107.76 ± 14.27 b
	High	16.02 ± 1.81	18.09 ± 1.31	4.00 ± 0.45 a	5.21 ± 0.38	280.58 ± 29.52 a	223.04 ± 41.34 a
Average		***15.95 ± 1.16 a***	***15.71 ± 3.04 a***	***3.98 ± 0.29 a***	***4.53 ± 0.87***	***220.19 ± 70.95 a***	***165.4 ± 68.94 a***
Significance							
Water Regime (WR)		*	**	*	ns	**	**
Nitrogen (N)		ns	*	*	**	****	****
WR x N		ns	ns	*	ns	****	**

ns, *, **, and **** denote not significant or significant at $p \leq 0.05$, 0.01, and 0.0001, respectively. Means followed by different letters in each column are significantly different according to the LSD test ($p = 0.05$). Reported values are averages of three replicates.

3.2.3.2. Optimal Spectral Bands

Table 4 shows the results of the principal components analysis carried out on 61 (10 nm) bands. The first two principal components (PCs) were associated with eigenvalues higher than one and explained 97.12 and 97.16% of the total variance in the 2019 and 2020 growing seasons, respectively. The first component was dominated by red-edge and green in 2019, and by red-edge and blue in 2020. The second component was dominated by NIR for both growing seasons.

Table 4. Results of PCA carried out on the 61 (10 nm) bands. For the mid-season phenological stage, the spectral bands with the largest loadings on the selected principal components (PCs) are reported.

Growing season	Percentage of variance explained		Bands centers (nm) with largest PC loadings									
	PC1	PC2	PC1					PC2				
2019	71.49	25.63	530	540	550	720	730	780	790	800	860	870
2020	78.63	18.53	420	430	440	720	730	760	770	780	790	800

3.2.3.3. Optimal Vegetation Indices

Correlations amongst variables were firstly checked using a Person correlation matrix (Fig.7). From this matrix, VIs were checked for correlation with yield, WP, NUptake, and physiological variables (A, gs, WUEi, Tr and LCC). For both growing seasons, the second principal component (F2, summarizing the contribution of NIR wavelengths) showed a strong positive relationship ($r > 0.4$) with all variables, except yield and WP in 2020. The first principal component (F1, summarizing the contribution of red-edge and green in 2019, and blue in 2020) showed a weak negative relationship with LCC in 2019 and a moderate negative relationship with WUEi in 2020.

The water indices (WBI, NWI1, NWI2, and WBI:NDVI) were strongly negatively correlated with NUptake and physiological variables for both growing seasons, except for NWI2 and WBI:NDVI, which were not correlated with LCC in 2020. In addition, in 2019, WBI, NWI1, and WBI:NDVI were strongly negatively correlated with yield and WP, while no significant correlations were observed in 2020.

The chlorophyll indices (Cl_{green}, $Cl_{red\text{-}edge}$, and Clred-edge710), DD, and DPI showed a strong positive relationship with yield, WP, NUptake, and physiological variables for both growing seasons except for: (i) Cl_{green}, which was not correlated with GY and WP in 2020; (ii) $Cl_{red\text{-}edge}$, which was not correlated with WUEi in 2020; and (iii) DPI, which was not correlated to either GY or WP in 2019, nor to GY, gs, Tr, or LCC in 2020.

For broad-band greenness indices (NDVI, RDVI, SAVI, OSAVI, GNDVI, and EVI) there were strong positive relationships with yield, WP, NUptake, and physiological variables for both growing seasons, except for GY and WP, which had no correlations in 2020, except for GNDVI. Also, EVI was not correlated with GY or WP in 2019, or with WUEi in 2020.

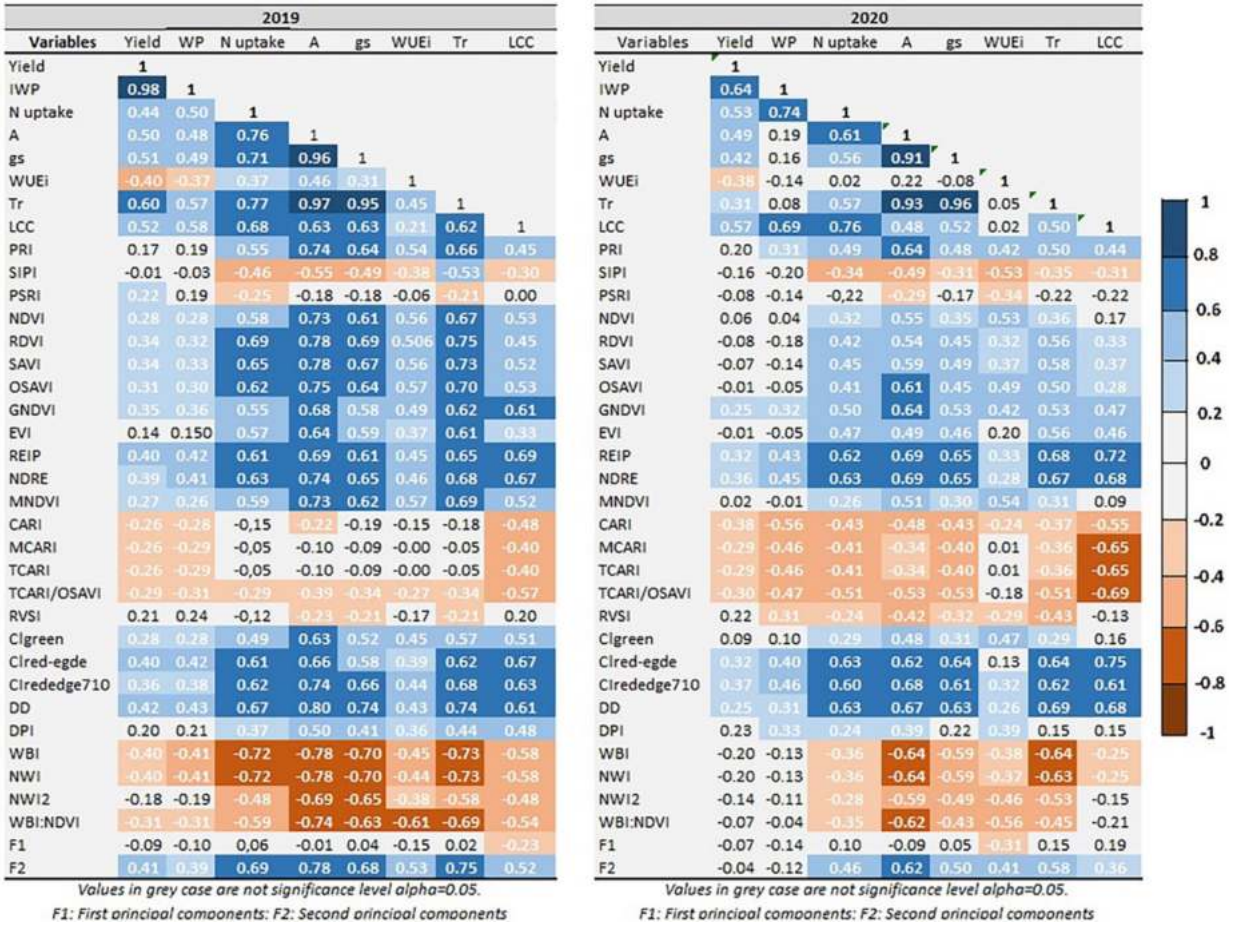

Figure 7. Correlations coefficients among fresh grain yield (GY), agronomic water productivity (WP), nitrogen uptake (NUptake) and physiological variables and vegetation indices for 2019 and 2020 growing season.

Table 5 shows stepwise regression models explaining GY, WP, NUptake and physiological variables variation from VIs across different water supplies and nitrogen levels in 2019 and 2020 growing seasons.

The best VIs explanatory variables to predict GY were DD and CARI indices in 2019 and 2020, respectively. However, the determination coefficients (R^2) of the regression model were low with values of 0.18 in 2019 and 0.14 in 2020. Similar results were obtained for WP; in addition, in 2020 also PSRI was selected, although it explained only a low portion of total variance. In 2019, 57% of the NUptake was explained by DD and water indices (WBI and NWI2), whereas in 2020, 40% of the NUptake was explained by DD index alone.

Among the five vegetation indices (DD, PSRI, OSAVI, MNDVI, RVSI) selected to predict the photosynthesis assimilation (A) in 2019, the DD gave the most accurate estimation of A (R^2 =0.64). In 2020, 54% of A was explained by REIP and WBI indices. In particular, REIP outperformed WBI index in providing an accurate estimation of A (R^2 =0.48).

In 2019, DD index provided a greater explaining capability of conductance (gs) as compared to NWI2, while in 2020, REIP gave more accurate estimation of gs than NWI1 and NWI2 (R^2 =0.42). The best model with two ($Cl_{red\text{-}edge710}$ and WBI: NDVI) and three (REIP, NDRE and WBI:NDVI) indices was selected to predict WUEi in 2019 and 2020 growing season, respectively. The ratio WBI:NDVI provided the most accurate estimation of WUEi with a R^2 of 0.37 and 0.31 in 2019 and 2020, respectively.

In 2019, 60% of Tr was explained by RDVI and NDRE indices with RDVI index giving the most accurate estimation of Tr (R^2 =0.56). On the other hand, DD, WBI and NWI2 were selected to predict Tr in 2020 with DD index explaining 48% of the data variation of Tr.

In 2020, 69% of the total variation in LCC under different N supply and water regimes was explained by PRI, GNDVI, $Cl_{red\text{-}edge}$ and WBI indices, with the chlorophyll index ($Cl_{red\text{-}edge}$) providing the most accurate estimation of the response variable (R^2=0.56). In 2019, 48% of the LCC was explained by REIP index alone.

Table 5. Multivariate regression models explaining fresh grain yield (GY), agronomic water productivity (WP), nitrogen uptake (NUptake), and physiological variables from vegetation indices (VIs) across different water supplies and nitrogen treatment in the 2019 and 2020 growing seasons.

Year	Response variables	VIs	Coefficients	p-value	Portion of variation	Year	Response variables	VIs	Coefficients	p-value	Portion of variation
2019	GY (R^2 = 0.18 R_{adj}^2 = 0.16)	Intercept	-0.500	0.873		2020	GY (R^2 = 0.14 R_{adj}^2 = 0.13)	Intercept	20.104	< 0.0001	
		DD	16.773	0.0008	1			CARI	-94.762	0.0078	1
	WP (R^2 = 0.18 R_{adj}^2 = 0.17)	Intercept	0.559	0.396			WP (R^2 = 0.38 R_{adj}^2 = 0.35)	Intercept	6.849	<.0001	
		DD	3.589	0.0007	1			CARI	-28.119	<.0001	0.32
								PSRI	-25.064	0.047	0.06
	NUptake (R^2 = 0.57 R_{adj}^2 = 0.56)	Intercept	2852.72	<.0001			NUptake (R^2 = 0.40 R_{adj}^2 = 0.39)	Intercept	51.555	<.0001	
		DD	113,25	0.038	0.02			DD	638.45	<.0001	1
		WBI	-3266.25	<.0001	0.52						
		NWI2	1456.42	0.005	0.03						
	A (R^2 = 0.77 R_{adj}^2 = 0.76)	Intercept	-148.048	<.0001			A (R^2 = 0.54 R_{adj}^2 = 0.53)	Intercept	-1493.387	0.0018	
		PSRI	217.972	0.0082	0.02			REIP	2.457	< 0.0001	0.48

	OSAVI	-951.677	<.0001	0.04		WBI	-251.036	0.003	0.06
	MNDVI	928.678	<.0001	0.04					
	RVSI	-132.312	<.0001	0.04					
	DD	100.540	<.0001	0.64					
gs (R^2 = 0.56 R_{adj}^2 = 0.55)	Intercept	-0.435	0.0196		gs (R^2 = 0.51 R_{adj}^2 = 0.49)	Intercept	-12.726	0.0026	
	DD	0.353	<.0001	0.54		REIP	0.018	0.0027	0.42
	NWI2	-1.393	0.0496	0.02		NWI1	-15.460	0.0027	0.05
						NWI2	8.018	0.0173	0.04
WUEi (R^2 = 0.40 R_{adj}^2 = 0.39)	Intercept	650.856	<.0001		WUEi (R^2 = 0.55 R_{adj}^2 = 0.53)	Intercept	-33427	<.0001	
	WBI:NDVI	-393.984	<.0001	0.37		REIP	48.306	<.0001	0.12
	Clred-edge710	-63.419	0.0444	0.03		NDRE	-2702.998	<.0001	0.08
						WBI:NDVI	-338.300	<.0001	0.31
Tr (R^2 = 0.60 R_{adj}^2 = 0.59)	Intercept	-9.712	<.0001		Tr (R^2 = 0.59 R_{adj}^2 = 0.58)	Intercept	185.980	0.0002	
	RDVI	12.230	<.0001	0.56		DD	14.365	0.0004	0.48
	NDRE	12.219	0.0040	0.04		WBI	-186.011	0.0002	0.06
						NWI2	188.534	0.0034	0.05
LCC (R^2 = 0.48 R_{adj}^2 = 0.47)	Intercept	-22399	<.0001		LCC (R^2 = 0.69 R_{adj}^2 = 0.67)	Intercept	-1297.836	0.1258	
	REIP	32.007	<.0001	1		PRI	4227.144	0.0005	0.03
						GNDVI	-1423.275	0.0004	0.03
						Clred-edge	2020.674	<.0001	0.56
						WBI	2036.023	0.0118	0.05

From the results of stepwise regression analysis, the linear regressions showing the highest explaining capability of some physiological variables (net assimilation, stomatal conductance and leaf chlorophyll content) with the VIs are presented in Figure 8.

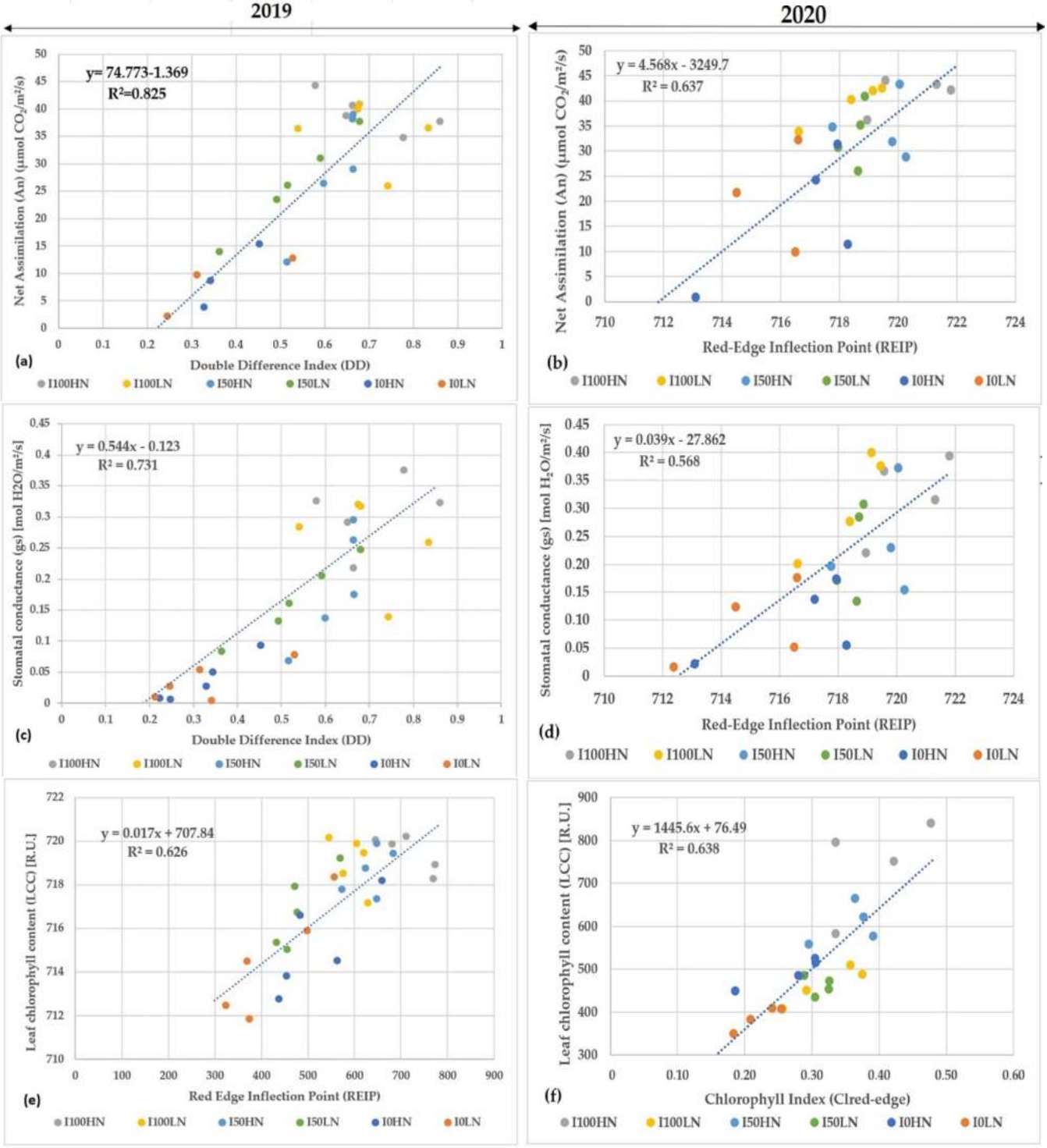

Figure 8. Linear regression parameters between net assimilation (a-b), stomatal conductance (c-d) and Double Difference Index (DD) and Red-edge Inflection Point (REIP), respectively. Linear regression parameters between leaf chlorophyll content (e-f) and Red-edge Inflection Point (REIP), Chlorophyll Index (Clred-edge), respectively. Each value is the mean of three replicates.

3.2.4. Discussion

3.2.4.1. Fresh Grain Yield, Agronomic Water Productivity and Nitrogen Uptake

Water and nitrogen (N) have been recognized as two primary limiting resources for maize production (Raun and Johnson, 1999; Plett et al., 2020). The maximum fresh grain yield values for well-irrigated and fertilized treatments were 16.0 and 18.1 t ha^{-1} in the 2019 and 2020 growing seasons, respectively. As a consequence of severe drought experienced by the crop in both years (seasonal precipitation was 119 and 56 mm in 2019 and 2020, respectively), the rainfed treatment did not reach the reproductive stage, because of either abortion of the floral ovary at the time of pollination, or, even worse, the failure of many silks to emerge from the husks, preventing fertilization. Several other studies (e.g., (Setter *et al.*, 2001; Gustin *et al*., 2018; Song *et al*., 2019)) reported that intense and prolonged water shortage in maize seriously compromises yield due to the lack of pollination.

As an average of the two years, WP ranged from 3.0 kg m^{-3} in I_{50} to 4.26 kg m^{-3} in I_{100} , which means that, under deficit irrigation conditions, less grain was produced per volume of water, compared with well-irrigated conditions. The WP values found in our study are similar to those reported by Kresovic *et al.* (2014) for maize cultivated in Serbia under different irrigation regimes. Similar to our findings, Farré and Faci (2006) reported that the WP of maize decreases with decreasing irrigation volumes in a Mediterranean area.

The highest values of NUptake were obtained in fully irrigated and fertilized regimes, with values of 280.6 kg ha^{-1} and 223.4 kg ha^{-1} in 2019 and 2020, respectively. NUptake in fully irrigated and low fertilized treatment decreased by 43% in 2019 and 51% in 2020. However, values in the I_{50} HN treatment averaged 215.2 kg ha^{-1} in 2019 and 195.9 kg ha^{-1} in 2020, reduced by 28% and 52% in the I_{50} LN treatment, respectively. Hence, our results highlight the importance of N fertilization and optimum water supply, which can facilitate crop N uptake, as irrigation increased N uptake and the ability of maize to efficiently use N from the soil. The results of our study confirm previously reported findings by several authors (Wang *et al*., 2010; Hammad *et al.,* 2016). Plant N uptake is facilitated through optimum irrigation; thus, both nitrogen and water use efficiencies may be simultaneously improved.

3.2.4.2. Spectral Reflectance

The principal component analysis (PCA) was conducted to identify optimal spectral bands for separating different combinations of water and N availability at the mid-season stage of both growing seasons. Reflectance in the green region is controlled by leaf color, whereas the wavebands in coastal blue are related to chlorophyll absorption, which peaks at 430–450 (Min and Lee, 2005). Wavebands

from the red-edge region are the most sensitive to stress-induced changes. The shape of the red-edge region has been shown to be strongly influenced by chlorophyll content, such that an increase in leaf chlorophyll content causes a shift in the red-edge position towards longer wavelengths (Delegido *et al.*, 2013). The red-edge wavelength ranges between 690 and 750 nm; the occurrence of a sharp change in reflectance indicates a transition from chlorophyll absorption to leaf scattering (Clevers *et al.*, 2002). Moreover, the differences in red edge position (up to 10 nm) in many studies were explained as the result of various factors, such as water stress (Ballester *et al.*, 2019; Zhang and Zhou, 2019), nutrient deficiency (Zhao *et al*., 2005), plant disease (Gazala *et al.*, 2013), etc. On the other hand, the internal leaf structure controls the NIR. The separation between coastal blue or green and red-edge, on one side, and NIR on the other side, were reported by several authors on many species (Wang *et al*., 2008; Stellacci *et al*.,2016; Abbasi *et al*., 2019). The difference in spectral behaviour in the visible region could be due to differences in the concentrations of biochemical substances, such as chlorophyll, carotenoid, nitrogen, and water, in the intra- and extracellular leaf structure. Therefore, healthy vegetation can be identified by high NIR reflectance and low visible reflectance, and even more precisely by analysing reflectance in narrow bands. The selection of optimal wavelengths through principal component analysis in our study underlined the separation between visible and NIR reflectance, and the role of red-edge region wavelengths in characterizing the sweet maize response to water and nitrogen stress in both growing seasons.

3.2.4.3. Spectral Indices

Multiple linear regression, with a stepwise algorithm, was used to select the VIs most able to estimate fresh grain yield, physiological variables, water productivity, and N uptake. The poor performance of the stepwise algorithm in selecting VIs for some response variables (GY and WP), also confirmed by the low R^2 and $Radj^2$ values, might be attributed to the high influence of collinearity of the predictors (Grossman *et al.*, 1996). As Strachan et al. (2002) reported, several VIs are needed to detect the stress status and health of maize. Many studies found that red-edge-derived indices outperformed broadband indices (Gupta *et al*., 2013; Putra and Soni, 2017; Imran *et al.,* 2020). However, in our study, broadband indices (NDVI, RDVI, SAVI, OSAVI, GNDVI, and EVI) show strong positive correlations with all investigated variables. This finding is in agreement with previous studies (Jiang *et al.,* 2006; Ranjan *et al*., 2012; Bolton and Freidl, 2013; Ghosh *et al*., 2018). In the multivariate regression results, the red-edge group indices, such as CARI, DD, REIP, and the $Cl_{red\text{-}edge}$ chlorophyll index, were observed to be better predictors, particularly of yield and physiological parameters (A, gs, and LCC) at the midseason stage, when differences among water supplies and nitrogen treatment are mainly related to chlorophyll content. This result confirms the role of the red-edge spectral region

that emerged from the principal component analysis. The DD, REIP, and $Cl_{red\text{-}edge}$ VIs can be used to discriminate temporary stress at the mid-season stage, or separate levels of water and N stress. Generally, these indices are sensitive to small variations of chlorophyll content and are reliable for most species, due to the presence of the red-edge region (Peng and Gitelson, 2013; Clever and Gitelson, 2013; Schlemmer *et al*., 2013). As previously reported, the high sensitivity to chlorophyll content highlights the importance of using red-edge-based VIs to characterize plant N deficiency and N requirement in the mid-season stage of sweet maize. According to Vogelmann *et al.* (1993), the red-edge position is related to environmental, developmental, and genetic factors that result in altered chlorophyll levels, and the red-edge position does not necessarily diagnose one particular type of stress. Here, the shift in red-edge position may be related to changes in the width of the maximum chlorophyll absorption in the red spectral region (Rock *et al.,* 1988), caused by the reduced activity of chlorophyll, and lower photosynthetic capacity as a consequence of low nitrogen supply. In addition, Ramachandiran and Pazhanivelan (2015) reported similar results. A relatively strong negative correlation was found between CARI index and its derivatives (MCARI, TCARI and TCARI/OSAVI) and both yield and physiological parameters (A, gs, and LCC), especially in the 2020 growing season. Zhang et al. showed a similar negative correlation between the MCARI index and leaf chlorophyll content. In addition, at later development stages close to harvest, when structural indices are not responsive to yield variability, the hyperspectral indices related to chlorophyll status (CARI and its derivatives) better reflect within-field yield variability (Zarco-Tejada *et al.,* 2005). Besides that, our results demonstrated a strong positive correlation between chlorophyll indices (Cl_{green}, $Cl_{red\text{-}edge}$ and $Cl_{red\text{-}edge710}$), DD and DPI, and physiological parameters, in agreement with some previous studies (Le Maire *et al*., 2004; Ju *et al*., 2010; Raper and Varco, 2014). This result confirms the critical role and sensitivity of the red-edge region (680–780 nm) to chlorophyll and nitrogen (Wu *et al*., 2008; Li *et al*., 2014; Wang *et al*., 2016).

A negative correlation was found between canopy water VIs and both NUptake and physiological parameters (Fig. 7). Water VIs are described in the literature as effective indicators of water stress and show a strong correlation with physiological variables (Ihuoma and Madramootoo, 2019; Cateregli *et al*., 2020), as was observed in our study. Under short-time water stress, crops adopt photo-protection strategies to prevent damage; however, under prolonged water stress, chlorophyll pigments are affected and changes in leaf optical properties occur (Zhang and Zhou, 2019). Generally, wavelengths between 900 and 1300 nm have strong correlations with leaf water content (Carter, 1991) and are effective predictors, as they can penetrate into canopies better than the rapidly-absorbed higher wavelengths (Sims and Gamon, 2003).

The canopy water content vegetation indices (WBI and WBI:NDVI) use the reflectance at 970 nm to indicate water absorption and a reference wavelength reflectance at 900 nm. This wavelength is used because there is no absorption by water at 900 nm, but it is subjected to the same changes in sample structure as the reading at 970 nm (Ihuoma and Madramootoo, 2017). Several authors show (Danson et al., 1992; Penuelas et al., 1993; Govind et al., 2005) that the WBI is higher in the initial or later stages of a nitrogen-stressed crop. According to Ramachandiran and Pazhanivelan (2015), the plants with high nitrogen status have lower values of WBI, and vice versa.

A decrease in NIR reflectance for stressed plants is mainly due to a decrease in LAI and green biomass (Govind *et al*., 2005), and reduced turgidity of the spongy-mesophyll layer in rainfed crops, compared to the turgidity levels of fully irrigated crops (Ramachandiran and Pazhanivelan, 2015). However, as the degree of absorption at 970 nm rises compared to 900 nm, the water content of plant canopies increases (Penuelas *et al*., 1995). On the contrary, under water-stress conditions, the 970 nm trough of the reflectance spectrum tends to shift towards lower wavelengths.

3.2.5. Conclusions

The results of this study demonstrated that hyperspectral reflectance can be used as a tool to detect the water and nitrogen status of sweet maize, even if no single index can describe the complexity of the eco-physiological behaviour of vegetation. The most effective indices to assess the combined effect of nitrogen and water stress in maize were red-edge-based VIs, such as CARI, DD, REIP, and $Cl_{red\text{-}edge}$ chlorophyll indices. Therefore, the use of spectral data at the mid-season stage could enhance precision agriculture by identifying stress patterns, and aid growers in making good decisions; for instance, allowing supplemental water and nutrient application to mitigate adverse stress effects.

The relationship between the spectral signature and the target variable might be affected by the structural properties of the canopy (i.e., plant size, age, and leaf angle) and physiological status, in response to biotic and abiotic stressors. Thus, in future perspectives, the integrated use of information derived from different sensors could help in discriminating the effects of multiple stresses on crop response.

3.2.6. References

Li, L.; Lin, D.; Wang, J.; Yang, L.; Wang, Y. Multivariate Analysis Models Based on Full Spectra Range and Effective Wavelengths Using Different Transformation Techniques for Rapid Estimation of Leaf Nitrogen Concentration in Winter Wheat. Front. Plant Sci. 2020, 11, 755.

Zhang, F.; Zhou, G. Estimation of vegetation water content using hyperspectral vegetation indices: A comparison of crop water indicators in response to water stress treatments for summer maize. BMC Ecol. 2019, 19, 18.

Shin, S.; Kim, S.G.; Lee, J.S.; Go, T.-H.; Shon, J.; Kang, S.; Lee, J.-S.; Bae, H.H.; Son, B.-Y.; Shim, K.-B.; et al. Impact of the consecutive days of visible wilting on growth and yield during tassel initiation in maize (Zea Mays L.). J. Crop Sci. Biotechnol. 2015, 18, 219–229.

Massignam, A.M.; Chapman, S.C.; Hammer, G.L.; Fukai, S. Physiological determinants of maize and sunflower grain yield as affected by nitrogen supply. Field Crops Res. 2009, 113, 256–267.

Leghari, S.J.; Wahocho, N.A.; Laghari, G.M.; HafeezLaghari, A.; MustafaBhabhan, G.; HussainTalpur, K.; Lashari, A.A. Role of nitrogen for plant growth and development: A review. Adv. Environ. Biol. 2016, 10, 209–219.

Maheswari, M.; Murthy, A.N.G.; Shanker, A.K. Nitrogen Nutrition in Crops and Its Importance in Crop Quality. In The Indian Nitrogen Assessment; Abrol, Y.P., Adhya, T.K., Aneja, V.P., Raghuram, N., Pathak, H., Kulshrestha, U., Eds.; Elsevier: Amsterdam, The Netherlands, 2017; pp. 175–186.

Tilling, A.K.; O'Leary, G.J.; Ferwerda, J.G.; Jones, S.D.; Fitzgerald, G.J.; Rodriguez, D.; Belford, R. Remote sensing of nitrogen and water stress in wheat. Field Crops Res. 2007, 104, 77–85.

Pinter, P.J., Jr.; Hatfield, J.L.; Schepers, J.S.; Barnes, E.M.; Moran, M.S.; Daughtry, C.S.; Upchurch, D.R. Remote sensing for crop management. Photogramm. Eng. Remote Sens. 2003, 69, 647–664.

Solari, F.; Shanahan, J.; Ferguson, R.; Schepers, J.; Gitelson, A. Active Sensor Reflectance Measurements of Corn Nitrogen Status and Yield Potential. J. Agron. 2008, 100, 571.

Walsh, O.S.; Klatt, A.R.; Solie, J.B.; Godsey, C.B.; Raun, W.R. Use of soil moisture data for refined GreenSeeker sensor based nitrogen recommendations in winter wheat (Triticum aestivum L.). Precis. Agric. 2013, 14, 343–356.

Taghvaeian, S.; Chávez, J.L.; Hansen, N.C. Ground-based remote sensing of corn evapotranspiration under limited irrigation practices. In Proceedings of the 32nd Annual American Geophysical Union Hydrology Days, Fort Collins, CO, USA, 21–23 March 2012; pp. 119–131.

Genc, L.; Inalpulat, M.; Kizil, U.; Mirik, M.; Smith, S.E.; Mendes, M. Paprastojo kukuruzo (Zea mays L.) dregmes streso nustatymas, taikant spektrini atspindi ir klasifikavimo medžio metoda. Zemdirbyste 2013, 100, 81–90. [CrossRef]

DeJonge, K.C.; Mefford, B.S.; Chávez, J.L. Assessing corn water stress using spectral reflectance. Int. J. Remote Sens. 2016, 37, 2294–2312.

Zhao, G.; Miao, Y.; Wang, H.; Su, M.; Fan, M.; Zhang, F.; Jiang, R.; Zhang, Z.; Liu, C.; Liu, P.; et al. A preliminary precision rice management system for increasing both grain yield and nitrogen use efficiency. Field Crop Res. 2013, 154, 23–30.

Din, M.; Zheng, W.; Rashid, M.; Wang, S.; Shi, Z. Evaluating Hyperspectral Vegetation Indices for Leaf Area Index Estimation of Oryza sativa L. at Diverse Phenological Stages. Front. Plant Sci. 2017, 8, 820.

Jones, H.G.; Vaughan, R.A. Remote Sensing of Vegetation: Principles, Techniques, and Applications; Jones, H.G., Vaughan, R.A., Eds.; Oxford University Press: Oxford, UK, 2010; p. 384. ISBN 978-0-19-920779-4.

Jain, N.; Ray, S.S.; Singh, J.P.; Panigrahy, S. Use of hyperspectral data to assess the effects of different nitrogen applications on a potato crop. Precis. Agric. 2007, 8, 225–239.

Carter, G.A.; Knapp, A.K. Leaf optical properties in higher plants: Linking spectral characteristics to stress and chlorophyll concentration. Am. J. Bot. 2001, 88, 677–684.

Mahajan, G.R.; Sahoo, R.N.; Pandey, R.N.; Gupta, V.K.; Kumar, D. Using hyperspectral remote sensing techniques to monitor nitrogen, phosphorus, sulphur and potassium in wheat (Triticum aestivum L.). Precis. Agric. 2014, 15, 499–522.

Carter, G.A.; Estep, L. General Spectral Characteristics of Leaf Reflectance Responses to Plant Stress and Their Manifestation at the Landscape Scale. In From Laboratory Spectroscopy to Remotely Sensed Spectra of Terrestrial Ecosystems; Muttiah, R.S., Ed.; Springer: Dordrecht, The Netherlands, 2002; pp. 271–293.

Feng, W.; Guo, B.-B.; Zhang, H.-Y.; He, L.; Zhang, Y.-S.; Wang, Y.-H.; Zhu, Y.-J.; Guo, T.-C. Remote estimation of above ground nitrogen uptake during vegetative growth in winter wheat using hyperspectral red-edge ratio data. Field Crops Res. 2015, 180, 197–206.

Gómez-Casero, M.T.; Castillejo-González, I.L.; García-Ferrer, A.; Peña-Barragán, J.M.; Jurado-Expósito, M.; García-Torres, L.; López-Granados, F. Spectral discrimination of wild oat and canary grass in wheat fields for less herbicide application. Agron. Sustain. Dev. 2010, 30, 689–699.

Stellacci, A.M.; Castrignanò, A.; Troccoli, A.; Basso, B.; Buttafuoco, G. Selecting optimal hyperspectral bands to discriminate nitrogen status in durum wheat: A comparison of statistical approaches. Environ. Monit. Assess. 2016, 188, 1–15.

Ye, X.; Sakai, K.; Sasao, A.; Asada, S. Potential of airborne hyperspectral imagery to estimate fruit yield in citrus. Chemom. Intell. Lab. Syst. 2008, 90, 132–144.

Kale, K.V.; Solankar, M.M.; Nalawade, D.B.; Dhumal, R.K.; Gite, H.R. A Research Review on Hyperspectral Data Processing and Analysis Algorithms. Proc. Natl. Acad. Sci. India Sect. A Phys. Sci. 2017, 87, 541–555.

Thenkabail, P.S.; Enclona, E.A.; Ashton, M.S.; Van Der Meer, B. Accuracy assessments of hyperspectral waveband performance for vegetation analysis applications. Remote Sens. Environ. 2004, 91, 354–376.

Choi, Y.H.; Kim, H.K.; Hazekamp, A.; Erkelens, C.; Lefeber, A.W.M.; Verpoorte, R. Metabolomic Differentiation ofCannabissativaCultivars Using1H NMR Spectroscopy and Principal Component Analysis. J. Nat. Prod. 2004, 67, 953–957.

Stellacci, A.M.; Castrignanò, A.; Diacono, M.; Troccoli, A.; Ciccarese, A.; Armenise, E.; Gallo, A.; De Vita, P.; Lonigro, A.; Mastro, M.A.; et al. Combined approach based on principal component analysis and canonical discriminant analysis for investigating hyperspectral plant response. Ital. J. Agron. 2012, 7, 247–253.

Ray, S.S.; Singh, J.P.; Panigraphy, S. Use of hyperspectral remote sensing data for crop stress detection: Ground-based studies. ISPRS Arch. 2010, 38, 562–570.

Krezhova, D.; Velichkova, K.; Petrov, N.; Maneva, S. The effect of plant diseases on hyperspectral leaf reflectance and biophysical parameters. In Proceedings of the 5th International Conference on Radiation and Application in Various Fields of Research (RAD-2017), Budva, Montenegro, 12–16 June 2017; pp. 11–16.

Morcillo-Pallarés, P.; Rivera-Caicedo, J.P.; Belda, S.; De Grave, C.; Burriel, H.; Moreno, J.; Verrelst, J. Quantifying the Robustness of Vegetation Indices through Global Sensitivity Analysis of Homogeneous and Forest Leaf-Canopy Radiative Transfer Models. Remote Sens. 2019, 11, 2418.

Carlson, T.N.; Ripley, D.A. On the relation between NDVI, fractional vegetation cover, and leaf area index. Remote Sens. Environ.1997, 62, 241–252.

Huete, A. A soil-adjusted vegetation index (SAVI). Remote Sens. Environ. 1988, 25, 295–309.[CrossRef]

Rondeaux, G.; Steven, M.; Baret, F. Optimization of soil-adjusted vegetation indices. Remote Sens. Environ. 1996, 55,

95–107.

Huete, A.; Didan, K.; Miura, T.; Rodriguez, E.; Gao, X.; Ferreira, L. Overview of the radiometric and biophysical performance of the MODIS vegetation indices. Remote Sens. Environ. 2002, 83, 195–213.

Gitelson, A.A.; Merzlyak, M.N. Remote sensing of chlorophyll concentration in higher plant leaves. Adv. Space Res. 1998, 22, 689–692.

Cristiano, P.M.; Posse, G.; Di Bella, C.M.; Jaimes, F.R. Uncertainties in fPAR estimation of grass canopies under different stress situations and differences in architecture. Int. J. Remote Sens. 2010, 31, 4095–4109.

Hansen, P.M.; Schjoerring, J.K. Reflectance measurement of canopy biomass and nitrogen status in wheat crops using normalized difference vegetation indices and partial least squares regression. Remote Sens. Environ. 2003, 86, 542–553.

Glenn, E.; Huete, A.; Nagler, P.; Nelson, S. Relationship Between Remotely-sensed Vegetation Indices, Canopy Attributes and Plant Physiological Processes: What Vegetation Indices Can and Cannot Tell Us About the Landscape. Sensors 2008, 8, 2136–2160.

Haboudane, D. Hyperspectral vegetation indices and novel algorithms for predicting green LAI of crop canopies: Modeling and validation in the context of precision agriculture. Remote Sens. Environ. 2004, 90, 337–352.

Gitelson, A.A.; Gritz, Y.; Merzlyak, M.N. Relationships between leaf chlorophyll content and spectral reflectance and algorithms for non-destructive chlorophyll assessment in higher plant leaves. J. Plant Physiol. 2003, 160, 271–282.

Gitelson, A.A.; Keydan, G.P.; Merzlyak, M.N. Three-band model for noninvasive estimation of chlorophyll, carotenoids, and anthocyanin contents in higher plant leaves. Geophys. Res. Lett. 2006, 33.

Wu, C.; Niu, Z.; Tang, Q.; Huang, W. Estimating chlorophyll content from hyperspectral vegetation indices: Modeling and validation. Agric. For. Meteorol. 2008, 148, 1230–1241.

Main, R.; Cho, M.A.; Mathieu, R.; O'Kennedy, M.M.; Ramoelo, A.; Koch, S. An investigation into robust spectral indices for leaf chlorophyll estimation. ISPRS J. Photogramm. Remote Sens. 2011, 66, 751–761.

Horler, D.N.H.; Dockray, M.; Barber, J. The red edge of plant leaf reflectance. Int. J. Remote Sens. 1983, 4, 273–288.

Prasad, B.; Carver, B.F.; Stone, M.L.; Babar, M.A.; Raun, W.R.; Klatt, A.R. Genetic Analysis of Indirect Selection for Winter Wheat Grain Yield Using Spectral Reflectance Indices. Crop Sci. 2007, 47, 1416.

Peñuelas, J.; Pinol, J.; Ogaya, R.; Filella, I. Estimation of plant water concentration by the reflectance Water Index WI (R900/R970). Int. J. Remote Sens. 1997, 18, 2869–2875.

Hayes, A. Multiple Linear Regression (MLR). 2021. Available online: https://www.investopedia.com/terms/m/mlr.asp (accessed on 30 March 2021).

Huang, Z.; Turner, B.J.; Dury, S.J.; Wallis, I.R.; Foley, W.J. Estimating foliage nitrogen concentration from HYMAP data using continuum removal analysis. Remote Sens. Environ. 2004, 93, 18–29.

Wang, F.; Huang, J.; Lou, Z. A comparison of three methods for estimating leaf area index of paddy rice from optimal hyperspectral bands. Precis. Agric. 2010, 12, 439–447.

Romero, A.P.; Alarcón, A.; Valbuena, R.I.; Galeano, C.H. Physiological Assessment of Water Stress in Potato Using Spectral Information. Front. Plant Sci. 2017, 8.

Kefauver, S.C.; Vicente, R.; Vergara-Díaz, O.; Fernandez-Gallego, J.A.; Kerfal, S.; Lopez, A.; Melichar, J.P.E.; Serret Molins, M.D.; Araus, J.L. Comparative UAV and Field Phenotyping to Assess Yield and Nitrogen Use Efficiency in Hybrid and Conventional Barley. Front. Plant Sci. 2017, 8.

Gracia-Romero, A.; Kefauver, S.C.; Vergara-Díaz, O.; Zaman-Allah, M.A.; Prasanna, B.M.; Cairns, J.E.; Araus, J.L. Comparative Performance of Ground vs. Aerially Assessed RGB and Multispectral Indices for Early-Growth

Evaluation of Maize Performance under Phosphorus Fertilization. Front. Plant Sci. 2017, 8, 4.

Soil Survey Staff. In Keys to Soil Taxonomy, 12th ed.; USDA-Natural Resources Conservation Service: Washington, DC, USA, 2014. Available online: http://www.nrcs.usda.gov/Internet/FSE_DOCUMENTS/nrcs142p2_051546.pdf (accessed on 30 March 2021).

Todorovic, M. An Excel-based tool for real time irrigation management at field scale. In Proceedings of the International Symposium on "Water and Land Management for Sustainable Irrigated Agriculture", Adana, Turkey, 4–8 April 2006; pp. 4–8.

Allen, R.G.; Pereira, L.S.; Raes, D.; Smith, M. Crop Evapotranspiration. In Guidelines for Computing Crop Water Requirements; Irrigation and Drainage Paper 56; Food and Agriculture Organization: Rome, Italy, 1998.

Piscitelli, L.; Colovic, M.; Aly, A.; Hamze, M.; Todorovic, M.; Cantore, V.; Albrizio, R. Adaptive Agricultural Strategies for Facing Water Deficit in Sweet Maize Production: A Case Study of a Semi-Arid Mediterranean Region. Water 2021, 13, 3285.

Von Caemmerer, S.; Farquhar, G.D. Some relationships between the biochemistry of photosynthesis and the gas exchange of leaves. Planta 1981, 153, 376–387.

Min, M.; Lee, W.S. Determination of Significant Wavelengths and Prediction of Nitrogen Content for Citrus. Trans. ASAE 2005, 48, 455–461.

De Mendiburu, F. Una Herramienta de Analisis Estadistico Para la Investigacion Agricola. Ph.D. Thesis, Universidad Nacional de Ingenieria (UNI-PERU), Rímac, Peru, 2009.

Wobbrock, J.O.; Findlater, L.; Gergle, D.; Higgins, J.J. The aligned rank transform for nonparametric factorial analyses using only anova procedures. In Proceedings of the 2011 Annual Conference on Human Factors in Computing Systems—CHI '11, British Columbia, BC, Canada, 7–12 May 2022; ACM Press: New York, USA, 2011; pp. 143–146.

R Core Team. R: A Language and Environment for Statistical Computing; R Foundation for Statistical Computing: Vienna, Austria, 2013. Available online: https://www.scirp.org/(S(vtj3fa45qm1ean45vvffcz55))/reference/ReferencesPapers.aspx?ReferenceID= 1742158 (accessed on 1 March 2021).

Addinsoft. XLSTAT Statistical and Data Analysis Solution. New York. 2020. Available online: https://www.xlstat.com (accessed on 1 March 2021).

Dunteman, G.H. Principal Components Analysis. In Quantitative Applications in the Social Sciences; Sage Publications: Newbury Park, CA, USA, 1989; Volume 69, pp. 96–101.

Matus, I.M.; Gonzales, G.; del Poso, A. Evaluation of phenotypic variation in a Chilean collection of garlic (Allium sativum L.) clones using multivariate analysis. Plant. Genet. Resour. Newslett. 1999, 117, 31–36.

Jain, A.K.; Flynn, P.; Ross, A.A. (Eds.) Handbook of Biometrics; Springer Science & Business Media: Boston, MA, USA, 2007; p. 556.

Friendly, M. Corrgrams: Exploratory Displays for Correlation Matrices; The American Statistician; Taylor & Francis, Ltd.: Boca Raton, FL, USA, 2002; Volume 56, pp. 316–324. Available online: http://www.jstor.org/stable/3087354 (accessed on 12 April 2020).

Rouse, J.W.; Hass, R.H.; Schell, J.A.; Deering, D.W.; Harlan, J.C. Monitoring the Vernal Advancement and Retrogradation (Green Wave Effect) of Natural Vegetation; Final Report, RSC 1978-4; Texas A&M University: College Station, TX, USA, 1974; pp. 1–120.

Jurgens, C. The modified normalized difference vegetation index (mNDVI) a new index to determine frost damages in

agriculture based on Landsat TM data. Int. J. Remote Sens. 1997, 18, 3583–3594.

Roujean, J.-L.; Breon, F.-M. Estimating PAR absorbed by vegetation from bidirectional reflectance measurements. Remote Sens.Environ. 1995, 51, 375–384.

Kim, M.S. The Use of Narrow Spectral Bands for Improving Remote Sensing Estimations of Fractionally Absorbed Photosynthetically Active Radiation. Doctoral Dissertation. 1994. Available online: http://hdl.handle.net/1903/24796 (accessed on 1 March 2021).

Daughtry, C. Estimating Corn Leaf Chlorophyll Concentration from Leaf and Canopy Reflectance. Remote Sens. Environ. 2000, 74, 229–239.

Haboudane, D.; Miller, J.R.; Tremblay, N.; Zarco-Tejada, P.J.; Dextraze, L. Integrated narrow-band vegetation indices for prediction of crop chlorophyll content for application to precision agriculture. Remote Sens. Environ. 2002, 81, 416–426.

Merzlyak, M.N.; Gitelson, A.A.; Chivkunova, O.B.; Rakitin, V.Y. Non-destructive optical detection of pigment changes during leaf senescence and fruit ripening. Physiol. Plant. 1999, 106, 135–141.

Gamon, J.A.; Serrano, L.; Surfus, J.S. The photochemical reflectance index: An optical indicator of photosynthetic radiation use efficiency across species, functional types, and nutrient levels. Oecologia 1997, 112, 492–501.

Peñuelas, J.; Baret, F.; Filella, I. Semi-empirical indices to assess carotenoids/chlorophyll a ratio from leaf spectral reflectance.Photosynthetica 1995, 31, 221–230.

Vogelmann, J.E.; Rock, B.N.; Moss, D.M. Red edge spectral measurements from sugar maple leaves. Int. J. Remote Sens. 1993, 14, 1563–1575.

Barnes, E.M.; Clarke, T.R.; Richards, S.E.; Colaizzi, P.D.; Haberland, J.; Kostrzewski, M.; Waller, P.; Choi, C.; Riley, E.; Thompson, T.; et al. Coincident detection of crop water stress, nitrogen status and canopy density using ground based multispectral data. In Proceedings of the Fifth International Conference on Precision Agriculture, Bloomington, MN, USA, 16–19 July 2000; Volume 1619, p. 15.

Merton, R.N. Monitoring community hysteresis using spectral shift analysis and the red-edge vegetation stress index. In Proceedings of the Seventh Annual JPL Airborne Earth Science Workshop, Pasadena, CA, USA, 12–16 January 1998; pp. 12–16.

Wang, L.; Qu, J.J. NMDI: A normalized multi-band drought index for monitoring soil and vegetation moisture with satellite remote sensing. Geophys. Res. Lett. 2007, 34.

Babar, M.A.; Reynolds, M.P.; van Ginkel, M.; Klatt, A.R.; Raun, W.R.; Stone, M.L. Spectral Reflectance to Estimate Genetic Variation for In-Season Biomass, Leaf Chlorophyll, and Canopy Temperature in Wheat. Crop Sci. 2006, 46, 1046.

Raun, W.R.; Johnson, G.V. Improving Nitrogen Use Efficiency for Cereal Production. J. Agron. 1999, 91, 357.

Plett, D.C.; Ranathunge, K.; Melino, V.J.; Kuya, N.; Uga, Y.; Kronzucker, H.J. The intersection of nitrogen nutrition and water use in plants: New paths toward improved crop productivity. J. Exp. Bot. 2020, 71, 4452–4468.

Setter, T.L.; Flannigan, B.A.; Melkonian, J. Loss of Kernel Set Due to Water Deficit and Shade in Maize. Crop Sci. 2001, 41, 1530.

Gustin, J.L.; Boehlein, S.K.; Shaw, J.R.; Junior, W.; Settles, A.M.; Webster, A.; Tracy, W.F.; Hannah, L.C. Ovary abortion is prevalent in diverse maize inbred lines and is under genetic control. Sci. Rep. 2018, 8. [CrossRef]

Song, L.; Jin, J.; He, J. Effects of Severe Water Stress on Maize Growth Processes in the Field. Sustainability 2019, 11, 5086.

Kresovic, B.; Matovic, G.; Gregoric, E.; Djuricin, S.; Bodroza, D. Irrigation as a climate change impact mitigation

measure: An agronomic and economic assessment of maize production in Serbia. Agric. Water Manag. 2014, 139, 7–16.

Farré, I.; Faci, J.M. Comparative response of maize (Zea mays L.) and sorghum (Sorghum bicolor L. Moench) to deficit irrigation in a Mediterranean environment. Agric. Water Manag. 2006, 83, 135–143.

Wang, Y.; Liu, F.; Andersen, M.N.; Jensen, C.R. Improved plant nitrogen nutrition contributes to higher water use efficiency in tomatoes under alternate partial root-zone irrigation. Funct. Plant Biol. 2010, 37, 175.

Hammad, H.M.; Farhad, W.; Abbas, F.; Fahad, S.; Saeed, S.; Nasim, W.; Bakhat, H.F. Maize plant nitrogen uptake dynamics at limited irrigation water and nitrogen. Environ. Sci. Pollut. Res. 2016, 24, 2549–2557.

Delegido, J.; Verrelst, J.; Meza, C.M.; Rivera, J.P.; Alonso, L.; Moreno, J. A red-edge spectral index for remote sensing estimation of green LAI over agroecosystems. Eur. J. Agron. 2013, 46, 42–52.

Clevers, J.G.P.W.; De Jong, S.M.; Epema, G.F.; Van Der Meer, F.D.; Bakker, W.H.; Skidmore, A.K.; Scholte, K.H. Derivation of the red edge index using the MERIS standard band setting. Int. J. Remote Sens. 2002, 23, 3169–3184.

Ballester, C.; Brinkhoff, J.; Quayle, W.C.; Hornbuckle, J. Monitoring the Effects of Water Stress in Cotton Using the Green Red Vegetation Index and Red Edge Ratio. Remote Sens. 2019, 11, 873.

Zhao, D.; Reddy, K.R.; Kakani, V.G.; Reddy, V.R. Nitrogen deficiency effects on plant growth, leaf photosynthesis, and hyperspectral reflectance properties of sorghum. Eur. J. Agron. 2005, 22, 391–403.

Gazala, I.F.S.; Sahoo, R.N.; Pandey, R.; Mandal, B.; Gupta, V.K.; Singh, R.; Sinha, P. Spectral reflectance pattern in soybean for assessing yellow mosaic disease. Indian J. Virol. 2013, 24, 242–249.

Wang, F.-M.; Huang, J.-F.; Wang, X.-Z. Identification of Optimal Hyperspectral Bands for Estimation of Rice Biophysical Parameters. J. Integr. Plant Biol. 2008, 50, 291–299.

Abbasi, M.; Verrelst, J.; Mirzaei, M.; Marofi, S.; Riyahi Bakhtiari, H.R. Optimal Spectral Wavelengths for Discriminating Orchard Species Using Multivariate Statistical Techniques. Remote Sens. 2019, 12, 63.

Grossman, Y.L.; Ustin, S.L.; Jacquemoud, S.; Sanderson, E.W.; Schmuck, G.; Verdebout, J. Critique of stepwise multiple linear regression for the extraction of leaf biochemistry information from leaf reflectance data. Remote Sens. Environ. 1996, 56, 182–193.

Strachan, I.B.; Pattey, E.; Boisvert, J.B. Impact of nitrogen and environmental conditions on corn as detected by hyperspectral reflectance. Remote Sens. Environ. 2002, 80, 213–224.

Gupta, V.; Reinke, K.; Jones, S. Changes in the spectral features of fuel layers of an Australian dry sclerophyll forest in response to prescribed burning. Int. J. Wildland Fire 2013, 22, 862–868.

Putra, B.T.W.; Soni, P. Evaluating NIR-Red and NIR-Red edge external filters with digital cameras for assessing vegetation indices under different illumination. Infrared Phys. Technol. 2017, 81, 148–156.

Imran, A.B.; Khan, K.; Ali, N.; Ahmad, N.; Ali, A.; Shah, K. Narrow band based and broadband derived vegetation indices using Sentinel-2 Imagery to estimate vegetation biomass. Glob. J. Environ. Sci. Manag. 2020, 6, 97–108.

Jiang, Z.; Huete, A.R.; Chen, J.; Chen, Y.; Li, J.; Yan, G.; Zhang, X. Analysis of NDVI and scaled difference vegetation index retrievals of vegetation fraction. Remote Sens. Environ. 2006, 101, 366–378.

Ranjan, R.; Chopra, U.K.; Sahoo, R.N.; Singh, A.K.; Pradhan, S. Assessment of plant nitrogen stress in wheat (Triticum aestivum L.) through hyperspectral indices. Int. J. Remote Sens. 2012, 33, 6342–6360.

Bolton, D.K.; Friedl, M.A. Forecasting crop yield using remotely sensed vegetation indices and crop phenology metrics. Agric. For.Meteorol. 2013, 173, 74–84.

Ghosh, P.; Mandal, D.; Bhattacharya, A.; Nanda, M.K.; Bera, S. Assessing Crop Monitoring Potential of Sentinel-2 in a SpatioTemporal Scale. Int. Arch. Photogramm. Remote Sens. Spat. Inf. Sci. 2018, XLII-5, 227–231.

Peng, Y.; Gitelson, A.A.; Sakamoto, T. Remote estimation of gross primary productivity in crops using MODIS 250 m data. Remote Sens. Environ. 2013, 128, 186–196.

Clevers, J.G.P.W.; Gitelson, A.A. Remote estimation of crop and grass chlorophyll and nitrogen content using red-edge bands on Sentinel-2 and -3. Int. J. Appl. Earth Obs. Geoinf. 2013, 23, 344–351.

Schlemmer, M.; Gitelson, A.; Schepers, J.; Ferguson, R.; Peng, Y.; Shanahan, J.; Rundquist, D. Remote estimation of nitrogen and chlorophyll contents in maize at leaf and canopy levels. Int. J. Appl. Earth Obs. Geoinf. 2013, 25, 47–

Rock, B.N.; Hoshizaki, T.; Miller, J.R. Comparison of in situ and airborne spectral measurements of the blue shift associated with forest decline. Remote Sens. Environ. 1988, 24, 109–127.

Ramachandiran, K.; Pazhanivelan, S. Determination of nitrogen and water stress with hyper spectral reflectance on maize using classification tree (CT) analysis. J. Agrometeorol. 2015, 17, 213.

Zarco-Tejada, P.J.; Ustin, S.L.; Whiting, M.L. Temporal and Spatial Relationships between Within-Field Yield Variability in Cotton and High-Spatial Hyperspectral Remote Sensing Imagery. Agron. J. 2005, 97, 641.

Le Maire, G.; François, C.; Dufrêne, E. Towards universal broad leaf chlorophyll indices using PROSPECT simulated database and hyperspectral reflectance measurements. Remote Sens. Environ. 2004, 89, 1–28.

Ju, W.; Gao, P.; Wang, J.; Zhou, Y.; Zhang, X. Combining an ecological model with remote sensing and GIS techniques to monitor soil water content of croplands with a monsoon climate. Agric. Water Manag. 2010, 97, 1221–1231.

Raper, T.B.; Varco, J.J. Canopy-scale wavelength and vegetative index sensitivities to cotton growth parameters and nitrogen status. Precis. Agric. 2014, 16, 62–76.

Li, F.; Miao, Y.; Feng, G.; Yuan, F.; Yue, S.; Gao, X.; Liu, Y.; Liu, B.; Ustin, S.L.; Chen, X. Improving estimation of summer maize nitrogen status with red edge-based spectral vegetation indices. Field Crops Res. 2014, 157, 111–123.

Wang, Z.; Wang, T.; Darvishzadeh, R.; Skidmore, A.K.; Jones, S.; Suarez, L.; Woodgate, W.; Heiden, U.; Heurich, M.; Hearne, J. Vegetation Indices for Mapping Canopy Foliar Nitrogen in a Mixed Temperate Forest. Remote Sens. 2016, 8, 491.

Ihuoma, S.O.; Madramootoo, C.A. Crop reflectance indices for mapping water stress in greenhouse grown bell pepper. Agric.Water Manag. 2019, 219, 49–58.

Caturegli, L.; Matteoli, S.; Gaetani, M.; Grossi, N.; Magni, S.; Minelli, A.; Corsini, G.; Remorini, D.; Volterrani, M. Effects of water stress on spectral reflectance of bermudagrass. Sci. Rep. 2020, 10, 1–12.

Carter, G.A. Primary and secondary effects of water content on the spectral reflectance of leaves. Am. J. Bot. 1991, 78, 919–924.

Sims, D.A.; Gamon, J.A. Estimation of vegetation water content and photosynthetic tissue area from spectral reflectance: A comparison of indices based on liquid water and chlorophyll absorption features. Remote Sens. Environ. 2003, 84, 526–537.

Ihuoma, S.O.; Madramootoo, C.A. Recent advances in crop water stress detection. Comput. Electron. Agric. 2017, 141, 267–275.

Danson, F.M.; Steven, M.D.; Malthus, T.J.; Clark, J.A. High-spectral resolution data for determining leaf water content. Int. J.Remote Sens. 1992, 13, 461–470.

Peñuelas, J.; Filella, I.; Biel, C.; Serrano, L.; Save, R. The reflectance at the 950–970 nm region as an indicator of plant water status.Int. J. Remote Sens. 1993, 14, 1887–1905.

Govind, A.M.B.; Kumari, J.; Govind, A. Efficacy of different indices derived from spectral reflectance of wheat for nitrogen stress detection. J. Plant Interact. 2005, 1, 93–105.

3.3. Hyperspectral Vegetation Indices to Assess Water and Nitrogen Status of Sweet Maize Crop

This chapter has been adapted from a previously published paper:
Colovic, M., Yu, K., Todorovic, M., Cantore, V., Hamze, M., Albrizio, R., & Stellacci, A. M. (2022). Hyperspectral Vegetation Indices to Assess Water and Nitrogen Status of Sweet Maize Crop. Agronomy, 12(9), 2181.

Abstract: The deployment of novel technologies in the field of precision farming has risen to the top of global agendas in response to the impact of climate change and the possible shortage of resources such as water and fertilizers. The present research addresses the performance of water and nitrogen-sensitive narrow-band vegetation indices to evaluate the response of sweet maize (Zea mays var. saccharata L.) to different irrigation and nitrogen regimes. The experiment was carried out in Valenzano, Bari (Southern Italy), during the 2020 growing season. Three irrigation regimes (full irrigation, deficit irrigation, and rainfed) and two nitrogen levels (300 and 50 kg ha^{-1}) were tested. During the growing season, a Field Spec Handheld 2 spectroradiometer operating in the range of 325–1075 nm was utilized to capture spectral data regularly. In addition, soil water content, biometric parameters, and physiological parameters were measured. The DATT index, based on near-infrared and red-edge wavelengths, performed better than other indices in explaining the variation in chlorophyll content, whereas the double difference index (DD) showed the greatest correlation with the leaf–gas exchange. The modified normalized difference vegetation index (NNDVI) and the ratio of water band index to normalized difference vegetation index (WBI/NDVI) showed the highest capacity to distinguish the interaction of irrigation x nitrogen, while the best discriminating capability of these indices was under a low nitrogen level. Moreover, red-edge-based indices had higher sensitivity to nitrogen levels compared to the structural and water band indices. Our study highlighted that it is critical to choose proper narrow-band vegetation indices to monitor the plant eco-physiological response to water and nitrogen stresses.

Keywords: vegetation reflectance; bio-physiological crop parameters; red-edge; water band indices; narrow-bands spectral indices; water and nitrogen stress

3.3.1. Introduction

Water and nitrogen (N) have long been known as two primary restricting inputs for crop production. Water stress directly affects crop growth and productivity (Osakabe *et al.*, 2014; Zhang and Zhou, 2019; Yuan *et al*., 2020; Piscitelli *et al*., 2020). According to several studies, crops in many regions, especially in the Mediterranean and other arid and semi-arid areas, experience severe effects of drought (Moriondo *et al*., 2011), which causes yield loss. Therefore, various studies have aimed to identify and assess the performance of water stress indicators and strategies for water use optimization (Holzman *et al*., 2011; Mladenova *et al*., 2017). Additionally, the application of essential nutrients in the optimal quantity is necessary to improve the crop growth and development; nitrogen is considered the most vital nutrient by having a fundamental role in the biochemical and physiological functions of plants (Massignam *et al*., 2009; Leghari *et al*., 2016; Maheswari *et al*., 2017). Normally, N deficit causes a decrease in biomass and leaf chlorophyll concentration, and an increment in leaf reflectance in the chlorophyll absorption bands of the visible part of the electromagnetic spectrum (Ranjan *et al*., 2012).

The interaction of water and nitrogen affects the biochemical and biophysical processes from the environmental to the molecular level. Some findings have shown that water–nitrogen interactions mainly affect the crop yield, grain size, protein content, root depth, and root-to-shoot translocation (Sadras *et al*., 2016; Cossani *et al*., 2018). Hence, matching N supply to water availability, both spatially and temporally, is essential to accomplish an optimal crop response, maximizing the efficiency of N application (Tilling *et al*., 2007). Consequently, the development of sustainable and efficient strategies is a priority for producers facing water shortages and nutrient deficiency (Bell *et al.*, 2018). As proximal and remote sensing methods enable rapid, non-destructive water and nutrient deficiency determination, they have been widely used in precision agriculture (Pinter *et al*., 2003).

Hyperspectral remote sensing, which records the radiation in hundreds of narrow contiguous spectral channels reflected from any feature, is an accurate technique to regain valuable information for applications in precision agriculture (Singh *et al.*, 2020). Such information provides significant progress in understanding the subtle changes in the biochemical and biophysical attributes of the crop and their different physiological processes, which otherwise are indistinct in multispectral remote sensing (Sahoo et al., 2015). Many studies have shown the high effectivity of narrow-band vegetation indices (VIs) to evaluate the crop biophysical parameters (Monteiro *et al*., 2012; Zhu *et al*., 2020), especially if the spectral and canopy structure information are integrated (Li *et al*., 2022). However, little is known about which VI can distinguish between the stress of different origins such as water and N, when combined.

Narrow-band vegetation indices have been favourably included in studies aiming to estimate the crop nitrogen concentration (Hansen and Schjoerring, 2003; Stroppiana *et al*., 2009; Chen *et al*., 2010; Yao *et al*., 2010), leaf chlorophyll content (Gitelson *et al*., 2005; Delegido *et al*., 2005; Vincini *et al*., 2011), light-use efficiency (Inoue *et al.*, 2008; Garbulsky *et al.*, 2010), as well as detect water stress (Ceccato *et al*., 2002; Zarco-Tejada *et al*., 2013; Ihouma, 2020) and diseases (Apan *et al.,* 2004; Ray *et al.*, 2011; Calderon *et al.*, 2013). The narrowband VIs use reflectance in red and infrared bands to collect the red-edge section of the spectrum. These indices provide information on numerous vegetation and environmental variations such as the leaf area index, leaf chlorophyll content, and background soil reflectance (Zou *et al*., 2018). For instance, the normalized difference red-edge index (NDRE) is considered susceptible to chlorophyll content changes in the leaves, variability in leaf area, and soil background effects (Fitzgerald *et al*., 2006; Thomposon *et al*., 2019; Boiarskii *et al*., 2019); the red-edge normalized difference vegetation index (RENDVI) has been shown to be superior to the normalized difference vegetation index (NDVI) for the late-season nitrogen determination (Shaver *et al*., 2017); and the modified chlorophyll absorption ratio index (MCARI) has been recommended as a valuable index that may afford upgraded sensitivity to nitrogen availability and soil moisture over NDVI (Perry and Davenport, 2007; Robersts *et al*., 2016). Additionally, concerning the water absorption properties, many reports have highlighted the great potential of water indices to estimate the crop water content and detect crop water stress (Penuelas et al., 1995; Zhao *et al.,* 2011; Wang *et al.*, 2015; McCall *et al.*, 2017).

Previous studies have shown that near-infrared and red-edge reflectance might lower the background influence and have excellent possibilities to predict the chlorophyll content, which helps to precisely determine the nitrogen quantity (Daugtry *et al*., 2000; Yang *et al*., 2003). Numerous studies have been conducted to relate the vegetation indices to the crop physiological and biometric parameters and a large number of relationships between them have been found (Casanova *et al*., 1998; Aparicio *et al*., 2000; Wang *et al.*, 2005; Riedel *et al*., 2005; Tsonev *et al*., 2014; Sivia-Perez *et al*., 2018; Chen *et al.*, 2020; Sellami *et al.*, 2022). Some findings have confirmed that spectral reflectance could be suitable for monitoring the photosynthetic parameters of crops (Heckmann *et al*., 2017; Yendreck *et al.*, 2017). Additionally, Weber *et al.* (2012) proved the high relevance of hyperspectral indices in predicting the maize grain yield. As maize has high water and nitrogen requirements, this crop needs proper water and nutrient management during all growth stages (Yuan *et al*., 2020). Nevertheless, the problem of saturation in predicting crop biophysical parameters has been found for many spectral indices (Haboudane *et al.,* 2004). It is not clear whether the current water and nitrogen indices can indicate the high water and nitrogen requirements in maize.

In this study, the canopy spectral reflectance data from the field spectrometry and bio-physiological measurements were simultaneously collected. The overall objective was to assess the performance of various narrow-band vegetation indices and sensitivity to different irrigation and nitrogen levels and their interaction. The specific objective was to find the best correlation in determining which vegetation index is the most efficient predictor of the crop eco-physiological parameters. The findings of this study will provide essential information for the non-destructive, real-time monitoring and assessment of sweet maize water stress and nitrogen deficiency using hyperspectral VIs.

3.3.2. Materials and Methods

3.3.2.1. Study Area and Experimental Design

The study was carried out in the 2020 growing season in Valenzano, Bari (41° 03′ N, 16° 53′ E, 77 m above sea level), Southern Italy, at the Mediterranean Agronomic Institute (IAMB) experimental field.

The climate of the location is typical of the Mediterranean, with moderate winters and dry summers. The average yearly precipitation is around 550 mm (30 years average), with most precipitation falling during the autumn and winter months. The average monthly air temperature varies from 8°C in January to 24°C in July and August. The research area's soil is silty-clay-loam (Staff, 2014).

The average values of the main physical and chemical soil properties are: sand 170 g kg^{-1}, clay 234 g kg^{-1}, silt 596 g kg^{-1}, USDA Textural Class: silty-loam; pH (H 2 O 1:2.5) 8.1, electrical conductivity (1:2) 0.24 dS m^{-1}, total carbonate 55 g kg^{-1}, organic C 11.6 g kg^{-1}, total N 0.9 g kg^{-1}, C/N ratio 12.9, available P 17 mg kg^{-1}, K exchangeable 465 mg kg^{-1} (Piscitelli *et al.,* 2021).

Sweet maize (*Zea mays* var. saccharata L.) was grown on 18 plots (sized 10 × 10 m) from June to September 2020, in rows-oriented north-south, 0.5 m apart and with a spacing between plants in the row of 0.2 m, with a plant density of 10 plants m^{-2}.

Three irrigation regimes (WR) were used in combination with two N levels. The irrigation regimes included: (i) full irrigation (I_{100}); (ii) deficit irrigation (I_{50}), which applied half of the crops' water needs; and (iii) rainfed treatment (I_0). The amounts of nitrogen were: (i) 50 kg ha^{-1}, which is a low level (LN) and (ii) 300 kg ha^{-1}, which is a high level (HN). The rainfed treatment received only one watering after sowing. Treatments were allocated in a split-plot experimental design with three replicates, considering the irrigation regime (WR) as the main-plot factor and the N level (N) as the sub-plot factor.

Before sowing, the fertilizers were applied to the whole experimental area as follows: nitrogen (N) 50 kg ha^{-1} as urea (46% of N), phosphorus (P_2O_5)—100 kg ha^{-1} as superphosphate (20% P_2O_5), and potassium (K_2O)—200 kg ha^{-1} as potassium sulfate (51% K_2O). On 22 June, 250 kg ha^{-1} of additional nitrogen as urea was supplied to HN treatment. The weeding control was conducted by milling before sowing and manually during the first growth stage.

During the experiment, a standard set of daily meteorological data (air temperature, relative humidity, solar radiation, wind speed and precipitation) was obtained from the weather station located next to the experimental field (Fig. 9). The average daily temperature (T_{avg}) ranged between 19 and 29°C, while the reference evapotranspiration (ETo) was between 1- and 5.6-mm d^{-1}. The total amount of precipitation was 56 mm, with the highest value of 23.6 mm recorded on 17 days after sowing (DAS). The crop evapotranspiration increased with the biomass growth until the flowering and initial maturity stages, and then it reduced approaching the harvesting (data not shown). Hence, the overall water deficit between crop evapotranspiration and precipitation increased during the growing season, which provoked strong water stress under rainfed cultivation.

Irrigation was performed by the surface drip method system using a drip line for each row and drippers (2.2 L h^{-1}) 0.50 m spaced apart. Crop water balance and irrigation scheduling were managed using an Excel-based model (Todorovic, 2006) that estimates day-by-day crop evapotranspiration and irrigation water requirements through the standard procedure proposed by Allen et al. (1998). Irrigation amounts of 291.2 mm were supplied in 12 waterings in the I_{100} treatment, while half of these amounts were applied in the I_{50} treatment.

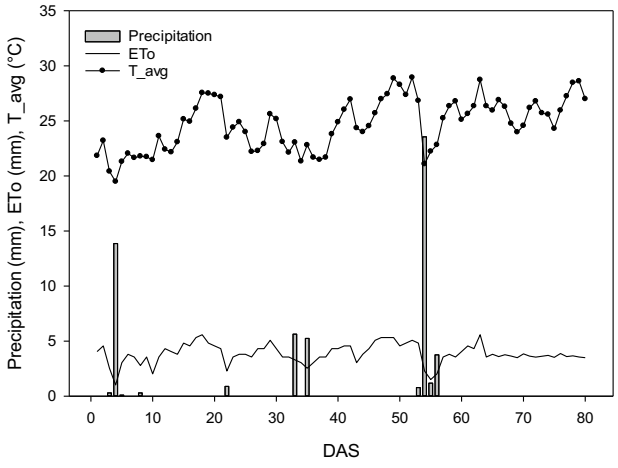

Figure 9. The daily precipitation, reference evapotranspiration (ETo), and average temperature (T_{avg}) during the crop growing cycle of sweet maize.

3.3.2.2. Measurements

All of the physiological measurements listed below were simultaneously taken five times from mid-July to the end of August.

3.3.2.2.1. Leaf Gas Exchange

A portable open system photosynthesis system (Li-6400XT, LiCor, Lincoln, NE, USA) was used to measure the net photosynthetic CO_2 assimilation, (An, μ mol m^{-2} s^{-1}) and stomatal conductance to water vapor (gs, mol m^{-2} s^{-1}) over a clipped leaf surface of 6.0 cm^2 on the intact, healthy green, and well-exposed up-leaves at solar noon (between 10:30 and 12:30 solar time). A saturating photosynthetic photon flux density (PPFD) of 2000 μ mol m^{-2} s^{-1} was used as the light source. To keep the CO_2 content in the leaf chamber at 400 μ mol mol^{-1} , an external bottled CO_2 source was employed. The von Caemmerer and Farquhar (1981) model was used to determine the different gas-exchange parameters (e.g., leaf transpiration (Tr, mmol m^{-2} s^{-1})) in the instrument software. The measurement was repeated three times per plot.

3.3.2.2.2. Leaf Chlorophyll Content

An optical meter (SPAD-502, Konica Minolta, Osaka, Japan) was used to measure the leaf chlorophyll content index (CC, r.u.) on 15 leaves per plot.

3.3.2.2.3. Relative Water Content

The relative water content (RWC) was measured in up-leaves blades similar to those used for the gas exchange measurements. At midday, nine leaf segments were gathered from three plants in each plot. Leaf-blade segments were weighed to obtain the fresh weight (FW, g), kept in distilled water overnight at 4 ◦ C to obtain the saturated weight (SW, g), and then weighed again. Afterward, they were dried at 80 ◦ C for 48 h and the dry weight (DW, g) was measured. Finally, the RWC was calculated as follows:

$$\mathrm{RWC} = \frac{\mathrm{FW}-\mathrm{DW}}{\mathrm{SW}-\mathrm{DW}} x100 \qquad (1)$$

3.3.2.2.4. Crop Reflectance

The crop reflectance was measured using a FieldSpec Handheld 2 spectroradiometer (Analytical Spectral Devices, Inc., Boulder, CO, USA). This spectroradiometer is designed to collect spectra with a resolution of <3 nm at 700 nm, accuracy of 1 nm, and a wavelength range of 325–1075 nm.

The field of view (FOV) of the bare fiber-optic probe was 25° . The spectrum of a white ($BaSO_4$) reference panel with known reflectance properties was acquired to derive the reflectance of the target. Ten spectra readings were averaged to obtain a single reflectance measurement. The measurements were acquired on three plants for each plot, at midday, under clear sky conditions. The crop spectrum was taken from a distance of 10 cm of height, with a spot size of about 14 cm^2 , and as the canopy cover grew and expanded, the distance from the vegetation increased to 60 cm.

The VIs were computed for each plot to analyze the relationships with the physiological crop parameters and evaluate their performance in distinguishing the water and nitrogen levels. These VIs were chosen on the basis of their sensitivity to (i) canopy structure; (ii) chlorophyll and other photosynthetic pigments; (iii) crop nitrogen status; and (iv) water status. However, in our study, the criteria for index selection were conducted on the previously successful use of them in numerous studies, as presented in Table 6.

Table 6. The indices derived from the hyperspectral visible and near-infrared bands.

Description	Abbreviation	Formulation	Reference
Narrow-Band Water and Nitrogen Sensitive Indices			
Red-edge inflection point	REIP	$700 + 40 \times [(((R_{670} + R_{780})/2) - R_{700})/(R_{740} - R_{700})]$	Guyot et al., 1988
Normalized difference red-edge	NDRE	$(R_{790} - R_{720})/(R_{790} + R_{720})$	Barnes et al., 2000
Narrow-band Normalized Difference Vegetation Index	NNDVI	$(R_{775} - R_{670})/(R_{775} + R_{670})$	Perry et al., 2008
Modified chlorophyll absorption reflectance index	MCARI	$[(R_{700} - R_{670}) - 0.2 \times (R_{700} - R_{550})] \times (R_{700}/R_{670})$	Daughtry et al., 2000
DATT index	DATT *	$(R_{760} - R_{720})/(R_{760} - R_{670})$	Shiratusuchi et al., 2011
MERIS terrestrial chlorophyll index	MTCI *	$(R_{760} - R_{720})/(R_{720} - R_{670})$	Shiratusuchi et al., 2011
Chlorophyll indices	Cl Cl_{green} $Cl_{red-edge}$	$Cl = (R_{880}/R_{590}) - 1$ $Cl_{green} = (R_{730}/R_{530}) - 1$ $CI_{red-edge} = (R_{850}/R_{730}) - 1$	Shiratusuchi et al., 2011
Double difference index	DD	$(R_{749} - R_{720}) - (R_{701} - R_{672})$	Le Maire et al., 2004
Structure intensive pigment index	SIPI	$(R_{800} - R_{445})/(R_{800} - R_{680})$	Penuelas et al., 1995
Water band index	WBI	R_{900}/R_{970}	Peñuelas et al., 1997
Ratio water band index and normalized difference vegetation index	(WBI/NDVI)	$(R_{900}/R_{970})/[(R_{800} - R_{680})/(R_{800} + R_{680})]$	Peñuelas et al., 1997

* DATT and MTCI indices were computed according to the equations reported in [69].

3.3.2.2.5. Canopy Temperature

The canopy temperature (Tc) was measured by a thermal imaging camera (FLIR B335, Wilsonville, OR, USA) with a 640 by 480-pixel resolution and 2% accuracy reading, the emissivity of 0.95, and the distance to the focal plane of 0.4 m. Thermal images were collected on three plants for each plot, between 11:00 and 13:00 (solar time) at 0.10 m from the crop, focusing as much as possible on the plant without soil disturbance in the background. Images were elaborated using FLIR Tools software for leaf temperature extraction. Canopy temperature was determined as the average temperature for each image.

3.3.2.2.6. Leaf Area Index and Dry-Above Ground Biomass

The leaf area index (LAI) was measured by using an optical leaf area meter (Li-COR, 3100, Lincoln NE, USA) on three plants for each plot. Dry-above ground biomass (DAGB) was measured on the same plants used for the LAI measurements. Samples were weighed after placing them in an oven at 70°C for 48 h.

3.3.2.2.7. Fresh Grain Yield and Irrigation Yield Water Use Efficiency

The harvesting was conducted on 3 September 2020, when the grain reached about 30% in dry matter, sampling 2 m^2 in the middle of each plot.
The irrigation yield water use efficiency ($IWUE_Y$) was calculated as the ratio of marketable yield and seasonal irrigation volume.

3.3.2.2.8. Statistical Analysis

The variables under study (vegetation indices VIs) were evaluated for normal distribution according to the Shapiro–Wilk W test and for homogeneity of variance using Bartlett's test. Multiple data taken over time on different plots were analyzed using a repeated-measures ANOVA approach to identify the effect of between-subject and within-subject factors on the measured variables. The general linear model (GLM) procedure was used. The vegetation indices (Table 1) were considered as dependent variables and the fixed factors (water treatment, nitrogen treatment and time) as categorical independent variables. The sphericity within all possible pairs was evaluated using Mauchly's test. The Greenhouse–Geisser adjustment was used to test the within-subject effects if Mauchly's test revealed that the assumption of sphericity was untenable since it was the case for a few variables.
The Student–Newman–Keuls (SNK) post hoc ($\alpha = 0.05$) test was used to make pairwise comparisons among the sample means group when significant differences were observed with ANOVA.

Moreover, simple linear regression analysis was applied to assess the relationship between the crop physiological and biometric data and vegetation indices, while the coefficient of determination (R^2) evaluated the strength of the relationships. All statistical analyses were performed using the R programming language (R Core Team).

3.3.3. Results

3.3.3.1. Crop Water Status, Yield, and Irrigation Yield Water Use Efficiency

In the beginning, all treatments had similar values, ranging from 64 to 73% (Fig. 10). However, after flowering, sweet maize under rainfed conditions experienced severe drought stress, which caused a remarkable reduction in the RWC. The peak RWC value of 82% was reached on 66 DAS in I_{100} HN. Plots under full irrigation treatment and high level of nitrogen (I_{100} HN) showed the greatest fresh yield (18.09 t ha^{-1}), while the yield of the same irrigation treatment (I_{100}) with a low nitrogen level (LN) was reduced by 26%. The water deficit treatments provided a yield of 9.74 and 7.56 t ha^{-1} under high and low nitrogen supply, respectively; these values were lower compared to the corresponding fully irrigated treatments. The yield reduction under deficit irrigation conditions was due to the decrement in the mean grain weight, the lessening in the number of ears, the weight of the ears, and grains per row (data not shown). Moreover, crops under rainfed conditions were strongly affected by the absence of water (irrigation or precipitation), particularly at the flowering stage; such severe water stress did not allow for the formation of grains. Irrigation yield water use efficiency ($IWUE_Y$) summarized these results: the greatest values were recorded for I_{50} HN (6.7 kg m^{-3}) and for I_{100} HN (6.2 kg m^{-3}), while under the corresponding treatments without N, reductions of 22 and 26% were observed. The lowest value of $IWUE_Y$ was detected in I_{100} LN.

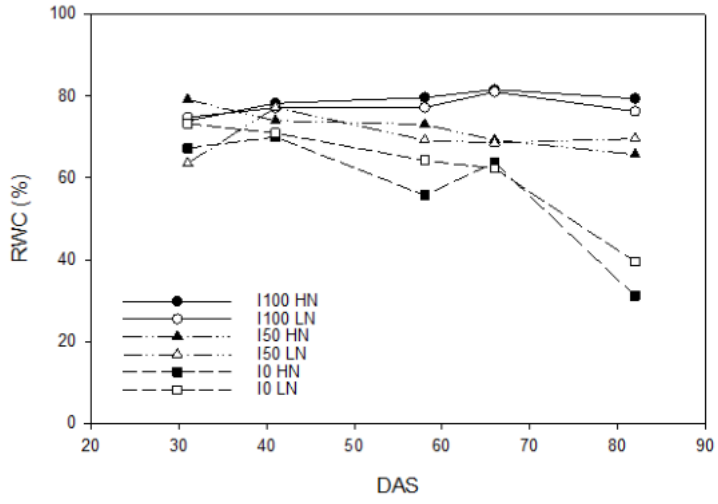

Figure 10. Variation in the relative water content (RWC) during the growing season of sweet maize for different water and nitrogen treatments.

3.3.3.2. Crop Reflectance and Vegetation Indices

A noteworthy difference in reflectance was observed between treatments experiencing stress and those well-watered. The crop spectral reflectance increased more rapidly in the infrared region and the slope of the red-edge became steeper, especially in the treatments under full irrigation and high nitrogen level, where a shift to longer wavelengths and an increase in the amplitude of the red-edge peak (Fig. 11) were observed. The values of spectral reflectance for non-stressed plants were higher in the range from 710 nm to 950 nm compared to the plants under stress.

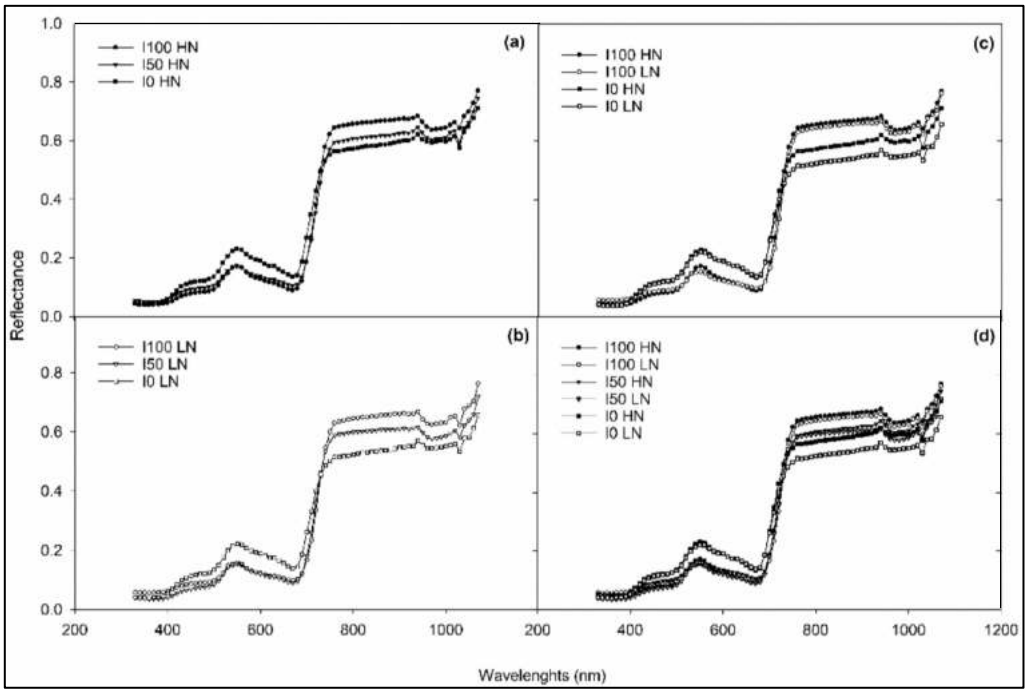

Figure 11. The average values of the spectral reflectance of sweet maize for different treatments, during the tasseling stage (73 DAS): (a) and (b) are the irrigation regimes under high nitrogen (HN) and low nitrogen (LN), respectively; (c) is the interaction among both full irrigation and rainfed treatments with nitrogen levels; (d) is the interaction among all the six treatments.

ANOVA allowed us to compare the sensitivity of the vegetation indices to different treatments and their interactions (Tab. 7).

Table 7. The analysis of variance of 13 vegetation indices (VIs) for different irrigation regimes, nitrogen levels, and the day after sowing (DAS) of sweet maize.

	Source of Variation	Irrigation	Nitrogen	DAS	Irrigation × Nitrogen	Irrigation × DAS	Nitrogen × DAS	Irrigation × Nitrogen X DAS
	Num DF	2	1	4	2	7	4	7
Vegetation Indices (VIs)	REIP	<0.0001 ***	0.0016 **	0.0064 **	0.5635 ns	<0.0001 ***	0.8752 ns	0.2969 ns
	NDRE	<0.0001 ***	<0.0001 ***	0.0024 **	0.6831 ns	<0.0001 ***	0.6765 ns	0.1399 ns
	NNDVI	0.0123 *	0.9880 ns	<0.0001 ***	0.0475 *	<0.0001 ***	0.0799 ns	0.4282 ns
	MCARI	0.5690 ns	0.0031 **	0.0033 **	0.5833 ns	0.0509 ns	0.3546 ns	0.4752 ns
	Cl	0.0020 **	0.0094 **	<0.0001 ***	0.1668 ns	0.0153 *	0.6765 ns	0.1394 ns
	Cl_{green}	0.0173 *	0.0709 ns	<0.0001 ***	0.0503 ns	0.06499 ns	0.1100 ns	0.1260 ns
	$Cl_{red-edge}$	<0.0001 ***	<0.0001 ***	0.0670 ns	0.8384 ns	<0.0001 ***	0.8025 ns	0.0422 *
	DD	<0.0001 ***	0.0025 **	<0.0001 ***	0.2713 ns	<0.0001 ***	0.7092 ns	0.5311 ns
	DATT	<0.0001 ***	<0.0001 ***	<0.0001 ***	0.65108 ns	<0.0001 ***	0.00524 **	0.39118 ns
	MTCI	<0.0001 ***	<0.0001 ***	<0.0001 ***	0.3292 ns	<0.0001 ***	0.8102 ns	0.1174 ns
	SIPI	0.0219 *	0.1610 ns	<0.0001 ***	0.4588 ns	0.0050 **	0.2390 ns	0.5465 ns
	WBI	<0.0001 ***	0.3500 ns	0.0095 **	0.2520 ns	<0.0001 ***	0.0934 ns	0.2770 ns
	WBI/NDV	<0.0001 ***	0.8780 ns	<0.0001 ***	0.0381 *	<0.0001 ***	0.217 ns	0.2158 ns

Not significant (ns); significant at $p \leq 0.05$ (*), $p \leq 0.01$ (**), and $p \leq 0.001$ (***).

All indices, except for MCARI and CI green , were significantly affected by irrigation and the effect varied over time (interaction irrigation × DAS).

The nitrogen levels significantly affected the red-edge based indices (REIP, NDRE, MCARI, CI red-edge , DD, DATT, MTCI, together with CI), whereas the structural (NNDVI, CI green) and water band indices (WBI, WBI/NDVI) did not vary significantly. The highest discriminating capability was shown by NDRE, CI red-edge , DATT, and MTCI.

Among all of the indices tested (Tab.8), the NNDVI and WBI/NDVI indices had the best ability to differentiate the interaction of irrigation x nitrogen, showing a greater discriminating capability under low nitrogen. CI red-edge was the only index affected by the interaction between irrigation, nitrogen, and DAS.

Table 8. The effect of the interaction of irrigation x nitrogen on the vegetation indices.

Index	Nitrogen	Irrigation		
		I0	I50	I100
NNDVI	LN	0.71c	0.76ab	0.79a
	HN	0.75b	0.75ab	0.76ab
WBI/NDVI	LN	1.47a	1.3bc	1.24c
	HN	1.36b	1.31bc	1.29bc

Means followed by different letters were significantly different at $p = 0.05$.

Figure 12 shows the trend in the vegetation indices during the growing season as a function of the irrigation regime (interaction irrigation × DAS). Red-edge indices (Figure 12a,c–g) showed a similar behavior: since V12–V14, the values of I 0 treatment started to gradually decrease, while those of the

two irrigated treatments started to differentiate after the tasseling stage with a more evident decrease for I_{50} compared to I_{100} . This behavior was more marked at 66 DAS for both CI red-edge (Figure 12a) and MTCI (Fig.12e). The CI index (Fig.12b) decreased for I 0 during the crop cycle with significant differences at 58 DAS, while lower values were observed only at 79 DAS for I_{50}; I_{100} treatment maintained almost constant values along the growing cycle. The trend of the NDVI index (Fig.12i) was smoothed for both irrigated treatments, while the values of the rainfed treatments significantly decreased from 0.80 to 0.61. The SIPI index (Fig.12h) displayed similar values for all irrigation treatments throughout the growing season. The WBI index (Fig.12j) showed a similar, but the specular trend to the red-edge indices, in particular, to REIP and DATT (Fig.2c,d), with values slightly increasing under water stress progressing and during the growing season.

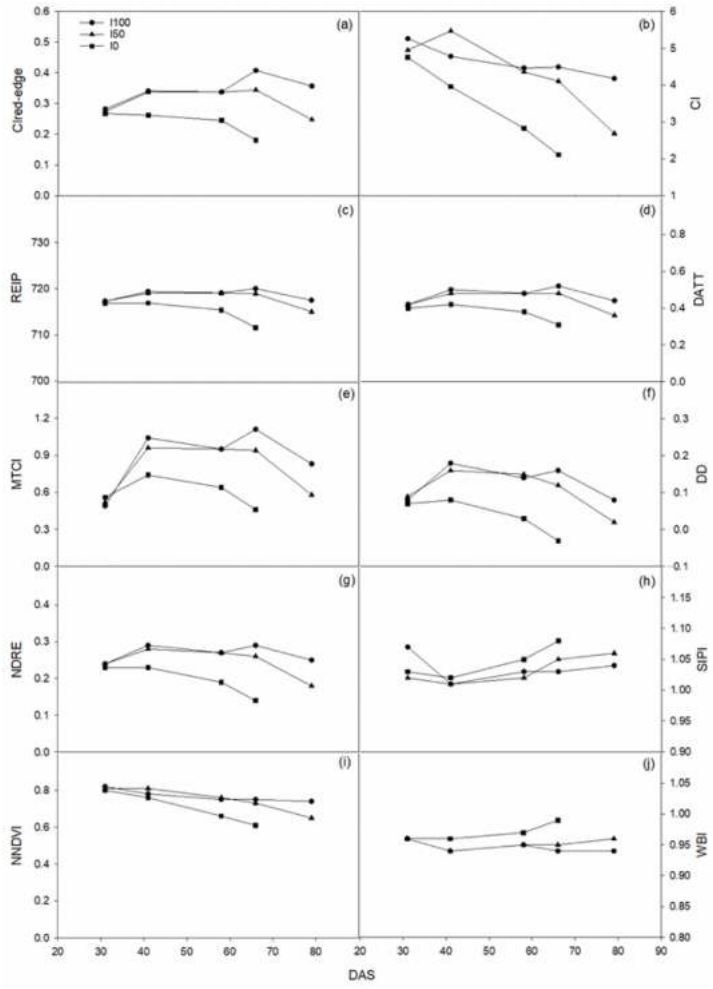

Figure 12. Variation in the CI red-edge (a), CI (b), REIP (c), DATT (d), MTCI (e), and DD (f). NDRE (g), SIPI (h), NNDVI (i), and WBI (j) during the growing season of sweet maize for different water and nitrogen treatments.

3.3.3.3. Correlation between Variables

Correlations among VIs (Tab.6) and both biometric and physiological parameters were checked using a Pearson correlation matrix (Fig.13). Among all of the analyzed indices, MTCI, DATT, and DD showed the strongest positive correlation with the chlorophyll content (CC). Similarly, LAI, as well as the gas-exchange parameters, showed the highest correlation with indices such as REIP, DD, NDRE, DATT, and MTCI. The WBI and WBI/NDVI displayed a negative correlation with all of the analyzed parameters, except for canopy temperature (Tc). However, canopy temperature had a moderately negative correlation with CI_{green} .

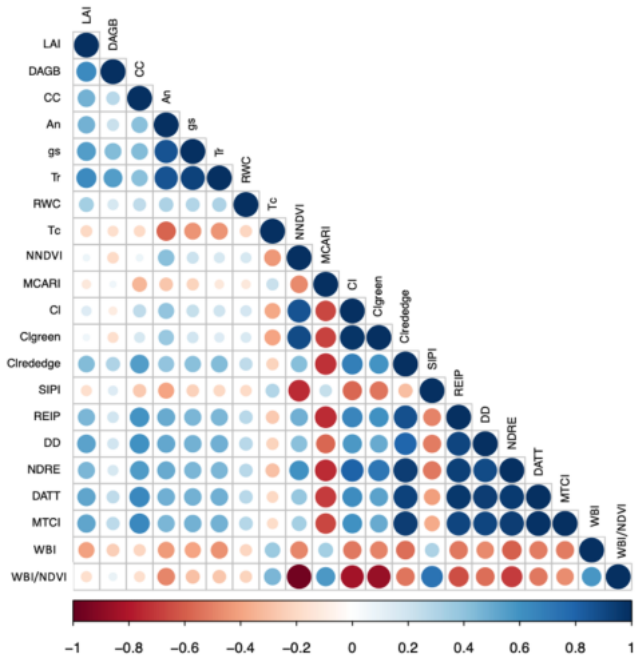

Figure 13. The correlation matrix for the bio-physiological parameters and vegetation indices for sweet maize.

The simple linear regression model was applied to link the measured eco-physiological variables and VIs. Among the parameters, the greatest coefficient of determination was found between the DATT index and chlorophyll content ($R^2 = 0.51$) as well as between the DD index and net assimilation rate ($R^2 = 0.4$) (Fig.14a,b).

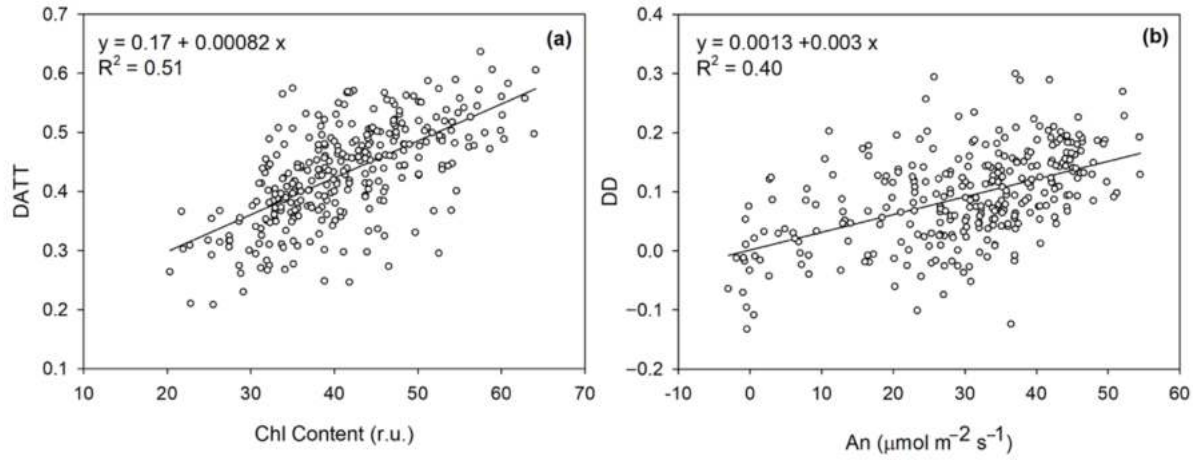

Figure 14. The linear regression parameters between the (a) DATT index and leaf chlorophyll content (Chl content); (b) DD index, and net assimilation rate (An).

3.3.4. Discussion

3.3.4.1. Differentiation between Drought and Nitrogen Deficiency

The experiment was carried out to evaluate the performance of the narrow-band vegetation indices to different water and nitrogen regimes and their interactions. The NNDVI and WBI/NDVI indices were highly affected by the interaction of water and nitrogen, showing the highest capability to distinguish low nitrogen treatment. On the other hand, in the interaction of irrigation and DAS, all indices were significantly affected, except for MCARI and CI_{green}. The red-edge-based indices (REIP, NDRE, MCARI, $CI_{red\text{-}edge}$, DD, DATT, MTCI, combined with CI) were significantly impacted by the nitrogen levels, while the structural (NNDVI, CI_{green}) and water band indices (WBI, WBI/NDVI) were not. Even though in our study the NNDVI separated the low nitrogen treatments, Shiratsuchi et al. (2011) showed a larger variation of this index due to the water supply and low ability to distinguish nitrogen treatments. It was previously confirmed that NNDVI performed better over many structural and narrow-band indices in detecting crop water stress (Kim *et al.*, 2011) and monitoring crop health (Sims *et al*., 2003). However, due to the relatively lower sensitivity to biomass and greater sensitivity to the crop chlorophyll content, Raper and Varco (2015) suggested that the red-edge-based indices be used as a more appropriate tool to determine the crop deficiency or demand for nitrogen fertilizer. Nitrogen deficiency causes red-edge reflectance and the peak of the first derivative of reflectance in the red-edge to shift toward shorter wavelengths.

Furthermore, spectral reflectance is less impacted by chlorophyll absorption characteristics beyond 730 nm in the NIR, and would only vary if the leaf morphology or water content changed in response to the stress (Raper and Varco, 2015). The effect of water absorption is better detected near 970 nm

if the stress is well-developed and in short-wave-infrared (1400–2500 nm) wavelengths (Garriha *et al.*, 2014). Water indices (WBI and WBI/NDVI) were found to be the most sensitive for distinguishing the water stress levels in crops (Ihuoma and Madramootoo, 2019). In comparison with WBI, the WBI/NDVI ratio has a stronger relationship with the crop water status because the NDVI is affected by structural and color changes (loss of pigments) in the irrigated plants, and is therefore indirectly related to the crop water content (Trunda *et al.*, 2015).

Many studies have reported the trends of VIs under different water levels. For example, Ma *et al.* (2022) found a correlation between the crop water status parameters and the $CI_{red\text{-}edge}$ and REIP indices, highlighting that the red-edge position has a high potential value for studying the canopy indices of drip irrigated cotton. Likewise, Zhang and Zhou (2019) demonstrated that the NNDVI, CI_{green} , and $CI_{red\text{-}edge}$, out of the 10 tested VIs, were the most sensitive to changes in water conditions between water treatments in a study on summer maize. Moreover, similar to our study, in the early stages, these VIs started to distinguish between the water and rainfed treatments, while the impacts of various water treatments on VIs were strongest during the peak of the growing season. In the case of our study, as observed in Figure 12, the difference between the irrigated treatments (I_{100} and I_0) was chiefly noticed for the MTCI and CI red-edge indices. Nevertheless, according to Shiratsuchi *et al.* (2011), the DATT and MTCI indices were the least affected by the irrigation levels, while the CI and $CI_{red\text{-}edge}$ indices were highly influenced, particularly at the V11 and R4 stages. In the present study, different water levels did not affect the SIPI (Fig.12), however, some studies showed a strong effect of water stress on the reduction in this index (Vincente *et al.,* 2018; Zhang *et al*., 2018).

3.3.4.2. Leaf Chlorophyll and Reflectance

Many structural indices use only two spectral bands in their formulation, the red and near-infrared regions, where light is scattered by leaf mesophyll, whereas chlorophyll indices use wavelengths in the red-edge region due to the linkage with chlorophyll content, allowing for the vegetation status to be monitored throughout the growing season. The red-edge identifies the steep transition between the reflectance absorption characteristic in red wavelengths and high NIR reflectance, with the red-edge position being defined as the point of maximum slope (inflection point). During the growth season, when there is a relatively large concentration of chlorophyll in the leaves, the red-edge spectrum is particularly sensitive to medium and high chlorophyll levels and it is considered as an excellent indicator of crop health (Kurbanov and Zakharova, 2020). Similarly, it was recently verified that the electromagnetic spectrum's red-edge area appeared to be the most responsive to the chlorophyll concentration (El-Metwalli *et al.,* 2020). This explains the positive correlation seen in our study between VIs, which were calculated using red-edge wavelengths (particularly $CI_{red\text{-}edge}$, REIP, DD,

NDRE, DATT, MTCI), and the leaf–gas exchange parameters. The peak at 705 nm is generally evident in leaves with low chlorophyll content, whereas the peak at 725 nm dominated in leaves with greater chlorophyll levels, as reported in Lamb *et al.* (2002); a similar trend was observed in our study for the REIP index.

These indicators aid researchers in a better understanding of the biophysical and biochemical processes of crop leaves as well as in crop yield prediction (Alordzinu *et al.,* 2021). Nitrogen deficit affects the leaf chlorophyll concentration, as it was widely recognized. In our study, before flowering, all treatments had close values of leaf chlorophyll content, but after the full developing stage, a separation occurred. As expected, the spectral reflectance values, starting from the NIR wavelengths, were greater in treatments of higher N levels.

In terms of VIs, DATT has already demonstrated the capacity to estimate the chlorophyll concentration with reasonable accuracy, as also observed in our work (Fig.14a). Similarly, the DD was shown to be indicative of the gas exchange parameters (Fig.14b) and by assessing the leaf chlorophyll concentration (Le Maire *et al.*, 2004; Ju *et al*., 2019).

However, the MCARI index, which has been considered as one of the most sensitive indices for chlorophyll variability, showed a slightly negative correlation with the physiological variables. A similar outcome was reported in the study of Zhang *et al.* (2019), where a negative correlation between the MCARI index and leaf chlorophyll content was found. Furthermore, the SIPI and CI indices were unable to accurately reflect the crop status, with minimal correlation with other variables. A lack of sensitivity of these indices to nutrient variation has been already described by (Blackburn *et al*., 1998; Marino *et al*., 2014).

3.3.4.3. Leaf Water and Reflectance

As expected, the water regime had a significant impact on RWC, which decreased gradually at the beginning and then rapidly as the drought progressed. The RWC increased following irrigation events in both the full and deficit irrigation treatments, with full irrigation showing greater values.

All of the calculated VIs showed a slightly negative or positive correlation with plant water content (expressed as RWC). Even though water loss from plant tissue is a result of drought-altering vegetation reflectance, in our study, a slightly negative correlation between water indices and RWC was found. However, it is currently being debated whether changes in plant reflectance can capture a minor decline in canopy water content during the early occurrence of water stress (Kovar *et al.*, 2019). Fernandes *et al.* (2020) found a negative relationship between the RWC and water indices. Furthermore, some studies have demonstrated that variations in leaf reflectance during dryness are

difficult to predict, as an increase in (Seelig *et al*., 2008), a decrease in (Jackson *et al.,*1985), and non-significant (Moore *et al*., 2008) changes were observed.

The hypothesis behind water indices (WIs) is that NIR wavelengths (970 nm) penetrate deeper into the canopy and may thus accurately evaluate the water content (Sims and Gamon, 2003). Consequently, water indices have the potential to detect early water stress in the absence of other types of stress. Water absorption bands occur in the NIR range, beyond the photosynthetically active radiation (PAR); it reduces the overlap with other abiotic stresses (Badzmierowski *et al*., 2019). In contrast to 900 nm, the degree of absorption at 970 nm increased as the water content of the plant canopies increased (Penuelas *et al*., 1996). Therefore, when plants are water-stressed, the 970 nm trough of the reflectance spectrum tends to disappear and shift toward lower wavelengths. The reflectance at 900 nm is utilized as a reference because it is affected by changes in the canopy structure as the measurement at 970 nm (Ihuoma and Madramootoo, 2017), although water has no absorption at this wavelength. Nevertheless, some studies (Wang *et al*., 2013; Katsoulas *et al*., 2016) have shown that some water-sensitive vegetation indices only give information about the water conditions, but not on the plant growth status. In the study of Zhang and Zhou (2019) on summer maize, the chlorophyll indices had a higher sensitivity to crop growth indicators (such as the canopy water content and leaf equivalent water thickness) than any of the water-sensitive indices tested.

In addition, in our study, the water indices were positively correlated to the vegetation temperature (Tc), which specifies the importance of the vegetation temperature for water stress detection. Since canopy temperature is an indicator of crop energy balance, a canopy under water stress appears to have a greater temperature than a well-watered one under the same environmental conditions. Moreover, previous research (Ihuoma and Madramootoo, 2020; Claudio *et al*., 2006) has demonstrated a positive correlation between canopy temperature and water indices (particularly WBI and WBI/NDVI).

3.3.5. Conclusions

The sweet maize response was affected by both the nitrogen and water supply. The effects of water stress were particularly evident at the flowering stage, not allowing for grain formation in the rainfed treatments. Both the water and nitrogen deficiencies reflected on the irrigation water use efficiency, which demonstrated the highest performance under deficit irrigation and nitrogen fertilization.

The analysis of the whole spectrum and the calculation of the vegetation indices demonstrated the importance of the red-edge vegetation indices in assessing the status of sweet maize. Thus, it is shown that remotely sensed reflectance indices are promising predictive tools for the impact of drought and

nutritional deficiency on the photosynthetic activity and water status. The findings of this study confirmed that, among all of the studied indices, NNDVI and WBI/NDVI were the only two indices affected by the interaction of water and nitrogen. Moreover, the red-edge indices had a high sensitivity to nitrogen levels, in particular, NDRE, $CI_{red\text{-}edge}$, DATT, and MTCI showed a great discrimination capability. Therefore, the detection of crop stress may become simpler by the appropriate selection of VIs. Since several indices did not show high sensitivity to the studied crop parameters, it is important to bear in mind that the link between the canopy-level spectral signal and the target property might be influenced by canopy structure factors including the plant size, age, and leaf angle. Moreover, it must be considered that under field conditions, water or/and nutrient deficits may be accompanied by changes in any other leaf and canopy properties that would affect the reflectance characteristics. Thus, in future steps, more complex experiments and comparative studies should be conducted to fully understand and differentiate the effects of stresses on the crop parameters. Multivariate techniques, such as partial least squares regression, and machine learning methods (random forest, multiple adaptive regression splines) may overcome certain limitations in assessing the vegetation parameters under different stresses, which should be investigated in future works.

3.3.6. References

Osakabe, Y.; Osakabe, K.; Shinozaki, K.; Tran, L.-S. Response of plants to water stress. Front. Plant Sci. 2014, 5, 86.

Zhang, F.; Zhou, G. Estimation of vegetation water content using hyperspectral vegetation indices: A comparison of crop water indicators in response to water stress treatments for summer maize. BMC Ecol. 2019, 19, 18.

Yuan, L.; Cui, S.; Zhang, Z.; Zhuang, K.; Wang, Z.; Zhang, Q. Determining effects of water and nitrogen input on maize (Zea mays) yield, water- and nitrogen-use efficiency: A global synthesis. Sci. Rep. 2020, 10, 9699.

Piscitelli, L.; Colovic, M.; Aly, A.; Hamze, M.; Todorovic, M.; Cantore, V.; Albrizio, R. Adaptive Agricultural Strategies for Facing Water Deficit in Sweet Maize Production: A Case Study of a Semi-Arid Mediterranean Region. Water 2021, 13, 3285.

Moriondo, M.; Giannakopoulos, C.; Bindi, M. Climate change impact assessment: The role of climate extremes in crop yield simulation. Clim. Chang. 2011, 104, 679–701.

Holzman, M.E.; Carmona, F.; Rivas, R.; Niclòs, R. Early assessment of crop yield from remotely sensed water stress and solar radiation data. ISPRS J. Photogramm. Remote Sens. 2018, 145, 297–308.

Mladenova, I.E.; Bolten, J.D.; Crow, W.T.; Anderson, M.C.; Hain, C.R.; Johnson, D.M.; Mueller, R. Intercomparison of soil moisture, evaporative stress, and vegetation indices for estimating corn and soybean yields over the US. IEEE J. Sel. Top. Appl. Earth Obs. Remote Sens. 2017, 10, 1328–1343.

Massignam, A.; Chapman, S.; Hammer, G.; Fukai, S. Physiological determinants of maize and sunflower grain yield as affected by nitrogen supply. Field Crop Res. 2009, 113, 256–267.

Leghari, S.J.; Wahocho, N.; Laghari, G.; Laghari, A.; Bhabhan, G.; HussainTalpur, K.; Ahmed, T.; Wahocho, S.; Lashari, A. Role of Nitrogen for Plant Growth and Development: A review. Adv. Environ. Biol. 2016, 10, 209–218.

Maheswari, M.; Murthy, A.N.G.; Shanker, A.K. 12-Nitrogen Nutrition in Crops and Its Importance in Crop Quality. In The Indian Nitrogen Assessment; Abrol, Y.P., Adhya, T.K., Aneja, V.P., Raghuram, N., Pathak, H., Kulshrestha, U., Sharma, C., Singh, B., Eds.; Elsevier: Amsterdam, The Netherlands, 2017; pp. 175–186, ISBN 978-0-12-811836-8.

Ranjan, R.; Chopra, U.K.; Sahoo, R.N.; Singh, A.K.; Pradhan, S. Assessment of plant nitrogen stress in wheat (Triticum aestivum L.) through hyperspectral indices. Int. J. Remote Sens. 2012, 33, 6342–6360.

Cossani, C.M.; Sadras, V.O. Water–nitrogen colimitation in grain crops. Adv. Agron. 2018, 150, 231–274.

Sadras, V.O.; Hayman, P.T.; Rodriguez, D.; Monjardino, M.; Bielich, M.; Unkovich, M.; Mudge, B.; Wang, E. Interactions between water and nitrogen in Australian cropping systems: Physiological, agronomic, economic, breeding and modelling perspectives. Crop Pasture Sci. 2016, 67, 1019–1053.

Tilling, A.K.; O'Leary, G.J.; Ferwerda, J.G.; Jones, S.D.; Fitzgerald, G.J.; Rodriguez, D.; Belford, R. Remote sensing of nitrogen and water stress in wheat. Field Crop Res. 2007, 104, 77–85.

Bell, J.; Schwartz, R.; Mcinnes, K.; Howell, T.; Morgan, C. Deficit irrigation effects on yield and yield components of grain sorghum. Agric. Water Manag. 2018, 203, 289–296.

Pinter, P.J., Jr.; Hatfield, J.L.; Schepers, J.S.; Barnes, E.M.; Moran, M.S.; Daughtry, C.S.T.; Upchurch, D.R. Remote sensing for crop management. Photogramm. Eng. Remote Sens. 2003, 69, 647–664.

Singh, P.; Pandey, P.; Petropoulos, G.; Pavlides, A.; Srivastava, P.; Koutsias, N.; Deng, K.; Bao, Y. Hyperspectral remote sensing in precision agriculture: Present status, challenges, and future trends. In Hyperspectral Remote Sensing: Theory and Applications; Pandey, P.C., Srivastava, P.K., Balzter, H., Bhattacharya, B., Petropoulos, G., Eds.; Elsevier: Amsterdam, The Netherlands, 2020.

Sahoo, R.; Ray, S.; Manjunath, R. Hyperspectral remote sensing of agriculture. Curr. Sci. 2015, 108, 848–859.

Monteiro, P.F.C.; Angulo Filho, R.; Xavier, A.C.; Monteiro, R.O.C. Assessing biophysical variable parameters of bean crop with hyperspectral measurements. Sci. Agric. 2012, 69, 87–94.

Zhu, W.; Sun, Z.; Gong, H.; Li, J.; Liao, X.; Peng, J.; Li, S.; Zhu, K. Estimating leaf chlorophyll content of crops via optimal unmanned aerial vehicle hyperspectral data at multi-scales. Comput. Electron. Agric. 2020, 178, 105786.

Li, H.; Li, D.; Xu, K.; Cao, W.; Jiang, X.; Ni, J. Monitoring of Nitrogen Indices in Wheat Leaves Based on the Integration of Spectral and Canopy Structure Information. Agronomy 2022, 12, 833.

Hansen, P.M.; Schjoerring, J.K. Reflectance measurement of canopy biomass and nitrogen status in wheat crops using normalized difference vegetation indices and partial least squares regression. Remote Sens. Environ. 2003, 86, 542–553.

Stroppiana, D.; Boschetti, M.; Brivio, P.A.; Bocchi, S. Plant nitrogen concentration in paddy rice from field canopy hyperspectral radiometry. Field Crop Res. 2009, 111, 119–129.

Chen, P.; Haboudane, D.; Tremblay, N.; Wang, J.; Vigneault, P.; Li, B. New spectral indicator assessing the efficiency of crop nitrogen treatment in corn and wheat. Remote Sens. Environ. 2010, 114, 1987–1997.

Yao, X.; Zhu, Y.; Tian, Y.; Feng, W.; Cao, W. Exploring hyperspectral bands and estimation indices for leaf nitrogen accumulation in wheat. Int. J. Appl. Earth Obs. Geoinf. 2010, 12, 89–100.

Gitelson, A.A.; Viña, A.; Ciganda, V.; Rundquist, D.C.; Arkebauer, T.J. Remote estimation of canopy chlorophyll content in crops. Geophys. Res. Lett. 2005, 32, L08403.

Delegido, J.; Fernandez, G.; Gandia, S.; Moreno, J. Retrieval of chlorophyll content and LAI of crops using hyperspectral techniques: Application to PROBA/CHRIS data. Int. J. Remote Sens. 2008, 29, 7107–7127.

Vincini, M.; Frazzi, E. Comparing narrow and broad-band vegetation indices to estimate leaf chlorophyll content in

planophile crop canopies. Precis. Agric. 2011, 12, 334–344.

Inoue, Y.; Peñuelas, J.; Miyata, A.; Mano, M. Normalized difference spectral indices for estimating photosynthetic efficiency and capacity at a canopy scale derived from hyperspectral and CO 2 flux measurements in rice. Remote Sens. Environ. 2008, 112, 156–172.

Garbulsky, M.F.; Peñuelas, J.; Papale, D.; Ardö, J.; Goulden, M.L.; Kiely, G.; Richardson, A.D.; Rotenberg, E.; Veenendaal, E.M.; Filella, I. Patterns and controls of the variability of radiation use efficiency and primary productivity across terrestrial ecosystems. Glob. Ecol. Biogeogr. 2010, 19, 253–267.

Ceccato, P.; Gobron, N.; Flasse, S.; Pinty, B.; Tarantola, S. Designing a spectral index to estimate vegetation water content from remote sensing data: Part 1: Theoretical approach. Remote Sens. Environ. 2002, 82, 188–197.

Zarco-Tejada, P.J.; González-Dugo, V.; Williams, L.E.; Suarez, L.; Berni, J.A.J.; Goldhamer, D.; Fereres, E. A PRI-based water stress index combining structural and chlorophyll effects: Assessment using diurnal narrow-band airborne imagery and the CWSI thermal index. Remote Sens. Environ. 2013, 138, 38–50.

Ihuoma, S.O. The Use of Spectral Reflectance Data to Assess Plant Stress and Improve Irrigation Water Management. Ph.D. Thesis, McGill University, Montreal, QC, Canada, 2020.

Apan, A.; Held, A.; Phinn, S.; Markley, J. Detecting sugarcane 'orange rust'disease using EO-1 Hyperion hyperspectral imagery. Int. J. Remote Sens. 2004, 25, 489–498.

Ray, S.S.; Jain, N.; Arora, R.K.; Chavan, S.; Panigrahy, S. Utility of hyperspectral data for potato late blight disease detection.J. Indian Soc. Remote Sens. 2011, 39, 161–169.

Calderón, R.; Navas-Cortés, J.A.; Lucena, C.; Zarco-Tejada, P.J. High-resolution airborne hyperspectral and thermal imagery for early detection of Verticillium wilt of olive using fluorescence, temperature and narrow-band spectral indices. Remote Sens. Environ. 2013, 139, 231–245.

Zou, X.; Haikarainen, I.; Haikarainen, I.P.; Mäkelä, P.; Mõttus, M.; Pellikka, P. Effects of crop leaf angle on LAI-sensitive narrow-band vegetation indices derived from imaging spectroscopy. Appl. Sci. 2018, 8, 1435.

Fitzgerald, G.J.; Rodriguez, D.; Christensen, L.K.; Belford, R.; Sadras, V.O.; Clarke, T.R. Spectral and thermal sensing for nitrogen and water status in rainfed and irrigated wheat environments. Precis. Agric. 2006, 7, 233–248.

Boiarskii, B.; Hasegawa, H. Comparison of NDVI and NDRE indices to detect differences in vegetation and chlorophyll content.J. Mech. Contin. Math. Sci. 2019, 4, 20–29.

Thompson, C.N.; Guo, W.; Sharma, B.; Ritchie, G.L. Using normalized difference red edge index to assess maturity in cotton. Crop Sci. 2019, 59, 2167–2177.

Shaver, T.M.; Kruger, G.R.; Rudnick, D.R. Crop canopy sensor orientation for late season nitrogen determination in corn. J. Plant Nutr. 2017, 40, 2217–2223.

Perry, E.M.; Davenport, J.R. Spectral and spatial differences in response of vegetation indices to nitrogen treatments on apple.Comput. Electron. Agric. 2007, 59, 56–65.

Roberts, D.A.; Roth, K.L.; Perroy, R.L. 14 hyperspectral vegetation indices. Hyperspectral Remote Sens. Veg. 2016, 2016, 306–327.

Penuelas, J.; Baret, F.; Filella, I. Semi-empirical indices to assess carotenoids/chlorophyll a ratio from leaf spectral reflectance.Photosynthetica 1995, 31, 221–230.

Zhao, T.J.; Zhang, L.X.; Shi, J.C.; Jiang, L.M. A physically based statistical methodology for surface soil moisture retrieval in the Tibet Plateau using microwave vegetation indices. J. Geophys. Res. Atmos. 2011, 116, D08116.

Wang, S.; Baig, M.H.A.; Zhang, L.; Jiang, H.; Ji, Y.; Zhao, H.; Tian, J. A simple enhanced water index (EWI) for percent surface water estimation using Landsat data. IEEE J. Sel. Top. Appl. Earth Obs. Remote Sens. 2015, 8, 90–97.

McCall, D.S.; Zhang, X.; Sullivan, D.G.; Askew, S.D.; Ervin, E.H. Enhanced soil moisture assessment using narrowband reflectance vegetation indices in creeping bentgrass. Crop Sci. 2017, 57, S-161–S-168.

Daughtry, C.S.T.; Walthall, C.L.; Kim, M.S.; De Colstoun, E.B.; McMurtrey Iii, J.E. Estimating corn leaf chlorophyll concentration from leaf and canopy reflectance. Remote Sens. Environ. 2000, 74, 229–239.

Yang, W.-H.; Peng, S.; Huang, J.; Sanico, A.L.; Buresh, R.J.; Witt, C. Using leaf color charts to estimate leaf nitrogen status of rice.Agron. J. 2003, 95, 212–217.

Casanova, D.; Epema, G.F.; Goudriaan, J. Monitoring rice reflectance at field level for estimating biomass and LAI. F. Crop. Res.1998, 55, 83–92.

Aparicio, N.; Villegas, D.; Casadesus, J.; Araus, J.L.; Royo, C. Spectral vegetation indices as nondestructive tools for determining durum wheat yield. Agron. J. 2000, 92, 83–91.

Wang, Z.; Wang, J.; Liu, L.; Huang, W.; Zhao, C.; Lu, Y. Estimation of Nitrogen Status in Middle and Bottom Layers of Winter Wheat Canopy by Using Ground-Measured Canopy Reflectance. Commun. Soil Sci. Plant Anal. 2005, 36, 2289–2302.

Riedel, S.M.; Epstein, H.E.; Walker, D.A. Biotic controls over spectral reflectance of arctic tundra vegetation. Int. J. Remote Sens.2005, 26, 2391–2405.

Tsonev, T.; Wahbi, S.; Sun, P.; Sorrentino, G.; Centritto, M. Gas exchange, water relations and their relationships with photochemical reflectance index in Quercus ilex plants during water stress and recovery. Int. J. Agric. Biol. 2014, 16, 335–341.

Silva-Perez, V.; Molero, G.; Serbin, S.P.; Condon, A.G.; Reynolds, M.P.; Furbank, R.T.; Evans, J.R. Hyperspectral reflectance as a tool to measure biochemical and physiological traits in wheat. J. Exp. Bot. 2018, 69, 483–496.

Chen, T.; Wang, L.; Qi, H.; Wang, X.; Zeng, R.; Zhu, B.; Lan, Y.; Zhang, L. Monitoring of water stress in peanut using multispectral indices derived from canopy hyperspectral. Int. J. Precis. Agric. Aviat. 2020, 3, 50–58.

Sellami, M.H.; Albrizio, R.; Colovic, M.; Hamze, M.; Cantore, V.; Todorovic, M.; Piscitelli, L.; Stellacci, A.M. Selection of Hyperspectral Vegetation Indices for Monitoring Yield and Physiological Response in Sweet Maize under Different Water and Nitrogen Availability. Agronomy 2022, 12, 489.

Heckmann, D.; Schlüter, U.; Weber, A.P.M. Machine learning techniques for predicting crop photosynthetic capacity from leaf reflectance spectra. Mol. Plant 2017, 10, 878–890.

Yendrek, C.R.; Tomaz, T.; Montes, C.M.; Cao, Y.; Morse, A.M.; Brown, P.J.; McIntyre, L.M.; Leakey, A.D.B.; Ainsworth, E.A.High-throughput phenotyping of maize leaf physiological and biochemical traits using hyperspectral reflectance. Plant Physiol. 2017, 173, 614–626.

Weber, V.S.; Araus, J.L.; Cairns, J.E.; Sanchez, C.; Melchinger, A.E.; Orsini, E. Prediction of grain yield using reflectance spectra of canopy and leaves in maize plants grown under different water regimes. Field Crop Res. 2012, 128, 82–90.

Haboudane, D.; Miller, J.R.; Pattey, E.; Zarco-Tejada, P.J.; Strachan, I.B. Hyperspectral vegetation indices and novel algorithms for predicting green LAI of crop canopies: Modeling and validation in the context of precision agriculture. Remote Sens. Environ. 2004, 90, 337–352.

Staff, S.S. Keys to Soil Taxonomy; United States Department of Agriculture: Washington, DC, USA, 2014.

Todorovic, M. An Excel-based tool for real time irrigation management at field scale. In Proceedings of the International Symposium on Water and Land Management for Sustainable Irrigated Agriculture, Adana, Turkey, 4–8 April 2006; pp. 4–8.

Allen, R.G.; Pereira, L.S.; Raes, D.; Smith, M. Crop Evapotranspiration. In Guidelines for Computing Crop Water

Requirements—FAO Irrigation and Drainage Paper 56; Food and Agriculture Organization: Rome, Italy, 1998.

Von Caemmerer, S.; Farquhar, G. Some relationships between the biochemistry of photosynthesis and the gas exchange of leaves.Planta 1981, 153, 376–387.

Guyot, G.; Baret, F. Utilisation de la haute resolution spectrale pour suivre l'etat des couverts vegetaux. Spectr. Signat. Objects Remote Sens. 1988, 287, 279.

Barnes, E.M.; Clarke, T.R.; Richards, S.E.; Colaizzi, P.D.; Haberland, J.; Kostrzewski, M.; Waller, P.; Choi, C.; Riley, E.; Thompson, T.Coincident detection of crop water stress, nitrogen status and canopy density using ground based multispectral data. In Proceedings of the Fifth International Conference on Precision Agriculture, Bloomington, MN, USA, 16–19 July 2000; Volume 1619.

Perry, E.M.; Roberts, D.A. Sensitivity of Narrow-Band and Broad-Band Indices for Assessing Nitrogen Availability and Water Stress in an Annual Crop. Agron. J. 2008, 100, 1211–1219.

Shiratsuchi, L.; Ferguson, R.; Shanahan, J.; Adamchuk, V.; Rundquist, D.; Marx, D.; Slater, G. Water and nitrogen effects on active canopy sensor vegetation indices. Agron. J. 2011, 103, 1815–1826.

Le Maire, G.; Francois, C.; Dufrêne, E. Towards universal broad leaf chlorophyll indices using PROSPECT simulated database and hyperspectral reflectance measurements. Remote Sens. Environ. 2004, 89, 1–28.

Peñuelas, J.; Pinol, J.; Ogaya, R.; Filella, I. Estimation of plant water concentration by the reflectance water index WI (R900/R970).Int. J. Remote Sens. 1997, 18, 2869–2875.

R Core Team. R: A Language and Environment for Statistical Computing; R Foundation for Statistical Computing: Vienna, Austria, 2018.

Kim, Y.; Glenn, D.M.; Park, J.; Ngugi, H.K.; Lehman, B.L. Hyperspectral image analysis for water stress detection of apple trees.Comput. Electron. Agric. 2011, 77, 155–160.

Sims, D.; Gamon, J. Estimation of vegetation water content and photosynthetic tissue area from spectral reflectance: A comparison of indices based on liquid water and chlorophyll absorption features. Remote Sens. Environ. 2003, 84, 526–537.

Raper, T.B.; Varco, J.J. Canopy-scale wavelength and vegetative index sensitivities to cotton growth parameters and nitrogen status. Precis. Agric. 2015, 16, 62–76.

Carter, G.A.; Knapp, A.K. Leaf optical properties in higher plants: Linking spectral characteristics to stress and chlorophyll concentration. Am. J. Bot. 2001, 88, 677–684.

Garriga, M.; Retamales, J.B.; Romero-Bravo, S.; Caligari, P.D.S.; Lobos, G.A. Chlorophyll, anthocyanin, and gas exchange changes assessed by spectroradiometry in Fragaria chiloensis under salt stress. J. Integr. Plant Biol. 2014, 56, 505–515.

Ihuoma, S.O.; Madramootoo, C.A. Sensitivity of spectral vegetation indices for monitoring water stress in tomato plants. Comput.Electron. Agric. 2019, 163, 104860.

Trunda, P.; Holub, P.; Klem, K. The effect of drought and nitrogen fertilization on the production, morphometry, and spectral characteristics of winter wheat. Glob. Chang. Complex Chall. 2015, 2015, 110.

Ma, L.; Chen, X.; Zhang, Q.; Lin, J.; Yin, C.; Ma, Y.; Yao, Q.; Feng, L.; Zhang, Z.; Lv, X. Estimation of Nitrogen Content Based on the Hyperspectral Vegetation Indexes of Interannual and Multi-Temporal in Cotton. Agronomy 2022, 12, 1319.

Vicente, R.; Vergara-Díaz, O.; Medina, S.; Chairi, F.; Kefauver, S.C.; Bort, J.; Serret, M.D.; Aparicio, N.; Araus, J.L. Durum wheat ears perform better than the flag leaves under water stress: Gene expression and physiological evidence. Environ. Exp. Bot. 2018, 153, 271–285.

Zhang, Y.J.; Hou, M.Y.; Xue, H.Y.; Liu, L.T.; Sun, H.C.; Li, C.D.; Dong, X.J. Photochemical reflectance index and solar-induced fluorescence for assessing cotton photosynthesis under water-deficit stress. Biol. Plant. 2018, 62, 817–825.

Kurbanov, R.K.; Zakharova, N.I. Application of vegetation indexes to assess the condition of crops. Agric. Mach. Technol. 2020, 14, 4.

El-Metwalli, A.; Tyler, A. Estimation of maize properties and differentiating moisture and nitrogen deficiency stress via ground—Based remotely sensed data. Agric. Water Manag. 2020, 242, 106413.

Lamb, D.; Steyn-Ross, M.; Schaare, P.; Hanna, M.; Silvester, W.; Steyn-Ross, A. Estimating leaf nitrogen concentration in ryegrass (Lolium spp.) pasture using the chlorophyll red-edge: Theoretical modelling and experimental observations. Int. J. Remote Sens. 2002, 23, 3619–3648.

Alordzinu, K.; Li, J.; Lan, Y.; Appiah, S.; Al Aasmi, A.; Wang, H.; Liao, J.; Sam-Amoah, L.; Qiao, S. Ground-Based Hyperspectral Remote Sensing for Estimating Water Stress in Tomato Growth in Sandy Loam and Silty Loam Soils. Sensors 2021, 21, 5705.

Elvanidi, A.; Katsoulas, N.; Ferentinos, K.; Bartzanas, T.; Kittas, C. Hyperspectral machine vision as a tool for water stress severity assessment in soilless tomato crop. Biosyst. Eng. 2018, 165, 25–35.

Ihuoma, S.O.; Madramootoo, C. Narrow-band reflectance indices for mapping the combined effects of water and nitrogen stress in field grown tomato crops. Biosyst. Eng. 2020, 192, 133–143.

Ju, C.H.; Tian, Y.C.; Yao, X.; Cao, W.X.; Zhu, Y.; Hannaway, D. Estimating Leaf Chlorophyll Content Using Red Edge Parameters.Pedosphere 2010, 20, 633–644.

Zhang, C.; Dai, X.; Qin, Q.; Li, J.; Zhang, T.; Sun, Y. Spectral characteristics of copper-stressed vegetation leaves and further understanding of the copper stress vegetation index. Int. J. Remote Sens. 2019, 40, 4473–4488.

Blackburn, G. Quantifying Chlorophylls and Caroteniods at Leaf and Canopy Scales: An Evaluation of Some Hyperspectral Approaches. Remote Sens. Environ. 1998, 66, 273–285.

Marino, G.; Pallozzi, E.; Cocozza, C.; Tognetti, R.; Giovannelli, A.; Cantini, C.; Centritto, M. Assessing gas exchange, sap flow and water relations using tree canopy spectral reflectance indices in irrigated and rainfed Olea europaea L. Environ. Exp. Bot. 2014, 99, 43–52.

Kovar, M.; Brestic, M.; Sytar, O.; Barek, V.; Hauptvogel, P.; Zivcak, M. Evaluation of Hyperspectral Reflectance Parameters to Assess the Leaf Water Content in Soybean. Water 2019, 443, 443.

Fernandes, A.; Fortini, E.; Areal de Carvalho Muller, L.; Batista, D.; Vieira, L.; Oliveira Silva, P.; Amaral, C.; Poethig, R.; Otoni, W.Leaf development stages and ontogenetic changes in passionfruit (Passiflora edulis Sims.) are detected by narrowband spectral signal. J. Photochem. Photobiol. B. 2020, 209, 111931.

Seelig, H.; Hoehn, A.; Stodieck, L.; Klaus, D.; Adams, W.W., III; Emery, W. The assessment of leaf water content using leaf reflectance ratios in the visible, near-, and short-wave-infrared. Int. J. Remote Sens. 2008, 29, 3701–3713.

Jackson, R.; Ezra, C. Spectral response of cotton to suddenly induced water stress. Int. J. Remote Sens. 1985, 6, 177–185.

Moore, J.; Vicré-Gibouin, M.; Farrant, J.; Driouich, A. Adaptations of higher plant cell walls to water loss: Drought vs. desiccation.Physiol. Plant. 2008, 134, 237–245.

Badzmierowski, M.J.; McCall, D.S.; Evanylo, G. Using Hyperspectral and Multispectral Indices to Detect Water Stress for an Urban Turfgrass System. Agronomy 2019, 9, 439.

Penuelas, J.; Filella, I.; Serrano, L.; Savé, R. Cell wall elasticity and Water Index (R970 nm/R900 nm) in wheat under different nitrogen availabilities. Int. J. Remote Sens. 1996, 17, 373–382.

Ihuoma, S.O.; Madramootoo, C. Recent advances in crop water stress detection. Comput. Electron. Agric. 2017, 141, 267–275.

Wang, L.; Hunt, E.R., Jr.; Qu, J.; Hao, X.; Daughtry, C. Remote sensing of fuel moisture content from ratios of narrow-band vegetation water and dry-matter indices. Remote Sens. Environ. 2013, 129, 103–110.

Katsoulas, N.; Elvanidi, A.; Ferentinos, K.; Kacira, M.; Bartzanas, T.; Kittas, C. Crop reflectance monitoring as a tool for water stress detection in greenhouses: A review. Biosyst. Eng. 2016, 151, 374.

Claudio, H.; Cheng, Y.; Fuentes, D.; Gamon, J.; Luo, H.; Oechel, W.; Qiu, H.-L.; Rahman, F.; Sims, D. Monitoring drought effects on vegetation water content and fluxes in chaparral with the 970 nm water band index. Remote Sens. Environ. 2006, 103, 304–311.

3.4. Comparative performance of Proximal Hyperspectral Vegetation Indices Vs. Aerial RGB indices for evaluation of sweet-maize behaviour

Abstract: In order to overcome some environmental limitations in crop production, remote sensing measures may be utilized to quickly evaluate crop performance and to cost-effectively monitor a large number of plots. In this work, we examined how well a set of RGB (red-green-blue) indices and hyperspectral vegetation indices described the response of sweet maize (*Zea mays* var. saccharata L.) under different nitrogen and water inputs. During two growing seasons of the sweet maize crop, measurements were conducted at two different levels: at the ground for collecting hyperspectral information and bio-physiological parameters and from an aerial platform for RGB indices acquisition. The greatest power was found for Green-Area index (GA) predicting Leaf Area Index (LAI) in 2020 (R^2=0.61) and Leaf Chlorophyll Concentration (CC) in 2021 (R^2=0.49). Moreover, the capacity of predicting gas-exchange parameters by red-edge positions was demonstrated. Several red-edge indices, including $Cl_{red\text{-}edge}$, NDRE, MTCI, DD, and REIP, were shown to be the best predictors of the bio-physiological parameters.
The usefulness of RGB-derived indices, which are less expensive and less time-consuming compared to hyperspectral indices, is showed by this study.

Keywords: RGB indices, Hyperspectral indices, drones in agriculture, bio-physiological crop parameters

3.4.1. Introduction

Precision agriculture, water stress and nutrient deficiency management have benefited from remote sensing approaches at the canopy level (Liaghat and Balasundram, 2010; Virnodkar *et al*., 2020). As a result, those spectral techniques have been presented as possible options for detecting crop N status and water stress across wide regions (Katsoulas *et al.,* 2016). These techniques can assist farmers in practising more sustainable agriculture, by providing (where feasible) the resources (such as water and fertilizer) required to ensure a higher yield (Shoshany *et al.*, 2013).
However, as the new technology adoption sometimes requires a big upfront investment, it is confined to large-scale production and/or farmers with significant financial resources (Mulla, 2013; Wachendorf *et al.*, 2018).

The use of both traditional laboratory procedures and remote sensing techniques to monitor crop development has certain drawbacks, including high costs and variability of weather conditions. Sometimes, even though some satellite images (such as Sentinel-2) are frequently available for free download, the low resolution (not higher than 100 square meters per pixel), intervals of data acquisition, weather factors (such as clouds), and the need for computer technical support and qualified people make this type of remote sensing inefficient for small-scale farmers (Khannal *et al*., 2020). An alternative option may be optical sensors, such as portable spectroradiometers. However, this approach has a limitation on portability and the time required to take measurements in different field locations (Haghighattalab *et al*., 2016).

Hence, using low-cost imaging approaches such as RGB (red-green-blue) imaging with a digital camera might help to improve agriculture monitoring in arid and semi-arid Mediterranean regions where irrigation and fertilization are sometimes not regulated in terms of time and volume (Danzi *et al.*, 2019).

Moreover, the use of RGB above canopy provides accurate results, since image capturing and data processing have become ever more commercially successful for different practical concerns in agriculture and biology as a result of recent advancements in remote sensing technology (Tsouros *et al.*, 2019). RGB images are an important discovery because of the colour variation dependence of different biological samples, as well as the ease with which they may be processed. Generally, the RGB imaging method has been developed for rapid and non-invasive determination of colour changes caused by nutritional stress such as chlorophyll content in the leaves (Yadav *et al.,* 2010). Furthermore, using information collected from digital RGB photos for calculating vegetation indices provides a low-cost alternative to using multispectral and hyperspectral bands (Yousfi *et al.,* 2019). Since RGB imaging approach detects leaf colour changes, it may be used to monitor the progress of a plant's development and health, water and nutritional level, plant disease, senescence, etc. Therefore, RGB VIs have previously been used for precision crop management at both the canopy and leaf levels aiming at improving crop performance under a variety of treatments (Norasma *et al*., 2018; Fernandez-Gallego *et al*., 2019; Buchaillot *et al.,* 2019; Zhang *et al.*, 2019; Wakabayashi *et al.,* 2021). Rorie *et al.* (2011) have reported that digital-image analysis is a simple method providing a determination of maize nitrogen status with the potential as a diagnostic tool for crop nitrogen needs evaluation. Besides that, measuring nitrogen status above crop tissue is cheaper and less time-consuming than soil tests (Li *et al.,* 2011).

Assessment of RGB and multispectral indices for maize under phosphorus fertilization and comparison between ground and UAV (Unmanned Aerial Vehicle) measurements done by Gracia-Romero *et al.* (2017) showed that ground-measured RGB indices such as hue, a*, u*, GA and GGA

indices were significantly affected by the absence of fertilizer and they had better performance in predicting grain yield than multispectral indices. Recently, it was found that the same RGB indices (a*, u*, GA and GGA) were associated with leaf wilting, with higher accuracy from proximally taken images (Sarkar *et al*., 2021). In a study on wheat under different irrigation regimes, vegetation indices, obtained from RGB conventional camera, showed similar or slightly better performance in yield predicting than NDVI (Casadesus *et al.*, 2007). According to Kefauver *et al.* (2015), RGB indices at both the canopy and at the leaf levels may successfully be employed for precise crop management in wheat and maize for fertilizers and irrigation treatments, monitoring disease and as effective high-throughput phenotyping techniques in breeding programs.

RGB images can be processed by analysing red, green, and blue light broadband reflectance values or by employing different colour spaces, as the Breedpix code suite does (Gracia-Romero *et al*., 2017).

In our study, RGB VIs described above are assessed for their potential to monitor sweet maize growth under different water and nitrogen treatments. The performance of RGB VIs was evaluated and compared to the performance of hyperspectral VIs collected by a spectroradiometer.

3.4.2. Materials and Methods

3.4.2.1. Study area and experimental design

Field trials were done at the experimental field of the Mediterranean Agronomic Institute (IAMB) (Fig.15) in Valenzano, Bari (41°03'N, 16°53'E, 77 m above sea level), Southern Italy, during two growing seasons in 2020 and 2021. The area experiences typical Mediterranean weather, with mild winters and dry summers. The soil in the study region is silty-clay-loam.

From June to September 2020 and 2021, sweet maize (*Zea mays* var. saccharata L.) was cultivated on 18 plots (each measuring 10 × 10 m). Sweet maize was grown under three irrigation regimes, including full irrigation (I100), deficit irrigation (I50) and rainfed (I0), and two Nitrogen treatments, which are High Nitrogen Level treatment (HN - 300 kg ha^{-1}) and Low Nitrogen Level (LN - 50 kg ha^{-1}). In HN level plots, in additionally to fertilization before sowing, 250 kg ha^{-1} as urea was applied. A split-plot experimental design with three replicates was used to distribute the treatments, with irrigation regime (WR) serving as the main plot component and N level (N) serving as the sub-plot factor.

A regular set of daily meteorological measurements (air temperature, relative humidity, solar radiation, wind speed, and precipitation) were collected from the weather station nearby to the experimental field.

For crops under irrigated treatments water was supplied by drip method system. Moreover, an Excel-Based model that calculates crop evapotranspiration and irrigation water needs on a day-by-day basis using the Allen et al. standard approach was used to manage crop water balance and irrigation schedule (1998).

Figure 15. Field experimental design

3.4.2.2. Data collection

3.4.2.2.1. RGB image acquisition and analysis

RGB images were collected using the digital camera (20 MP) installed on a drone (Mavik-2 DJI). Each image was taken from the (Fig.16) of the plots, holding aircraft 80-100 cm above the canopy in the zenithal plane. Image acquisition has been done on sunny days, during both growing seasons, from development stage until harvesting.

Thereafter, the Breedpix 0.2 program, which was modified for JAVA 8 and included as a plugin in FIJI (https://github.com/George-haddad/CIMMYT), was then used to analyse RGB images. This program makes it possible to extract RGB vegetation indices (VIs) in connection to various colour characteristics (Casades *et al.,* 2007) and is a free program that can quickly analyse hundreds of images at once and output a number of indices. Utilizing BreedPix functions, RGB values were changed to hue-saturation-intensity (HSI) values, which are based on how people see colour, to make interpretation simpler. Chromatic coordinates from the CIELab and CIELuv color spaces were simultaneously determined as in Trussell *et al*., (2011).

Hence, the indices (Tab.9) are calculated using either the average colour of the entire image in various units related to "greenness" or the proportion of pixels classified as green canopy relative to the total number of pixels in the image. The Hue (H) component of the HSI colour space describes the colour spanning the visible spectrum in the form of an angle between 0^O and 360^O, where 0^O corresponds to red, 60^O to yellow, 120^O to green, and 180^O to cyan.

Green Area Index (GA) is the percentage of pixels with $60 < Hue < 120$ from the total amount of pixels, whereas the greener area (GGA) is a little more limiting since the index corresponds to $80 <$

Hue < 120, excluding yellowish-green tones. Moreover, GGA is proposed to capture the active photosynthetic area excluding senescent leaves.

In the CIELab colour space model, the L* dimension denotes lightness, while the a* component represents the green to red range, with a greater positive value signifying a purer red and a lower positive value indicating a greener hue. Meanwhile, the b* component expresses the transition from blue to yellow, with the more positive value being closer to pure yellow and the more negative value being closer to blue. In the CIELuv colour space model, dimensions u* and v* are perceptually uniform coordinates, where L* is again lightness and u* and v* represent axes similar to a* and b* in separating the colour spectrum, respectively.

Furthermore, both CIELab and CIELuv include colour calibration corrections by separating the colour hue from the illumination elements of the input RGB signal. For that reason, as it was proposed by Buchaillot et al. (2019), we used two new vegetation indices based on these colour spaces, using the normalized difference between a* and b* (NDLab) and the normalized difference between u* and v* (NDLuv) in a manner similar to the conceptual basis for NDVI.

As a result, the CIElab and CIEluv colour spaces may contrast green vegetation abundance with both the reddish/brown soil background (fractional vegetation cover or plant growth) and yellowing induced by chlorosis (loss of foliar chlorophyll), both of which are typical indications of nitrogen deficit.

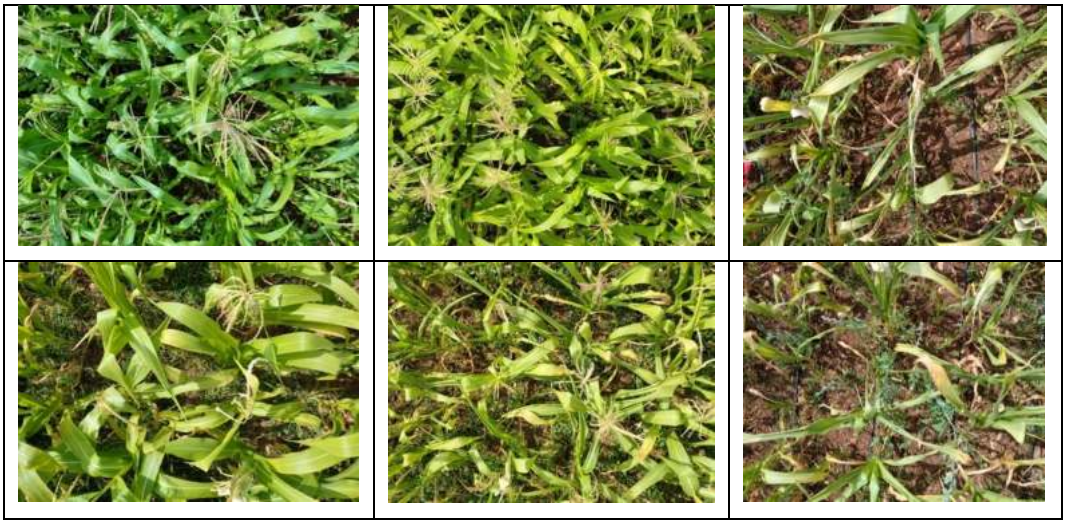

Figure 16. RGB images taken during the flowering season in 6 different treatments (I100 HN, I100 LN, I50 HN, I50 LN, I0 HN, I0 LN)

Table 9. Indices derived from RGB digital camera

RGB vegetation indices		
Model	***Index***	
HSI model	Hue (H)	0° - red
		60° - yellow
		120° - green
		180° - cyan
pixels	Green Area (GA)	60° - 180° → yellow-bluish green
pixels	Greener Area (GGA)	80° - 180° → exclude yellowish tones
CIELab	a*	green – red
	b*	blue - yellow
CIELuv	u*	blue – green (v*) – red (u*)
	v*	
CIELab	NDLab	(((1 − a*) − b*)/ ((1 − a*) + b*) + 1).
CIELuv	NDLuv	(((1 − u*) − v*)/ ((1 − u*) + v*) + 1)

3.4.2.2.2. Spectral reflectance and bio-physiological parameters

ASD FieldSpec Hand-Held 2 Spectro-radiometer with high spectral resolution was used to assess plant reflectance (Analytical Spectral Devices, Inc., Boulder, CO, USA). The device measures reflectance with a wavelength range of 325–1075 nm, a resolution of 3 nm at 700 nm, and a precision of 1 nm. Thereafter, vegetation indices (Tab.6) were calculated using different spectral bands.

Moreover, during the growing season different bio-physiological crop parameters were measured. In order to measure the net photosynthetic CO_2 assimilation rate (An, μmol m^{-2} s^{-1}), stomatal conductance (gs, mol m^{-2} s^{-1}), and leaf transpiration (Tr, mmol m^{-2} s^{-1}), a portable open-system gas-exchange analyser (Li-6400XT, Li-Cor Biosciences, Lincoln, NE, USA) was used. On 25 repetitions per plot, the Chlorophyll Content (CC) of leaves was indirectly quantified using an optical meter (SPAD-502, Konica Minolta, Osaka, Japan). Also, relative water content (RWC) was calculated as a ratio of the difference between fresh weight (FW) of leaf segments and their dry weight (DW) and the difference between fresh weight and saturated weight (SW). Furthermore, a thermal imaging camera (FLIR B335, Wilsonville, OR, USA) was used to measure the canopy temperature (Tc) and then, for leaf temperature extraction, FLIR Tools software was used to enhance the images. Finally, the leaf area index (LAI) was assessed using an optical leaf area meter (Li-COR, 3100, Lincoln NE, USA) and then dry-above ground biomass was measured on the same samples used for LAI, weighting them after drying in the oven at 70°C for 48 h.

3.4.2.3. Statistical analysis

Using the free and open-source software RStudio, data was statistically analyzed (R Foundation for Statistical Computing, Vienna, Austria). A two-factor analysis of variance was used to investigate the

impact of growing conditions (water and nitrogen regime) and their interaction on various bio-physiological parameters. Fisher's LSD (Least Significant Difference) test was used to identify post hoc differences at each growing condition. Moreover, bivariate Pearson correlation coefficients were computed to examine the correlation between the bio-physiological parameters and tested RGB indices. Multiple linear regression was calculated using a stepwise algorithm with bio-physiological parameters as dependent variables and RGB and hyperspectral vegetation indices as independent variables.

3.4.3. Results

The results of the analysis of variance for Leaf Area Index (LAI), Chlorophyll content (CC) and net assimilation rate (An) for two growing seasons (2020 and 2021) are reported in Table 10. The water treatments significantly affected all three presented variables, while nitrogen regimes were significant only in the case of CC in both years and An in 2020. However, the interaction between water and nitrogen was only significant for CC in 2021, where also the biggest differences between each treatment were found, except for two rainfed treatments that showed similar performance. Other parameters displayed the difference mainly between water treatments. Moreover, the importance of nitrogen for CC was shown also by values that were the highest in treatments with high nitrogen level (I_{100} HN, I_{50} HN, I_0 HN).

Table 10. Effects of irrigation regime and nitrogen levels on Leaf Area Index (LAI), Chlorophyll content (CC) and net assimilation rate (An)

Treatment		LAI (m^2 m^{-2})		CC (r.u.)		An (□mol m^{-2} s^{-1})	
		2020	2021	2020	2021	2020	2021
Water regime	Nitrogen						
I0	Low	1.08±0.34c	0.24±0.03c	33.34±5.71c	17.65±1.30e	1.54±2.58c	1.17±0.25c
	High	0.92±0.13c	0.34±0.05c	39.96±7.08bc	19.91±1.59e	1.06±0.94c	1.47±0.56c
I50	Low	2.10±0.19b	1.53±0.45b	38.26±2.96c	24.58±1.91d	33.25±3.21b	19.67±1.42b
	High	2.56±0.12ab	1.62±0.42b	46.62±3.03b	34.16±2.36b	34.76±1.93b	21.25±1.09b
I100	Low	2.54±0.24ab	2.53±0.31a	38.32±4.41c	29.89±1.54c	39.67±2.31a	29.96±2.59a
	High	3.12±0.27a	2.78±0.12a	53.83±2.95a	44.72±1.68a	41.48±0.99a	33.81±3.45a
Significance							
Water regime		***	***	*	***	***	***
Nitrogen		ns	ns	***	***	*	ns
WR x N		ns	ns	ns	***	ns	ns

Table 11 shows stepwise regression models explaining different physiological variables variations from RGB and narrow-band VIs across different water supplies and nitrogen levels in the 2020 and 2021 growing seasons. All presented models were found to be significant. The best-performing model was obtained in 2020 when 63.7% of LAI was explained, considering indices such as GA, NDLuv and v*. The same indices, together with index b*, explained 61.8 % of CC in 2020. Moreover, in 2020, the GA index was considered as one of the best indices for explaining response variables, since it explained 61.6% of LAI, 46.1% of stomatal conductance, 56.3% of transpiration rate and 35.7% of RWC. In the growing season of 2021, GA has been included only in the model chosen for CC, where this index provided the most accurate estimation (R^2=0.49).In 2021, the GGA index was included in more models, but not with high prediction ability. The best model of 2021 was found for CC that includes GA, GGA and NDLab indices.

Table 11. Multilinear stepwise regression of different bio-physiological parameters and RGB indices

Year 2020	Response Variable	VIs	Coefficient	p value	Portion of variance	Year 2021	Response Variable	VIs	Coefficient	p value	Portion of variance
	LAI (R^2=0.637, R_{adj}^2=0.633)	Constant	-1.20	<0.001			LAI (R^2=0.491, R_{adj}^2=0.485)	Constant	-1.517	<0.001	
		GA	6.84	<0.001	0.616			v*	0.059	<0.001	0.393
		NDLuv	-1.38	<0.001	0.009			GGA	1.547	<0.001	0.098
		v*	-0.02	0.003	0.012						
	DAGB (R^2=0.498, R_{adj}^2=0.490)	Constant	-995.25	<0.001			DAGB (R^2=0.236, R_{adj}^2=0.226)	Constant	-121.884	<0.001	
		GA	4734.94	<0.001	0.146			b*	10.132	<0.001	0.185
		u*	46.53	<0.001	0.203			GGA	489.834	<0.001	0.025
		b*	-25.50	<0.001	0.091			NDLuv	-335.562	0.008	0.026
		NDLuv	-1275.89	<0.001	0.058						
	CC (R^2=0.618, R_{adj}^2=0.612)	Constant	19.83	<0.001			CC (R^2=0.508, R_{adj}^2=0.501)	Constant	24.764	<0.001	
		NDLuv	58.03	<0.001	0.502			GA	32.738	<0.001	0.49
		u*	1.62	<0.001	0.081			GGA	8.682	<0.001	0.008
		GA	35.38	<0.001	0.026			NDLab	-21.978	0.05	0.01
		b*	-0.19	0.016	0.009						
	An (R^2=0.535, R_{adj}^2=0.531)	Constant	-19.75	<0.001			An (R^2=0.496, R_{adj}^2=0.491)	Constant	-30.163	<0.001	
		v*	0.79	<0.001	0.374			v*	0.81	<0.001	0.45
		GGA	29.68	<0.001	0.161			NDLab	23.802	<0.001	0.046
	gs (R^2=0.474, R_{adj}^2=0.470)	Constant	-0.12	<0.001			gs (R^2=0.354, R_{adj}^2=0.347)	Constant	-0.225	<0.001	
		GA	0.63	<0.001	0.461			v*	0.005	<0.001	0.3
		a*	0.01	0.013	0.013			NDLab	0.217	<0.001	0.054
	Tr (R^2=0.604, R_{adj}^2=0.600)	Constant	-3.77	<0.001			Tr (R^2=0.447, R_{adj}^2=0.41)	Constant	-4.362	<0.001	
		GA	13.97	<0.001	0.563			v*	0.148	<0.001	0.421
		a*	0.19	<0.001	0.014			GGA	4.205	0.003	0.026
		v*	0.07	<0.001	0.024						

RWC (R^2=0.560, R_{adj}^2=0.555)	Constant	23.45	<0.001		RWC (R^2=0.267, R_{adj}^2=0.256)	Constant	-51.968	<0.001	
	GA	70.49	<0.001	0.357		u*	6.215	<0.001	0.087
	u*	3.18	<0.001	0.054		v*	2.539	<0.001	0.107
	NDLuv	86.87	<0.001	0.149		GGA	125.257	<0.001	0.073
Tc (R^2=0.575, R_{adj}^2=0.570)	Constant	13.43	<0.001		Tc (R^2=0.412, R_{adj}^2=0.406)	Constant	38.965	<0.001	
	NDLuv	49.77	<0.001	0.232		v*	-0.167	<0.001	0.384
	u*	1.44	<0.001	0.255		u*	0.082	0.003	0.028
	v*	0.30	<0.001	0.088					

For the purpose of testing how the combinations of narrow-band indices may improve the strength and accuracy of the assessment of different physiological variables, stepwise regression was performed (Tab.12). The best explanatory variables to predict LAI were DD and WINDVI in 2020 season, while in 2021 REIP and WI. However, the determination coefficients (R^2) of the regression model were low in both growing seasons, as also observed for DAGB prediction.

In 2020, the $Cl_{red-edge}$ index explained 55.2% of CC, while WINDVI and DD 15.4 and 3.5 %, respectively. However, in 2021, the ability of DD index to predict CC was noticeably higher (R^2=0.446). In 2020, 45.7% of total variation of An was explained by Cl_{green}, DD and WINDVI , while in 2021 the model included NDRE, WINDVI and WI, explaining 50.1%.

The same indices (NDRE and Cl) were selected in models to predict gs and Tr in 2020, while in 2021, gs and Tr were mainly explained by MTCI (R^2=0.396) and NDRE (R^2=0.477), respectively. The variation of RWC in each growing season was very well explained by WI, with significant variation of coefficient of determination (R^2), with values of 70.5% in 2020, while 13% in 2021 .

The best model, with two (WI and $Cl_{red-edge}$) and three (DD, WI and WINDVI) indices, was selected to predict Tc in 2020 and 2021, respectively. Moreover, in 2020, WI explained 76.5% of Tc, which was the best performance compared to other indices included in all models.

Table 12. Multilinear stepwise regression of different bio-physiological parameters as the dependent variable and hyperspectral indices

Year 2020	Response Variable	VIs	Coefficient	p value	Portion of variance	Year 2021	Response Variable	VIs	Coefficient	p value	Portion of variance
	LAI (R^2=0.408, R_{adj}^2=0.404)	Constant	0.08	0.719			LAI (R^2=0.387, R_{adj}^2=0.381)	Constant	-70.631	<0.001	
		DD	9.38	<0.001	0.343			REIP	0.09	<0.001	0.366
		WINDVI	0.82	<0.001	0.065			WI	7.746	0.011	0.021
	DAGB (R^2=0.244, R_{adj}^2=0.238)	Constant	207.19	0.002			DAGB (R^2=0.368, R_{adj}^2=0.359)	Constant	-8601.66	0.001	
		$Cl_{red-edge}$	3287.90	<0.001	0.105			$Cl_{red-edge}$	314.34	0.219	0.313
		Cl	-168.11	<0.001	0.139			WI	2623.148	0.001	0.037
								REIP	8.57	0.017	0.018
	CC (R^2=0.741, R_{adj}^2=0.738)	Constant	1.50	0.328			CC (R^2=0.493, R_{adj}^2=0.485)	Constant	385.933	0.01	
		$Cl_{red-edge}$	38.50	<0.001	0.552			DD	104.517	<0.001	0.446
		WINDVI	17.14	<0.001	0.154			Cl_{green}	-3.664	0.003	0.03
		DD	54.21	<0.001	0.035			REIP	-0.541	0.012	0.017
	An (R^2=0.457, R_{adj}^2=0.451)	Constant	2.23	0.399			An (R^2=0.501, R_{adj}^2=0.494)	Constant	-60.825	0.129	
		Cl_{green}	6.17	<0.001	0.353			NDRE	81.859	<0.001	0.477
		DD	76.57	<0.001	0.094			WINDV	-8.964	0.005	0.016
		WINDVI	4.22	0.024	0.01			WI	74.419	0.068	0.008
	gs (R^2=0.349, R_{adj}^2=0.346)	Constant	-0.02	0.289			gs (R^2=0.436, R_{adj}^2=0.428)	Constant	-0.798	0.023	
		NDRE	1.32	<0.001	0.334			MTCI	0.16	<0.001	0.396
		Cl	-0.02	0.012	0.015			WINDV	-0.064	0.009	0.02
								WI	0.89	0.009	0.02
	Tr (R^2=0.435, R_{adj}^2=0.431)	Constant	0.34	0.376			Tr (R^2=0.495, R_{adj}^2=0.485)	Constant	-26.077	0.011	
		NDRE	32.53	<0.001	0.41			NDRE	27.54	<0.001	0.421
		Cl	-0.55	0.001	0.025			WINDV	-3.858	<0.001	0.015
								Cl_{green}	-2.489	<0.001	0.031
								WI	34.815	0.01	0.028
	RWC (R^2=0.755, R_{adj}^2=0.752)	Constant	0.70	0.779			RWC (R^2=0.194, R_{adj}^2=0.182)	Constant	-637.804	<0.001	
		WI	69.10	<0.001	0.705			WI	688.902	<0.001	0.13
		DD	57.39	<0.001	0.05			DD	-154.241	<0.001	0.048
								Cl	5.906	0.051	0.016
	Tc (R^2=0.823, R_{adj}^2=0.821)	Constant	2.76	<0.001			Tc (R^2=0.422, R_{adj}^2=0.413)	Constant	66.171	<0.001	
		WINDVI	16.74	<0.001	0.765			DD	-6.392	0.025	0.337
		$Cl_{red-edge}$	16.63	<0.001	0.058			WI	3.079	<0.001	0.043
								WINDV	-35.621	<0.001	0.042

Correlations among the RGB indices and both bio-physiological parameters were checked using a Pearson correlation matrix (Fig.17). In 2020, the GA index and LAI had the highest positive correlation (0.79). The GA index was favourably connected with all parameters in the season of 2021, with CC having the strongest correlation (0.74). Other indices performed similarly, particularly GGA,

NDLab, and NDLuv, but indices b* and v* had lower values of correlation with the examined parameters. In contrast, all parameters in both seasons had a highly or moderately negative correlation with indices a* and u*.

However, very poor correlation values were found for DAGB, particularly throughout the 2020 season. Similar to that, with the exception of the b* and v* indices, the correlation between RWC and indices in 2021 had values that were extremely low, close to zero.

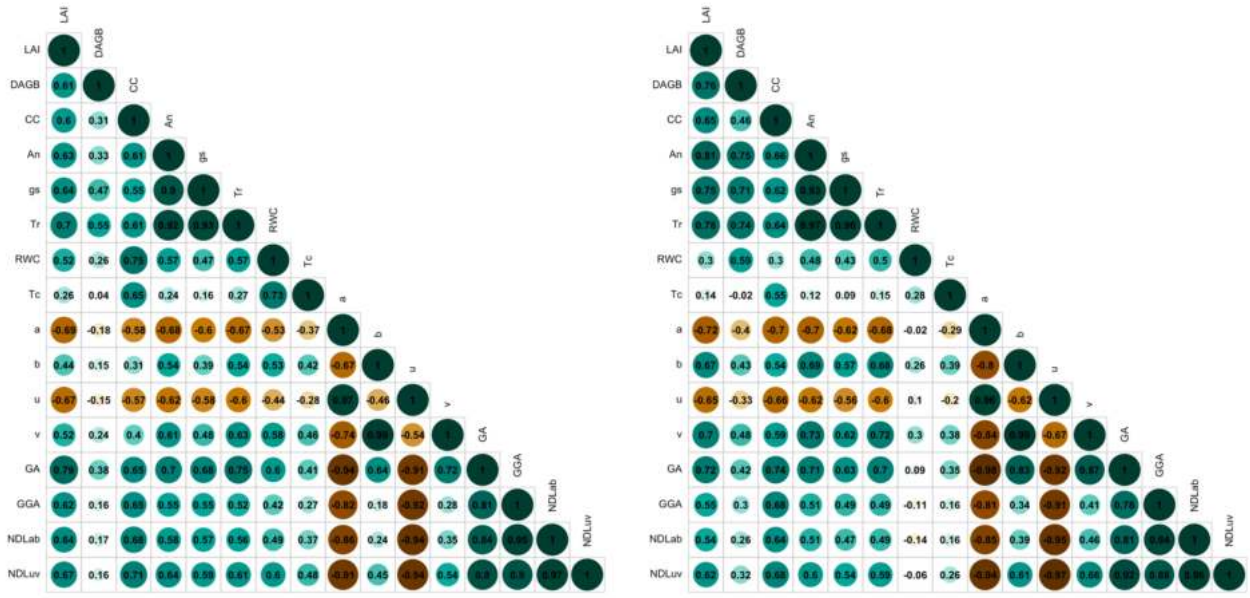

Figure 17. Correlation matrix for the bio-physiological parameters and RGB indices for sweet maize in 2020 (left) and 2021 (right)

3.4.4. Discussion

3.4.4.1. Effect of water and nitrogen treatments on Leaf Area Index, leaf chlorophyll content and net assimilation rate

Water scarcity, together with N deficiency, is a significant limiting factor of the main physiological processes, such as photosynthesis, respiration, nitrogen accumulation, etc (Santos *et al*., 2022). Those two factors have a marked effect on LAI (Liaghat and Balasundram, 2018), leaf chlorophyll content (Wang *et al*., 2021), net assimilation rate (Li *et al.,* 2016) and therefore, they are strongly linked with crop production.

In our study, the maximum LAI, with values of 3.12 and 2.78 in 2020 and 2021, respectively, was obtained in full irrigated and high nitrogen level conditions. However, water stress that occurred in rainfed plots led to much lower values of LAI, especially in the 2021 season. Numerous studies have linked leaf area index to water stress in maize (Cakir, 2004; Farre and Faci, 2009). Moreover, in our

study, water stress had a significant effect on LAI in both growing years, while N and interaction of water and N were not significant for this parameter.

As Table 10 showed, the values of leaf chlorophyll content ranged between 33.3 and 53.8 (r.u) in 2020, while in 2021 between 17.7 and 44.7 (r.u). Nitrogen significantly affected CC in both years, while in 2021 also significant interaction of water and nitrogen was observed. Many studies determined that the leaf chlorophyll content increases with the increment of doses of nitrogen fertilizers (Prsa *et al*., 2007; Uysal, 2018).

Furthermore, some studies explained that the decrease in chlorophyll concentration in nitrogen-limited conditions is frequently a factor contributing to lower rates of photosynthesis.

N deficit causes maize to lower photosynthetic activity, which has a significant impact on grain productivity (Bertheloot *et al*., 2008). Compared to full irrigated treatments, in deficit irrigation treatments, An decreased by 16% and 37% in 2020 and 2021, respectively. It is worth noticing that the reduction of the net assimilation rate in rainfed conditions, usually occurring in severe water stress conditions, results in closing stomata and impairing the photosynthetic activity. Hence, this parameter has great significance in determining the lowest limit of water demand in plant physiology and represents a key indicator of the shift from mild to severe drought conditions (Bacelar *et al*., 2009).

3.4.4.2. Performance of RGB and hyperspectral vegetation indices

The fundamental advantage of integrating imaging approaches into aerial-based platforms is that researchers may quickly cover larger experimental regions, limiting the impact of diurnal fluctuation in environmental factors such variations in radiation and temperature or the presence of clouds (Costa *et al*., 2013).

It has been suggested that the vegetation indices acquired by digital RGB images may be useful to estimate the green biomass, yield production and other physiological parameters of maize and other crops under stress (Ahmed and Reid, 1996). As all measurements in both seasons were done at the same time on the same day, fluctuations in environmental factors could be almost negligible.

Compared with other RGB-based indices, the GA index presented the greatest ability to predict examined parameters (Tab.11). It was surprising to notice that the GGA index was not capable to perform in the same way as GA, knowing that both indices compare the percentage of green pixels to all the pixels in the picture (Lukina *et al*., 1999) and previous studies reported very similar behaviors of these two indices (Gracia-Romero *et al.*, 2019; Buchaillot *et al*., 2019).

In our study, a* index was not included in predicted models, even though a* index was found to be strongly linked to green biomass and the detection of crop stress (Sarkar *et al.*, 2021). However, the explaining ability of the NDLuv index in the 2020 season was the best in the case of predicting the

CC, where 50% of this parameter was explained. A study of Buchaillot *et al.* (2019) demonstrated the similar contribution of NDLuv, together with NDLab, to predict the grain yield of maize, which overperformed NDVI and some other multispectral indices.

It was observed a high positive correlation of GA and LAI, as well as gas-exchange parameters, followed by similar values of other indices such as GGA, NDLab, NDLuv and the same parameters. However, the correlation of those indices with DAGB in 2020 and RWC and Tc in 2021 was not significant.

Multilinear stepwise regression of bio-physiological variables and hyperspectral indices resulted in the best model of canopy temperature explained by the ratio of WI/NDVI and $Cl_{red\text{-}edge.}$ A canopy under water stress seems to have a higher temperature than one that is well-watered under the same climatic conditions because canopy temperature is a measure of the energy balance (Ihuoma and Madramootoo, 2020). This may explain the great capability of water indices (WI and WI/NDVI) to explain variables such as Tc and RWC.

Furthermore, the high capacity of red-edge position to predict the gas-exchange parameters was proved again. Different red-edge indices such as $Cl_{red\text{-}edge}$, NDRE, MTCI, DD, REIP were obtained as best predictors of examined bio-physiological parameters. As it was previously explained, the red-edge position is defined as the point of greatest slope (inflexion point), and it indicates the sharp transition between the reflectance absorption characteristic in red wavelengths and NIR reflectance. Recent findings reported that the red-edge region of the electromagnetic spectrum showed a very high sensitivity to the chlorophyll content variation (El-Metwalli and Tyler, 2020). This explains the favorable association between the leaf-gas exchange parameters and the VIs based on red-edge wavelengths.

3.4.5. Conclusion

The use of RGB vegetation indicators to predict the performance of a set of sweet maize parameters during the two growing seasons is highlighted in this study. In terms of assessing crop bio-physiological parameters, the RGB and hyperspectral indices had similar results. Overall, the GA index demonstrated the greatest correlation and capability to explain examined parameters. On the other hand, hyperspectral vegetation indices indicated the potential of red-edge wavelengths for the assessment of important crop parameters. Hence, due to the similarities between the outcomes of the proximal evaluation and those attained from aerial platforms, the use of vegetation indices produced from RGB photographs may constitute a particularly cost-effective strategy for crop stress monitoring. Digital photography is a viable method, despite being relatively low-tech and

inexpensive, and its derived indices have shown potential for the assessment of crop management in maize, making it appropriate for developing countries in particular.

3.4.6. References

Liaghat, S., Balasundram, S. K. (2010). A review: The role of remote sensing in precision agriculture. American Journal of Agricultural and Biological Sciences, 5(1), 50-55.

Virnodkar, S. S., Pachghare, V. K., Patil, V. C., & Jha, S. K. (2020). Remote sensing and machine learning for crop water stress determination in various crops: a critical review. Precision Agriculture, 21(5), 1121-1155.

Katsoulas, N., Elvanidi, A., Ferentinos, K. P., Kacira, M., Bartzanas, T., & Kittas, C. (2016). Crop reflectance monitoring as a tool for water stress detection in greenhouses: A review. Biosystems Engineering, 151, 374-398.

Shoshany, M., Goldshleger, N., & Chudnovsky, A. (2013). Monitoring of agricultural soil degradation by remote-sensing methods: A review. International Journal of Remote Sensing, 34(17), 6152-6181.

Mulla, D. J. (2013). Twenty five years of remote sensing in precision agriculture: Key advances and remaining knowledge gaps. Biosystems engineering, 114(4), 358-371.

Wachendorf, M., Fricke, T., & Möckel, T. (2018). Remote sensing as a tool to assess botanical composition, structure, quantity and quality of temperate grasslands. Grass and forage science, 73(1), 1-14.

Khanal, S., Fulton, J., & Shearer, S. (2017). An overview of current and potential applications of thermal remote sensing in precision agriculture. Computers and Electronics in Agriculture,139, 22–32. https://doi.org/10.1016/j.compag.2017.05.001.

Haghighattalab, A., González Pérez, L., Mondal, S., Singh, D., Schinstock, D., Rutkoski, J., ... & Poland, J. (2016). Application of unmanned aerial systems for high throughput phenotyping of large wheat breeding nurseries. Plant Methods, 12(1), 1-15.

Danzi, D., Briglia, N., Petrozza, A., Summerer, S., Povero, G., Stivaletta, A., ... & Janni, M. (2019). Can high throughput phenotyping help food security in the mediterranean area?. Frontiers in Plant Science, 10, 15.

Tsouros, D. C., Bibi, S., & Sarigiannidis, P. G. (2019). A review on UAV-based applications for precision agriculture. Information, 10(11), 349.

Yadav, S. P., Ibaraki, Y., & Dutta Gupta, S. (2010). Estimation of the chlorophyll content of micropropagated potato plants using RGB based image analysis. Plant Cell, Tissue and Organ Culture (PCTOC), 100(2), 183-188.

Yousfi, S., Gracia-Romero, A., Kellas, N., Kaddour, M., Chadouli, A., Karrou, M., ... & Serret, M. D. (2019). Combined use of low-cost remote sensing techniques and δ13C to assess bread wheat grain yield under different water and nitrogen conditions. Agronomy, 9(6), 285.

Norasma, C. Y. N., Sari, M. A., Fadzilah, M. A., Ismail, M. R., Omar, M. H., Zulkarami, B., ... & Tarmidi, Z. (2018, June). Rice crop monitoring using multirotor UAV and RGB digital camera at early stage of growth. In IOP Conference Series: Earth and Environmental Science (Vol. 169, No. 1, p. 012095). IOP Publishing.

Fernandez-Gallego, J. A., Kefauver, S. C., Vatter, T., Gutiérrez, N. A., Nieto-Taladriz, M. T., & Araus, J. L. (2019). Low-cost assessment of grain yield in durum wheat using RGB images. European Journal of Agronomy, 105, 146-156.

Buchaillot, M. L., Gracia-Romero, A., Vergara-Diaz, O., Zaman-Allah, M. A., Tarekegne, A., Cairns, J. E., ... &

Kefauver, S. C. (2019). Evaluating maize genotype performance under low nitrogen conditions using RGB UAV phenotyping techniques. Sensors, 19(8), 1815.

Zhang, L., Niu, Y., Zhang, H., Han, W., Li, G., Tang, J., & Peng, X. (2019). Maize canopy temperature extracted from UAV thermal and RGB imagery and its application in water stress monitoring. Frontiers in plant science, 10, 1270.

Wakabayashi, H., Matsuda, O., Fujita, T., & Kume, A. (2021). Practical application of proximal sensing for monitoring the growth of Physcomitrium patens. Biological Sciences in Space, 35, 32-40.

Rorie, R. L., Purcell, L. C., Mozaffari, M., Karcher, D. E., King, C. A., Marsh, M. C., & Longer, D. E. (2011). Association of "greenness" in corn with yield and leaf nitrogen concentration. Agronomy Journal, 103(2), 529-535.

Li, B., Xu, X., Zhang, L., Han, J., Bian, C., Li, G., ... & Jin, L. (2020). Above-ground biomass estimation and yield prediction in potato by using UAV-based RGB and hyperspectral imaging. ISPRS Journal of Photogrammetry and Remote Sensing, 162, 161-172.

Gracia-Romero, A., Kefauver, S. C., Vergara-Díaz, O., Zaman-Allah, M. A., Prasanna, B. M., Cairns, J. E., & Araus, J. L. (2017). Comparative performance of ground vs. aerially assessed RGB and multispectral indices for early-growth evaluation of maize performance under phosphorus fertilization. Frontiers in Plant Science, 8, 2004.

Sarkar, S., Ramsey, A. F., Cazenave, A. B., & Balota, M. (2021). Peanut leaf wilting estimation from RGB color indices and logistic models. Frontiers in plant science, 12, 713.

Casadesús, J., Kaya, Y., Bort, J., Nachit, M. M., Araus, J. L., Amor, S., ... & Villegas, D. (2007). Using vegetation indices derived from conventional digital cameras as selection criteria for wheat breeding in water-limited environments. Annals of applied biology, 150(2), 227-236.

Kefauver, S. C., El-Haddad, G., Vergara-Diaz, O., & Araus, J. L. (2015, October). RGB picture vegetation indexes for high-throughput phenotyping platforms (HTPPs). In Remote Sensing for Agriculture, Ecosystems, and Hydrology XVII (Vol. 9637, pp. 82-90). SPIE.

Allen, R. G., Pereira, L. S., Raes, D., & Smith, M. (1998). Crop evapotranspiration-Guidelines for computing crop water requirements-FAO Irrigation and drainage paper 56. Fao, Rome, 300(9), D05109.

Trussell, H. J., Lin, J., & Shamey, R. (2011, June). Effects of texture on color perception. In 2011 IEEE 10th IVMSP Workshop: Perception and Visual Signal Analysis (pp. 7-11). IEEE.

LIU, X. J., Qiang, C. A. O., YUAN, Z. F., Xia, L. I. U., WANG, X. L., TIAN, Y. C., ... & Yan, Z. H. U. (2018). Leaf area index based nitrogen diagnosis in irrigated lowland rice. Journal of integrative agriculture, 17(1), 111-121.

Wang, N., Fu, F., Wang, H., Wang, P., He, S., Shao, H., ... & Zhang, X. (2021). Effects of irrigation and nitrogen on chlorophyll content, dry matter and nitrogen accumulation in sugar beet (Beta vulgaris L.). Scientific Reports, 11(1), 1-9.

Li, W., Xiong, B., Wang, S., Deng, X., Yin, L., & Li, H. (2016). Regulation effects of water and nitrogen on the source-sink relationship in potato during the tuber bulking stage. PloS one, 11(1), e0146877.

Cakir, R. (2004). Effect of water stress at different development stages on vegetative and reproductive growth of corn. Field Crops Research, 89(1), 1-16.

Farré, I., & Faci, J. M. (2009). Deficit irrigation in maize for reducing agricultural water use in a Mediterranean environment. Agricultural water management, 96(3), 383-394.

Prsa, I., Stampar, F., Vodnik, D., & Veberic, R. (2007). Influence of nitrogen on leaf chlorophyll content and photosynthesis of 'Golden Delicious' apple. Acta Agriculturae Scandinavica Section B-Soil and Plant

Science, 57(3), 283-289.

UYSAL, E. (2018). Effects of Nitrogen Fertilization on the Chlorophyll Content of Apple. Meyve Bilimi, 5(1), 12-17.

Bertheloot, J., Martre, P., & Andrieu, B. (2008). Dynamics of light and nitrogen distribution during grain filling within wheat canopy. Plant physiology, 148(3), 1707-1720.

Bacelar, E. A., Moutinho-Pereira, J. M., Gonçalves, B. C., Lopes, J. I., & Correia, C. M. (2009). Physiological responses of different olive genotypes to drought conditions. Acta Physiologiae Plantarum, 31(3), 611-621.

Costa, L., Nunes, L., & Ampatzidis, Y. (2020). A new visible band index (vNDVI) for estimating NDVI values on RGB images utilizing genetic algorithms. Computers and Electronics in Agriculture, 172, 105334.

Ahmed, M. A., Reid, E., Cooke, A., Arngrimsson, R., Tolmie, J. L., & Stephenson, J. B. (1996). Familial hemiplegic migraine in the west of Scotland: a clinical and genetic study of seven families. Journal of Neurology, Neurosurgery & Psychiatry, 61(6), 616-620.

Lukina, E. V., Stone, M. L., & Raun, W. R. (1999). Estimating vegetation coverage in wheat using digital images. Journal of Plant Nutrition, 22(2), 341-350.

Gracia-Romero, A., Kefauver, S. C., Fernandez-Gallego, J. A., Vergara-Díaz, O., Nieto-Taladriz, M. T., & Araus, J. L. (2019). UAV and ground image-based phenotyping: a proof of concept with durum wheat. Remote Sensing, 11(10), 1244.

Ihuoma, S. O., & Madramootoo, C. A. (2020). Narrow-band reflectance indices for mapping the combined effects of water and nitrogen stress in field grown tomato crops. Biosystems Engineering, 192, 133-143.

Chapter 4

Conclusion

Remote and proximal sensing (RS) technologies give the agricultural community a diagnostic tool that can act as an early warning system, enabling early intervention to prevent possible issues before they adversely affect crop production. Due to recent developments in sensor technologies, data management and analysis, the agricultural community now has accessed to several RS choices.

This study focused on the evaluation of proximal and aerial sensing techniques for accurate soil and crop management and sustainable use of nitrogen and water. Specifically, the performance of those techniques was assessed for evaluating the sweet maize growth under different water (I_{100}, I_{50}, I_0) and nitrogen regimes (HN and LN). Ground-based, aerial, and bio-physiological measurements were made throughout the growing seasons.

The crop's physiological characteristics were evaluated using hyperspectral reflectance data. The outcomes of our study underlined the key role of the red-edge spectral region by demonstrating that red-edge group indices including CARI (Chlorophyll Absorption Reflectance Index), DD (Double Difference Index), REIP (Red- Edge Inflection Point), and $Cl_{red\text{-}edge}$ (Chlorophyll Red-Edge) were reliable predictors of yield and physiological parameters. At the mid-season stage, DD, REIP, and $Cl_{red\text{-}edge}$ VIs were able to distinguish crop stress, as well as differentiate water and N stress levels.

We assessed how responsive hyperspectral indices were to various nitrogen and water treatments. The DATT index, which is based on near-infrared and red-edge wavelengths, performed better than other indices in explaining variation in chlorophyll content. In contrast, the double difference index (DD) exhibited the strongest relation with the leaf-gas exchange. The modified normalized difference vegetation index (NNDVI) and the ratio of the water band index to the normalized difference vegetation index (WBI/NDVI) were the best indicators to identify the interaction of irrigation and nitrogen. Additionally, red-edge-based indicators were more responsive to nitrogen status than the structural and water band indices.

This study highlighted the importance of selecting the suitable narrow-band vegetation indicators to monitor the plant's eco-physiological response to water and nitrogen availability.

Our study has demonstrated the success of using RGB indices to monitor the growth of sweet maize. It was obtained high accuracy in predicting Leaf Area Index (LAI) (R^2=0.61) in 2020 and Leaf Chlorophyll Content (CC) (R^2=0.49) in 2021 by the Green-Area index (GA). Thus, these vegetation indices may serve as a very affordable and low-cost alternative tool for monitoring water and

nutritional status. Consequently, one of the top concerns in current agriculture should be further study and practical application of RGB indices in crop growth monitoring, whether used from the ground or drones and other unmanned aerial vehicles (UAVs). Undoubtedly, it will demand the development of uniform monitoring processes and data elaboration methods that will make it easier to calibrate the methods and enable data comparison across various crops and regions. Additional agricultural personnel and professional training are required for this purpose.

Based on the conclusions and data gathered in this work, it can be confirmed the effectiveness of the adopted indices and procedures in advancing knowledge of the soil-plant continuum and facilitating real-time crop water and nutrient status monitoring.

However, it is always very important to take into account that, depending on the field conditions, changes in any other leaf and canopy features can have an impact on the reflectance characteristics occurring in conjunction with water or nutrient deficits. Hence, the employment of machine learning and deep learning algorithms, which are being used frequently to build up complex prediction models for estimating crop characteristics using spectral data, may represent a challenging strategy to overcome existing limitations.